2012-12-06

# Microfluidic Devices with Integrated Sample Preparation for Improved Analysis of Protein Biomarkers

Pamela Nsang Nge
*Brigham Young University - Provo*

# Microfluidic Devices with Integrated Sample Preparation for Improved Analysis of Protein Biomarkers

Pamela Nsang Nge

A dissertation submitted to the faculty of
Brigham Young University
in partial fulfillment of the requirements for the degree of

Doctor of Philosophy

Adam T. Woolley, Chair
Milton L. Lee
David V. Dearden
James E. Patterson
Aaron R. Hawkins

Department of Chemistry and Biochemistry

Brigham Young University

December 2012

# ABSTRACT

## Microfluidic Devices with Integrated Sample Preparation for Improved Analysis of Protein Biomarkers

Pamela N. Nge
Department of Chemistry and Biochemistry, BYU
Doctor of Philosophy

Biomarkers present a non-invasive means of detecting cancer because they can be obtained from body fluids. They can also be used for prognosis and assessing response to treatment. To limit interferences it is essential to pretreat biological samples before analysis. Sample preparation methods include extraction of analyte from an unsuitable matrix, purification, concentration or dilution and labeling. The many advantages offered by microfluidics include portability, speed, automation and integration. Because of the difficulties encountered in integrating this step in microfluidic devices most sample preparation methods are often carried out off-chip. In the fabrication of micro-total analysis systems it is important that all steps be integrated in a single platform.

To fabricate polymeric microdevices, I prepared templates from silicon wafers by the process of photolithography. The design on the template was transferred to a polymer piece by hot embossing, and a complete device was formed by bonding the imprinted piece with a cover plate. I prepared affinity columns in these devices and used them for protein extraction. The affinity monolith was prepared from reactive monomers to facilitate immobilization of antibodies. Extraction and concentration of biomarkers on this column showed specificity to the target molecule. This shows that biomarkers could be extracted, purified and concentrated with the use of microfluidic affinity columns.

I prepared negatively charged ion-permeable membranes in poly(methyl methacrylate) microchips by *in situ* polymerization just beyond the injection intersection. Cancer marker proteins were electrophoretically concentrated at the intersection by exclusion from this membrane on the basis of both size and charge, prior to microchip capillary electrophoresis. I optimized separation conditions to achieve baseline separation of the proteins. Band broadening and peak tailing were limited by controlling the preconcentration time. Under my optimized conditions a 40-fold enrichment of bovine serum albumin was achieved with 4 min of preconcentration while >10-fold enrichment was obtained for cancer biomarker proteins with just 1 min of preconcentration.

I have also demonstrated that the processes of sample enrichment, on-chip fluorescence labeling and purification could be automated in a single voltage-driven platform. This required the preparation of a reversed-phase monolithic column, polymerized from butyl methacrylate monomers, in cyclic olefin copolymer microdevices. Samples enriched through solid phase extraction were labeled on the column, and much of the unreacted dye was rinsed off before elution. The retention and elution characteristics of fluorophores, amino acids and proteins on

these columns were investigated. A linear relationship between eluted peak areas and protein concentration demonstrated that this technique could be used to quantify on-chip labeled samples. This approach could also be used to simultaneously concentrate, label and separate multiple proteins.

Keywords: biomarkers, capillary electrophoresis, capillary electrochromatography, microfluidics, sample preparation

## ACKNOWLEDGEMENTS

First, I would like to express sincere gratitude to my advisor Dr. Adam T. Woolley whose scientific guidance, dedication, patience and understanding has helped me overcome the challenges of doctoral studies and shaped my career goals. He has been a great mentor and I will always be grateful for the experience I have gained from working with him. I also thank my graduate committee members Dr. Lee, Dr. Dearden, Dr. Patterson and Dr. Hawkins for their valuable suggestions and great ideas. I am equally grateful to the entire faculty and staff of the Department of Chemistry and Biochemistry at Brigham Young University. I am immensely grateful to all my lab mates for their help and support. Those in the microfluidics area, especially Dr. Weichun Yang, Dr. Ming Yu, Jayson Pagaduan, Chad Rogers and Debolina Chatterjee, have all contributed directly to this work. I appreciate the collaborative discussions I've had with other students in the Department of Chemistry and Biochemistry, especially those in Dr. Lee's lab. I am indebted to my family and friends for their support and encouragement. My sisters Nabi, Ndim, Nafoin, Yiwumi and Futih have been incredibly supportive and I will never take their love for granted.

## TABLE OF CONTENTS

## LIST OF TABLES

## LIST OF FIGURES

# 1. INTRODUCTION*

## 1.1 MINIATURIZED BIOANALYTICAL SYSTEMS

### 1.1.1 Introduction to micro-total analysis systems (μTAS)

Microfluidics consist of microfabricated structures for liquid handling, with cross-sections in the 1-500 μm range, and small volume capacity (fL-nL). Though micromachined systems for gas chromatography were introduced in the 1970's,[1] the field of microfluidics did not gain much traction until the 1990's.[2] Microelectromechanical systems (MEMS) contain integrated electrical and mechanical parts that create a sensor or system.[3] Micro-total analysis systems, also known as lab-on-a-chip, are the chemical analogues of MEMS, as integrated microfluidic devices that are capable of automating multiple processes relevant to laboratory sciences. For example, a typical lab-on-a-chip system can integrate multiple processes (like labeling, purification, separation, and detection) in a microfluidic device, which can be highly enabling for many applications.

The field of microfluidics offers many advantages compared to bulk solution chemistry, one of which is faster diffusion rates due to the smaller interaction distances. Reduced channel dimensions also lead to smaller sample volumes (fL-nL), as well as portable devices that enable on-site testing, for example. Due to the multitude of advantages of microfluidics, many applications have been demonstrated, often with a biological focus such as point-of-care (POC) diagnostics, single-cell analysis, nucleic acid analysis, drug discovery and development, or biosensing.[4] Additional applications are found in environmental monitoring, forensics, food analysis and space exploration.

---

* Parts of this chapter are adapted with permission from Chemical Reviews, Nge, P. N.; Rogers, C. I.; Woolley, A. T., *Chem. Rev.* 2012, In revision. Copyright 2012 American Chemical Society.

### 1.1.2 Materials

Microfluidic device materials initially consisted of silicon and glass substrates; as the field advanced, other materials were evaluated. These materials can be organized into three broad categories: inorganic, polymeric, and paper. Polymer-based materials can be further divided into elastomers and thermoplastics. Paper microfluidics is an emerging and substantially different platform from devices made from either polymer or inorganic materials.

Silicon, the first material used for microfluidics,[1] has a well-developed surface chemistry based on the silanol group (–Si-OH), so surface modification is easily accomplished via silanes. Silicon is transparent to infrared but not visible light, making typical fluorescence detection or fluid imaging challenging for embedded structures in silicon. This issue can be overcome by having a transparent material (polymer or glass) bound to silicon in a hybrid system. Glass has large, composition-dependent elastic modulus, low background fluorescence, and as with silicon, modification chemistries are silanol based. Glass is compatible with biological samples, has relatively low nonspecific adsorption, and is not gas permeable.

Polymers are organic-based, long-chain materials that are increasingly being used for microfluidic device fabrication because they are relatively inexpensive, amenable to mass production processes and adaptable through formulation changes and chemical modification. Polydimethylsiloxane (PDMS), first introduced as a microfluidic substrate in the late 1990's,[5] is arguably the most common material in use due to its reasonable cost, rapid fabrication, and ease of implementation. A hydrophobic material, PDMS is susceptible to nonspecific adsorption and permeation by hydrophobic molecules.[6] However, chemical modification of PDMS by methods

such as plasma treatment[7] and reaction of silanes with silanols[8] can often address these issues. Thermoplastics are densely crosslinked polymers that are moldable when heated above their glass transition temperature but retain their shape when cooled. These materials are generally durable, amenable to micromachining processes, optically clear, resistant to permeation of small molecules, and stiffer than elastomers. The most frequently used thermoplastic is poly(methyl methacrylate) (PMMA), formed through the polymerization of methyl methacrylate and better known under the commercial names of Plexiglas or Lucite. PMMA has an elastic modulus of 3.3 GPa and good optical clarity.[9] Other advantages of this material include biological compatibility, gas impermeability, and ease of micromachining at relatively low temperatures (~100°C). Cyclic-olefin copolymer (COC)[10] is an optically transparent thermoplastic, with good moldability, low background fluorescence, and suitability for use with both organic solvents and aqueous solutions.[11, 12] Since COC is hydrophobic, surface modification is necessary to analyze proteins in these devices.[10]

Paper is a flexible, cellulose-based material that has recently emerged as a promising microfluidic substrate because it is cheap, readily available, biologically compatible and can be chemically modified through composition/formulation changes or through surface reactions.[13, 14] Microfluidic paper-based analytical devices (μPADs) rely on the passive mechanism of capillary action to pull solutions through a device. They are potentially useful for quantitative analysis in developing countries, home care services and other places where resources are limited,[15] and generally employ colorimetric or electrochemical detection that does not require complex instrumentation.[16] Initially, μPADs were one-dimensional devices that had some limitations including loss of fluid by evaporation and increased chances of contamination during analysis.

More complex three-dimensional μPADs address some of the problems observed with one-dimensional devices.[17,18]

### 1.1.3 Fabrication techniques

Fabrication of microfluidic devices involves several techniques depending on the type of material. Most of the techniques for the fabrication of silicon and glass devices are adapted from the semiconductor industry and are either subtractive processes in which structures are formed within the substrate (bulk micromachining), or additive processes in which structures are formed on the surface of the substrate (surface micromachining). In this section, only the more common bulk micromachining processes will be discussed.

#### 1.1.3.1 Glass and silicon devices

Conventional microfabrication techniques for glass and silicon devices involve photolithography, etching and bonding. In photolithography the desired microchannel design is patterned on a photomask and subsequently transferred to the silicon or glass. First the substrate is coated with a light-sensitive photoresist and exposed to UV radiation using a mask aligner. During the process of chemical development for a positive photoresist, the exposed region is removed while the parts not exposed to light stay intact. The reverse occurs for a negative photoresist. Features on the substrate are then created by etching, which can either be done in the liquid or gas phase, with isotropic or anisotropic directionality. This is followed by bonding. Bonding methods include direct bonding,[19] anodic bonding[20] and use of adhesives[21] such as Parylene C, SU-8, benzocyclobutene, and polyimide.[22]

#### 1.1.3.2 Polymer devices

Pattern transfer and bonding in polymer materials depend on the type of polymer. Soft lithography is usually employed for pattern transfer in elastomers like PDMS while hot embossing, injection molding and laser ablation are commonly used for thermoplastics. Activation of the polymer surface by plasma oxidation is the most common method for enabling bonding in elastomers, while thermal and solvent bonding are commonly employed for thermoplastics.

Soft lithography has become popular because the fabrication process is simple.[23] Though PDMS is the most commonly used polymer with soft lithography, other materials including polyurethane and thermally curable epoxy have also been used.[24,25] In the process of soft lithography a prepolymer mixture is poured on the master mold (fabricated by photolithography or e-beam lithography) with positive features, and cured. The patterned polymer replica produced is then detached from the master mold and bonded to another polymer piece, glass or silicon, to form a complete device. One drawback of this technique is that photolithography is still required for the production of the master mold.[26]

For hot embossing, a master template with positive features is pressed against a polymer piece at a defined temperature and time, either with an oven or a hydraulic press at temperatures above the glass transition temperature of the material. This imprints the structure from the template onto the plastic material.[27] In injection molding, which is the preferred commercial method because of its good reproducibility,[28] molten polymer is injected into a molding machine containing a patterned mold insert capable of withstanding high temperatures and pressures. The

replica formed is removed after cooling.[29,30] In laser ablation, a high-power laser is used to create features in the thermoplastic by the removal of materials according to a programmed pattern.[31,32] While the method is fast and patterns can be easily changed through the control software, not many polymers are suitable for this process and the surface chemistry obtained is different from the native polymer.[30]

Thermoplastics can be bonded using heat, solvent or adhesives. Thermal bonding is achieved by pressing two cleaned substrates together and heating the unit above the glass transition temperature of the polymer in an oven or hot press. Bonding occurs as a result of mixing of the polymer chains between the two surfaces.[33] This process is simple; however, microchannel deformation can occur and the bond strength, though good, is weaker than that achieved by solvent bonding.[34,35] Solvent bonding is accomplished by exposing the substrate surfaces to a solvent that is capable of dissolving the polymer. A variety of organic solvents can be used depending on the polymer type. To prevent the solvents from dissolving the polymers and deforming channels, sacrificial layers made from wax[36,37] or ice[38] can be used. Modification of the polymer surface by plasma oxidation has also been shown to improve bond strength in thermoplastics.[39] Adhesive bonding is a simple method of sealing thermoplastic devices.[33] The approach is similar to that of solvent bonding except that it employs glue, epoxies or acrylates. The main limitation of this technique is channel clogging caused by the flow of adhesives into the channel.[40]

### 1.1.4 Limits of miniaturized systems

Microfluidic channels have small overall volumes, laminar flow and a large surface-to-volume ratio. Dimensions of a typical separation channel in microchip electrophoresis (μCE) are: 50 μm width, 15 μm height and 5 cm length for a volume of 37.5 nL. Flow in these devices is normally nonturbulent due to low Reynold's number resulting in diffusion-limited mixing, which is a slower process than that obtained with turbulent flow. Therefore, improved mixing is usually achieved by the use of complex geometries or the integration of micromixers.[41] These small channel sizes have a high surface-to-volume ratio, leading to nonspecific adsorption and surface fouling. Microfluidic devices also have lower separation efficiencies than conventional techniques which separate samples better with longer separation columns.[42] Additionally, the optical pathlength for a channel height of about 15 μm is shorter than for traditional separation columns, resulting in reduced detection sensitivities.[43]

## 1.2 MICROCHIP ELECTROPHORESIS

### 1.2.1 Introduction

Electrophoresis is a powerful liquid-phase separation technique that can be used to separate a diverse range of analytes. Microchip electrophoresis, first demonstrated in the early 1990s, is one of the best miniaturized separation techniques because it is fast, has good resolution, and does not need moving parts.[44, 45] Unlike with traditional capillary electrophoresis instrumentation, which consists of one or more discrete capillaries, many different fluidic channels can be patterned on a microfluidic device for integration and throughput.[45] The use of microscale channels reduces the effects of Joule heating, facilitating the use of higher voltages for more efficient separations.[46] Advantages of electrophoretic methods include high efficiency and speed,

and low sample consumption. However, as indicated above limitations are concentration sensitivity, constrained by the injection of small volumes, and the short optical pathlength.[47]

### 1.2.2 Theory

In both conventional capillary electrophoresis and μCE, analytes are separated according to their electrophoretic mobilities.[48] When an electric field is applied to a buffer in a capillary the analytes acquire different velocities described by equation 1.1.

$$\nu = \mu_e E \qquad (1.1)$$

where ν is the migration velocity (m $s^{-1}$), $\mu_e$ is the electrophoretic mobility ($m^2$ $V^{-1}s^{-1}$) and E is the electric field. The electrophoretic mobility is given by

$$\mu_e = q/6\pi\eta r \qquad (1.2)$$

where q is the charge on the molecule, η is the viscosity of the solution and r is the Stokes radius of the molecule. Differences in analyte charge and size will therefore affect electrophoretic mobility, with a faster mobility achieved for smaller analytes with higher charge. [45]

Electroosmotic flow (EOF) is generated from capillary or microchannel walls during electrophoresis. When voltage is applied to a buffer solution in contact with a charged surface, an electrical double layer of charge (an inner rigid or Stern Layer and an outer diffuse layer) is created as oppositely charged ions from the buffer are attracted to the surface charges.[49] An electrokinetic potential known as the Zeta potential is formed in this double layer and its potential decreases with distance from the capillary wall. Figure 1.1 depicts the formation of such a layer on a negatively charged wall.

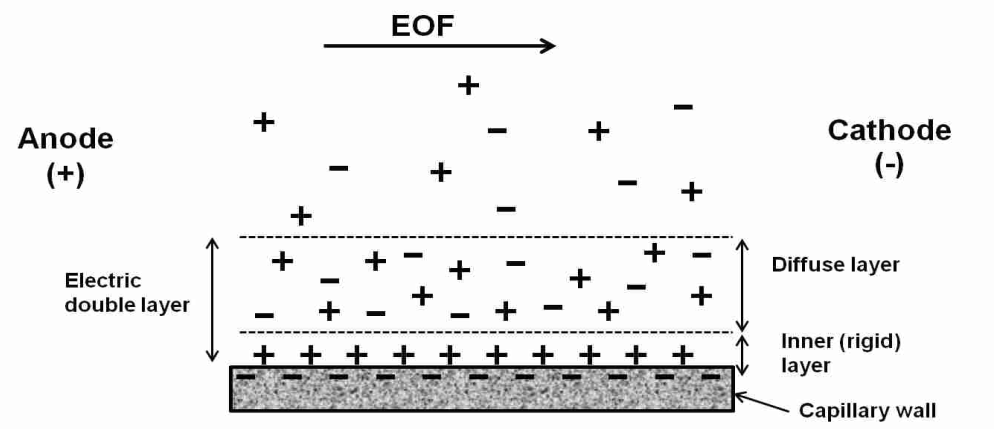


**Figure 1.1.** Direction of EOF of a buffer solution in a negatively charged channel.

This double layer is the basis for EOF, where an applied voltage causes cations within the loosely bound diffuse layer to move towards the cathode, dragging the bulk solution along. The velocity of this flow is given by:

$$\nu_{eof} = (\varepsilon_o \varepsilon \zeta / 4\pi\eta)E \qquad (1.3)$$

where, $\varepsilon_o$ is the dielectric constant of vacuum, $\varepsilon$ is the dielectric constant of the buffer and $\zeta$ is the zeta potential. Electroosmotic mobility ($\mu_{eof}$) is therefore $\varepsilon_o \varepsilon \zeta / 4\pi\eta$.[50] Since both electroosmosis and electrophoresis occur concurrently,[51] the overall velocity ($\nu_{net}$) of an analyte is dictated by the combination of its electrophoretic and electroosmotic mobilities:[45, 50]

$$\nu_{net} = (\mu_{ep} + \mu_{eof})\, E \qquad (1.4)$$

Factors such as pH, electric field, surfactants, organic solvents and wall coatings that affect the zeta potential, dielectric constant and viscosity will also affect EOF.[48]

EOF has both advantages and disadvantages. A disadvantage of EOF is that its reproducibility from run to run is affected by changes in capillary surface properties, for example caused by adsorption.[50,51] However, EOF has many advantages including the fact that it can be used to

control the overall migration speed, making it possible for the simultaneous separation of anions, cations and neutral molecules. When electroosmosis and electrophoresis are in opposite directions and EOF is strong ($v_{EOF} > v_e$) migration by EOF will dominate. Additionally, since the flow profile of EOF is flatter than the parabolic or laminar flow profiles generated by hydraulic pressure (Figure 1.2), broadening of the analyte zone is minimized resulting in improved separation efficiencies.[50]

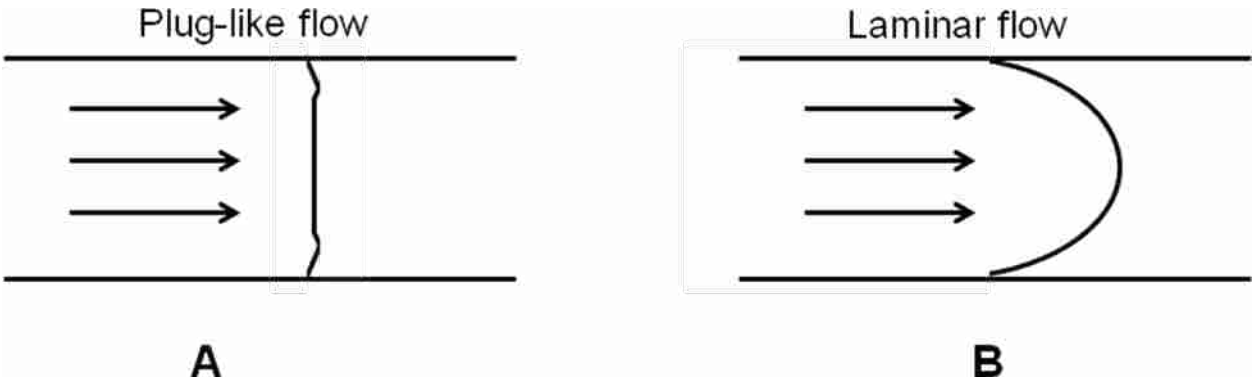


**Figure 1.2.** Flow profiles generated by (a) EOF, and (b) pressure.

### 1.2.3 Operation of μCE devices

The basic operations performed in μCE are sample injection, separation and detection. The fundamentals of these basic steps employed in microdevices are discussed below.

#### 1.2.3.1 Injection

Reproducible introduction of sample into the separation channel is an essential requirement for analysis in microfluidic devices.[52] The sample plug must be distinct because sample leaking into the separation channel after injection will cause band-broadening and result in poor separation efficiency.[53,54] Many configurations or channel geometries have been used to facilitate injection

in microdevices. The most common configurations are the simple cross (Figure 1.3A) and offset T (Figure 1.3B). The offset T configuration is used to inject a larger volume of sample than simple cross devices.[55] Two methods commonly used for sample introduction in microdevices are electrokinetic and hydrodynamic injection, with electrokinetic being the most common method. With conventional CE hydrodynamic injection is more widely used.[56]

Electrokinetic injection involves the manipulation of voltages between the injection and separation channels such that a defined sample plug at the intersection between these channels is moved into the separation channel. The popularity of this method relies on its simplicity and flexibility since no added equipment is needed.[54,57] However, this technique is prone to bias in favor of analytes with higher mobility, resulting in reduced loading of low-mobility components.[52,58] Another problem sometimes encountered is the leakage of sample into the separation channel, which can cause peak tailing and decreased resolution.

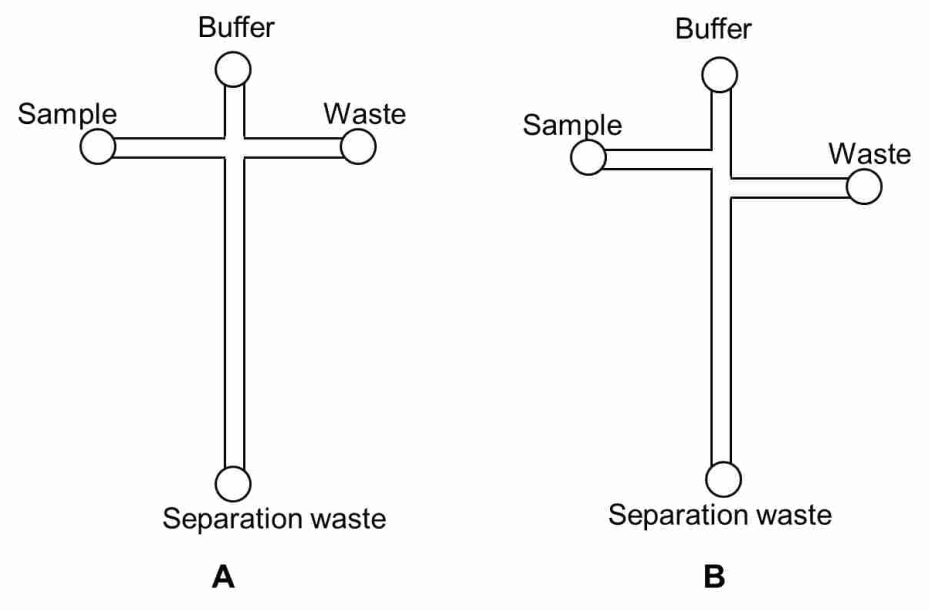


**Figure 1.3.** Schematic designs for μCE. (a) Simple cross. (b) Offset T.

Samples can be injected electrokinetically by either the "float", "pinched" or "gated" techniques. The float technique was the original approach employed for sample injection in microdevices.[59] In this technique sample is injected by application of voltage only between the sample and waste reservoirs (Fig. 1.3) while the other two reservoirs are floated. For separation, the sample and waste reservoirs are floated while voltage is applied between the buffer and separation waste reservoirs. Because this technique was prone to sample leakage into the separation channel, resulting in poor resolution and tailing, the pinched and gated modes were explored.[52, 59]

Pinched injection is the major technique used because it delivers discrete sample plugs into the separation channel. For pinched injection, voltage is applied to the sample waste reservoir while the sample reservoir as well as the reservoirs at each end of the separation channel are grounded (Figure 1.4A). This ensures that the sample does not migrate into the cross channel as it moves through the intersection to the waste reservoir. Then, application of voltage across the separation channel (Figure 1.4B) transfers the sample from the intersection into the separation channel for analysis. Sample leakage into the separation channel is prevented by simultaneous application of voltages to the sample and sample waste reservoirs to pull back excess sample towards these reservoirs.[55]

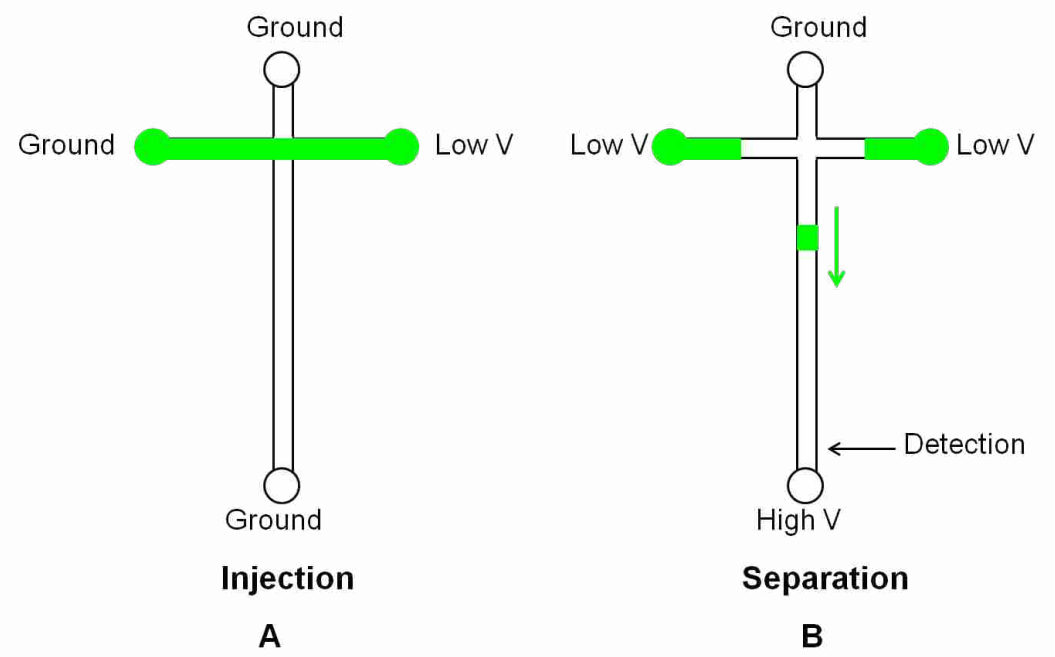


**Figure 1.4.** Schematic representation of "pinched" injection. (a) Injection. (b) Separation.

In gated injection the sample and buffer reservoirs in Figure 1.3 are interchanged such that with the application of voltage the sample flows in an L-pattern from the sample reservoir to the waste reservoir (Fig. 1.5A). Simultaneously, buffer from the buffer reservoir flows to the separation waste to minimize sample leakage. Injection of sample is performed by momentarily turning off the voltage between the buffer and separation waste reservoirs to allow a sample plug to be transferred into the separation channel (Fig. 1.5B). The voltage set-up is then switched back to the original mode for separation (Fig. 1.5C).[60] The volume of sample injected depends on the injection time, which is advantageous in that the injected volume of sample can be varied from run to run, unlike in "pinched" injection.[53] However, sample mobility bias in this method is greater than for pinched injection.[61]

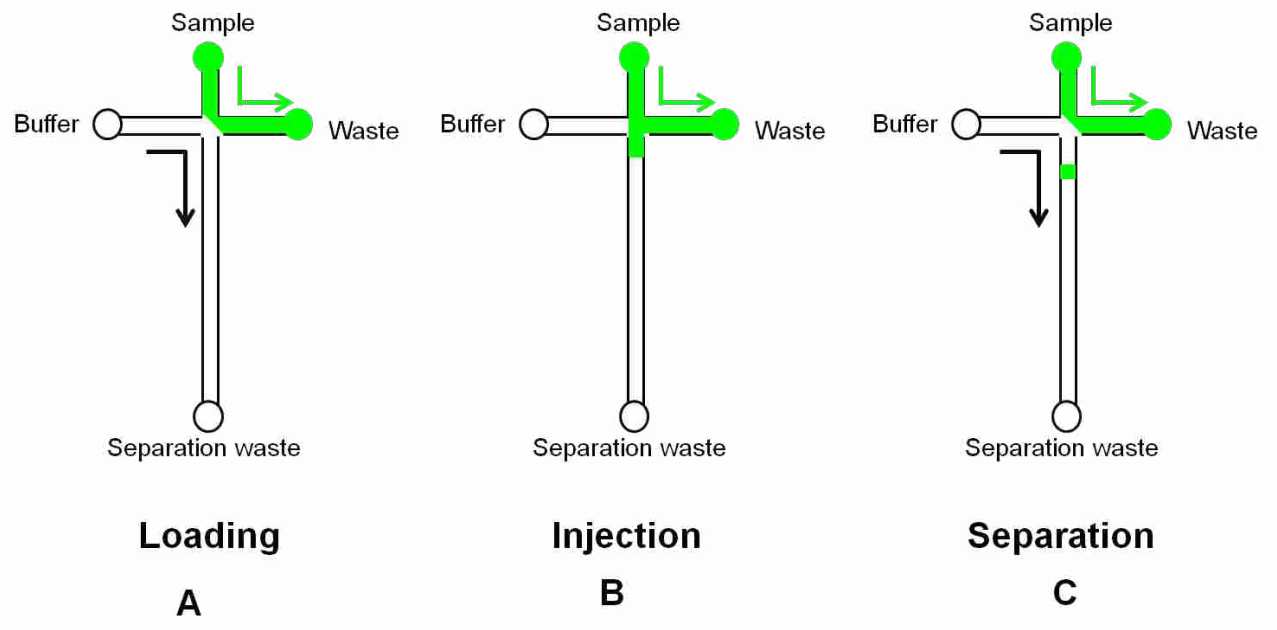


**Figure 1.5.** Schematic representation of "gated" injection. a) Sample loading. b) Injection of sample into separation channel. c) Separation of sample.

Hydrodynamic injection can be accomplished by the application of pressure or vacuum. The main advantage offered by hydrodynamic injection is the lack of injection bias commonly encountered with electrokinetic injection, which is the main reason it is commonly used in conventional capillary electrophoresis. However, hydrodynamic injection in microfluidic systems requires a more complex set-up, which may include external or integrated pumps such as ones involving membranes.[52,58] Various mechanisms that have been used for hydrodynamic injection include hydrostatic pressure, from unequal filling heights for the sample and sample waste reservoirs,[62] syringe pumps[52] and pneumatic valves.[61]

### 1.2.3.2 µCE modes

All of the electrophoresis modes described here that have been demonstrated in microfluidic devices were originally developed for regular capillary electrophoresis. Free solution

electrophoresis is the most common method and is discussed in Section 1.2.2 above. In addition to free solution electrophoresis, other variants are also employed for specific purposes as discussed below.

Gel electrophoresis uses a sieving matrix to enhance fractionation. The resolution and reproducibility of this method is better than for free solution electrophoresis.[63] The most common matrix employed is polyacrylamide, usually in the linear or cross-linked form.[64] Linear polyacrylamide is easy to use and can be replaced after each run for lower viscosity formulations, which improves run-to-run reproducibility. However, linear polyacrylamide has lower resolving power than cross-linked polyacrylamide.[65] The main difficulty encountered with *in situ* polymerization of cross-linked polyacrylamide is precise control of conditions to avoid polymerization in other locations of the channel.[66] Addition of SDS to the matrix can enable size-based protein separation.[67]

A hybrid of chromatography and electrophoresis, capillary electrochromatography (CEC) has a mobile phase moved by EOF, with separation based on both electrophoretic mobility and interaction with a chromatographic stationary phase. Compared to free solution electrophoresis, a better separation efficiency is obtained for both charged and uncharged species since the stationary phases used provide additional interaction for uncharged molecules.[68,69] CEC benefits from reduced zone broadening compared to HPLC because of plug-like flow.[68,70] CEC is well suited for miniaturized formats, and the designs of the microfluidic devices used are similar to those for μCE. Jacobson et al.[71] first reported CEC in microchips using an open channel coated with octadecylsilane as stationary phase. Other stationary phases now used include coated silica

beads,[72] coated microfabricated column structures[69, 73] and polymer monoliths.[74] With porous polymer monoliths different monomers can be selected to achieve a specific type of separation.[75] For example, EOF can be tailored by copolymerization of a negatively or positively charged monomer,[74,76] although even neutral monoliths can exhibit EOF despite the absence of fixed charges.[77]

#### 1.2.3.3 Detection

Various detection methods have been employed in microfluidic systems including optical and electrochemical detection, and mass spectrometry. Some of the methods require conjugation of the analyte to enable detection while other methods are label-free.

Optical detection methods are most commonly employed in microdevices because they have low detection limits, are isolated from the fluid and can be used to monitor a wide variety of compounds.[78] Several approaches to optical detection are currently being implemented in microfluidic devices; these are label-based (such as fluorescence and chemiluminescence) or label free (such as UV absorbance).

Laser-induced fluorescence is the most frequently used optical method in microfluidic systems because of its low detection limits.[79] However, samples that do not fluoresce naturally need to be derivatized, often with variants of either fluorescein or rhodamine, which fluoresce in the green and red regions of the spectrum, respectively.[79] In many instances the optics for detection in microfluidics are external to the chip itself. For LIF a laser is used for excitation and a photomultiplier or CCD is used for detection (Fig. 1.6.).[80, 81] While label-based methods require

time consuming sample derivatization, the detection limits of LIF are typically better than for label-free methods.

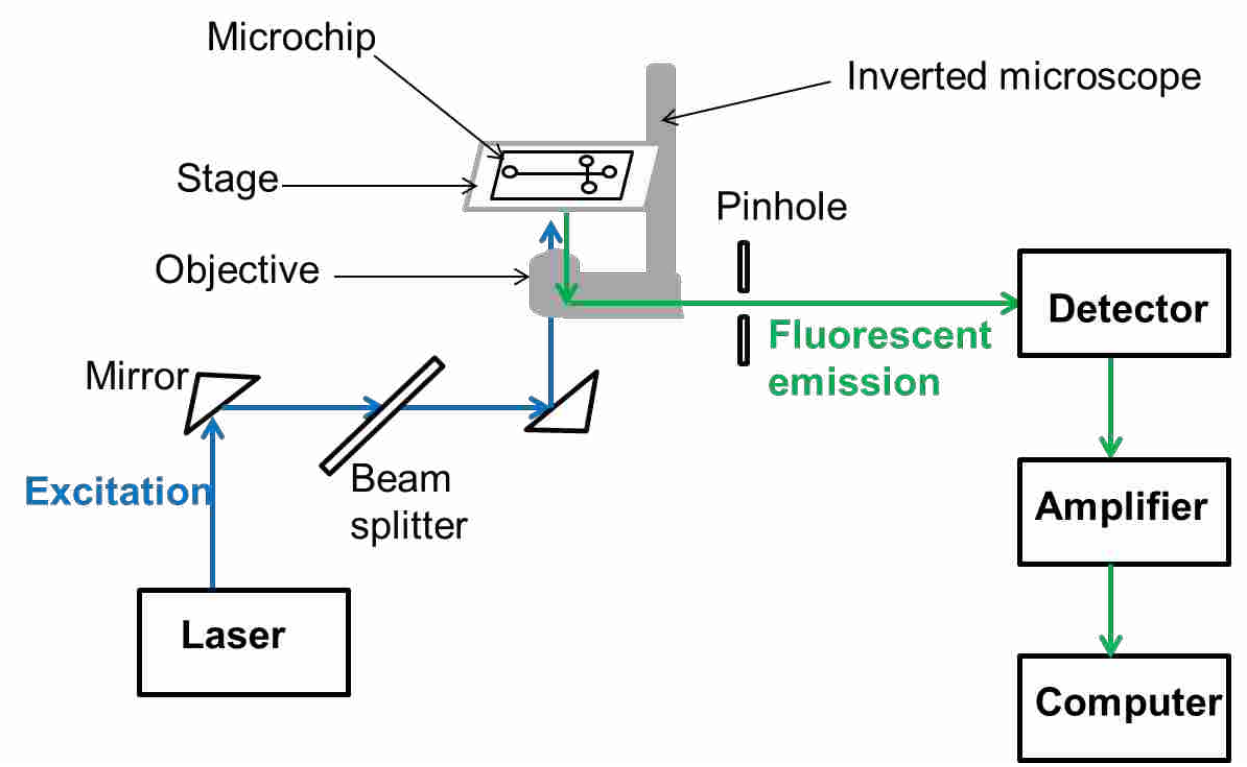


**Figure 1.6.** Schematic of a laser-induced fluorescence system for μCE detection.

Chemiluminescence (CL) is based on the production of light through a chemical reaction or when a reaction product transfers its energy to another molecule that then emits light.[82] CL detection has the advantage of not requiring an excitation source that raises background; however, very sensitive detectors are required.

UV absorbance is a label-free method commonly used in HPLC and electrophoresis systems. However, its sensitivity is reduced by the short optical path lengths commonly encountered in microfluidic channels.[43] Both off- and on-chip UV absorbance formats have been shown in

microdevices. The off-chip format is more commonly employed because it avoids complications of fabrication of integrated systems. In the on-chip format, a detection cell which measures absorbance along the plane of the device is used, which increases the pathlength and results in improved sensitivity.[43]

Native UV-excited fluorescence is a label-free detection method that typically entails excitation between 210 and 325 nm.[43, 83] This method, which requires a UV excitation source and a detection system, is not commonly employed in microfluidic systems. Its sensitivity is usually inferior to visible LIF.[83] The devices used with this detection method must be transparent to UV light; acceptable materials include quartz and fused silica, as many glass and plastic materials are not UV transparent.[43]

Electrochemical detectors are increasingly being used because they can be miniaturized without reducing sensitivity.[84] Conductivity, amperometry and potentiometry are the most commonly used electrochemical detection methods in microfluidics. Conductivity detection takes advantage of the conductivity difference between the background electrolyte in solution and the analyte.[85] Two modes have been implemented in microfluidic devices. In the contact conductivity mode, the detection electrodes are in direct contact with fluid inside the channel.[86] With contactless conductivity, the electrodes are isolated from the solutions in the device, avoiding issues such as electrode fouling and bubble formation.[87, 88] Amperometric detection relies on the electrical current produced from the oxidation or reduction of a species by a voltage applied between a reference and a working electrode.[89] This method is advantageous in that the electrodes can be fabricated by photolithographic processes within the microfluidic device.[90] In potentiometric

methods the potential of an ion-selective electrode relative to a reference electrode is probed. The resulting charge separation that occurs generates a potential between the working and reference electrodes that depends on the type of ion and its concentration.[89] As for amperometric detection, microfabrication technologies can be used to integrate potentiometric electrodes in microfluidic devices.[91-93]

Interfacing microfluidics with MS detection produces valuable data, enabling discrimination based on small differences in mass.[94,95] ESI and matrix-assisted laser desorption/ionization (MALDI) are two ionization methods for interfacing microfluidic chips with MS. ESI-MS[76, 96, 97] is the more common approach for coupling microdevices to MS, and these systems are simpler but less suitable for parallel analysis, compared to MALDI-MS.[95]

## 1.3 ANALYSIS OF CANCER BIOMARKERS

### 1.3.1 Introduction

Biomarkers are measurable molecules that can indicate a difference between normal and disease states, or therapeutic response.[98,99] An ideal biomarker should be easy to measure in a non-invasive manner and with high sensitivity and specificity.[98] Cancer biomarkers can be obtained from tissue samples or body fluids and play a key role in early detection and treatment. Considerable research has focused on the discovery of cancer biomarkers in body fluids. Though single biomarkers have been useful for screening, diagnosis and prognosis, more reliable results are obtained with a panel of biomarkers.[100] Cancer biomarkers can be proteins, nucleic acids, peptides, carbohydrates, or other metabolites. However, all of the FDA approved biomarkers are

proteins, and protein markers are considered to be more useful than other markers since protein molecules directly influence molecular pathways in cells.[101,102]

### 1.3.2 Protein biomarkers

Of the numerous proteins proposed as cancer biomarkers, only those shown in Table 1.1 have been approved by the FDA.[103] Their sensitivities, specificities and threshold values are shown in the table. The specificity of these biomarkers is reasonable (70-98%) but their sensitivity is somewhat worse (40-96%), which is one of the reasons why better diagnosis is provided by a combination of biomarkers. The cut off concentration (above which a positive diagnosis is made) for most of the biomarkers is low, below 20 ng/mL. Therefore, improved sensitivity will be obtained if the biomarkers are concentrated prior to detection. Here, I focus on five protein biomarkers that I have studied: alpha-fetoprotein (AFP), carcinoembryonic antigen (CEA), heat shock protein 90 (HSP90), thymidine kinase 1 (TK1), and cytochrome c.

AFP is a diagnostic marker for hepatocellular carcinoma (HCC). AFP is a 67 kDa glycoprotein which is present in high levels in fetal sera.[104] Its concentration decreases to trace levels soon after birth; therefore, raised AFP levels in adult serum usually indicate a disease state. AFP concentrations above 20 ng/mL are indicative of HCC, with reported sensitivity between 50 and 85%, and specificity between 70 and 90%.[105] Recent studies have shown that AFP concentrations can also be used to predict the outcome for HCC treatment. Patients with elevated levels of AFP who were treated with sorafenib and showed >20% decrease in AFP concentration within 8 weeks of treatment had improved survival and lowered disease progression than those that did not show a decrease in AFP concentration.[103, 106]

**Table 1.1** Sensitivities and specificities for the nine FDA approved cancer biomarkers.[103] (NA – not available; SPIgR– secreted chain of polymeric immunoglobulin receptor).

| Marker | Disease | Cut off | Sensitivity | Specificity | Reference |
|---|---|---|---|---|---|
| CEA | malignant pleural effusion | NA | 57.5% | 78.6% | 107 |
| CEA | peritoneal cancer dissemination | 0.5 ng/mL | 75.8% | 90.8% | 108 |
| Her-2/neu | stage IV breast cancer | 15 ng/mL | 40% | 98% | 109 |
| Bladder Tumor Antigen | urothelial cell carcinoma | NA | 52.8% | 70% | 110 |
| Thyroglobulin | thyroid cancer metastasis | 2.3 ng/mL | 74.5% | 95% | 111 |
| Alpha-fetoprotein | hepatocellular carcinoma | 20 ng/mL | 50% | 70% | 105 |
| PSA | prostate cancer | 4.0 ng/mL | 46% | 91% | 112 |
| CA 125 | ovarian cancer | 41U/mL | 62% | 98% | 113 |
| CA 19.9 | pancreatic cancer | NA | 75% | 80% | 114 |
| CA 15.3 | breast cancer | 40 U/mL | 58.2% | 96% | 115 |
| Leptin, prolactin, osteopontin, and IGF-II | ovarian cancer | NA | 95% | 95% | 116 |
| CD98, fascin, sPIgR, and 14-3-3 eta | lung cancer | NA | 96% | 77% | 117 |

CEA is a 180 kDa glycoprotein that is overexpressed in colorectal and other epithelial cancers, and is also useful in predicting recurrence of these cancers.[118-120] It is produced by the fetal gut but its level decreases in adults, and it functions as a cell adhesion molecule.[121] The sensitivity of CEA in predicting peritoneal cancer at a cutoff level of 0.5 ng/mL was found to be 76% while the specificity was 91% which is among the best of the biomarkers in Table 1.1. Apart from epithelial tumors, CEA level is also increased in smokers, and people with pancreatitis and liver disease.[119]

Another biomarker of interest is HSP90, a 90 kDa molecular chaperone that oversees the proper folding, stability and maturation of newly formed proteins.[122] Many HSP90 clients are proteins whose mutation or overproduction promotes cancer, making HSP90 inhibition a target in cancer therapy.[123, 124] Some of these mutated client proteins have shown a greater dependence on HSP90 than their normal counterparts,[125] and within certain drug concentration limits, inhibition of HSP90 had a greater impact on cancer cells compared to healthy cells.[126] For example, significant degradation of mutant as opposed to normal epidermal growth factor receptor, whose overexpression has been implicated in lung cancer, was seen with the administration of an HSP90 inhibitor.[125] Therefore, although HSP90 is presently not FDA approved, its elevated levels in many human cancer types and the depletion of client proteins by its inhibition indicate potential utility for diagnosis and the monitoring of response to treatment.[122,127]

TK1 is a cytosolic enzyme that is crucial in the deoxyribonucleotide salvage pathway involved in DNA synthesis and repair, catalyzing the phosphorylation of thymidine to its monophosphate form.[128-130] TK1 interchanges between the dimeric, low catalytic form to the tetrameric high

catalytic form depending on the presence or absence of ATP. Each subunit is ~25.5 kDa.[129] TK1 expression is closely related to cell proliferation, with low or no activity in resting cells,[131] but increased activity in the S phase coinciding with greater DNA synthesis.[129] Extensive studies have shown that TK1 is a biomarker for a variety of cancer types,[132] with serum and tissue levels correlating with the stage and aggressiveness of the cancer.[128] Inefficient cell-cycle control of TK1 by cancer cells has been implicated in the increased levels found in cancer patients.[133] Diagnostic concentrations of serum TK1 have been found to be >2 pM, with sensitivities and specificities depending on the cancer type.[134] Serum TK1 levels have also been shown to be helpful in prognostics in many cancer types including leukemia, breast, prostate and bladder cancers, as well as small-cell and non-small-cell lung carcinomas. [130,133]

Cytochrome c is a heme protein with a molecular weight of ~12 kDa that plays an important role in electron transport during respiration and the onset of apoptosis.[135,136] Though cytochrome c is not a classic cancer biomarker, elevated levels observed in some cancer patients were found to gradually decrease during treatment.[137,138] Its usefulness is thus limited to patients known to have cancer since elevated levels also occur in other non-malignant diseases.[138]

### 1.3.3 Detection methods

Though a lot of progress has been made in the early detection of cancer using biomarkers, ultimate diagnosis still requires a biopsy because elevated levels of some biomarkers also indicate other benign conditions.[99] One of the challenges encountered in the application of cancer biomarkers in clinical settings is the detection of low concentration analytes in a matrix containing many other proteins which are usually present at much higher concentrations.[103]

#### 1.3.3.1 ELISA

The most common technique used for the detection of biomarkers is enzyme-linked immunosorbent assay (ELISA). In this method a monoclonal antibody immobilized on a solid surface is used to capture a specific biomarker from a biological fluid. An enzyme-conjugated or fluorescently labeled secondary antibody is then complexed to the biomarker via a different site from the first antibody to generate a measurable signal. This technique is commonly referred to as sandwich ELISA because the antigen is trapped between two antibodies.[100,139] This format has good throughput and reproducibility but is not desirable for parallel detection of multiple biomarkers.[140] Further challenges with ELISA-based methods are the limited availability of high quality antibodies and lengthy analysis times.[101,141] A microarray ELISA format provides high throughput multiplex biomarker analysis, which is advantageous for early detection of cancer.[99,100] In the microarray format hundreds of monoclonal antibodies are spotted in an ordered manner on a surface to perform an array of assays. This platform presents a cost-effective method for high throughput screening of multiple proteins.[142] The microarray format, however, is susceptible to reagent cross-reactivity resulting in errors due to reduced specificity; therefore, its implementation in a microchip format requires complex designs to minimize these errors.[142]

#### 1.3.3.2 Proteomic methods

The availability of high-resolution MS has led to progress in proteomics[143] and the detection of protein biomarkers. Traditional proteomics methods that have been used for cancer markers include two-dimensional polycarylamide gel electrophoresis (2D-PAGE) with MS detection,[144] capillary electrophoresis-MS[145] and liquid chromatography coupled to hyphenated MS.[146,147]

Capillary electrophoresis is a powerful separation method and its combination with MS has been shown to be useful for the analysis of intact proteins.[145] 2D-PAGE with MS detection is more suitable for biomarker discovery than routine detection of biomarkers,[144] while LC-MS/MS can be applied to both biomarker discovery and routine detection of biomarkers.[102] However, LC-MS cannot be used for POC detection.[99]

#### 1.3.3.3 Microfluidc methods

The significance of microfluidic technology for biomarker analysis in POC settings has been demonstrated in several publications. Wang et al.[148] developed a microchip sandwich ELISA technique for POC detection of the ovarian cancer biomarker, human epididymis protein 4 (HE4) in urine. Colorimetric detection was accomplished with a cell phone/camera, and analysis with an integrated mobile application allowed reporting of the pixel value for each channel. The method successfully differentiated ovarian cancer patients from the control group. An integrated PMMA microfluidic device with a monolithic affinity column coupled to μCE was used for the extraction and quantification of cancer biomarkers in human blood serum. The microchip was designed with multiple reservoirs to enable automated transfer of the different fluids required for loading, rinsing, eluting and separating the sample.[149] Simultaneous detection of four biomarkers in the serum of oral cancer patients was achieved with a microfluidic array consisting of immobilized antibody-functionalized magnetic beads. This method detected oral cancer with a sensitivity of 89% and a specificity of 98%.[150]

## 1.4 SAMPLE PREPARATION METHODS

### 1.4.1 Overview

Conventional sample preparation methods involving filtration, extraction, enrichment and labeling are time consuming and can lead to sample loss before analysis.[151] Filtration is a size-based method wherein small molecule contaminants are separated from the sample with the use of filter membranes as in ultrafiltration and gel filtration. Alternatively, centrifugation or dialysis can be used. Classical sample extraction techniques are liquid-liquid extraction (LLE) or solvent extraction and solid phase extraction (SPE). In LLE, a separation funnel is used to transfer a compound from one solvent into a second immiscible solvent. SPE, on the other hand, employs the adsorptive power of a stationary phase to retain components from solution. The most common methods for concentrating samples involve filtration with a membrane, SPE and dialysis. Stacking and focusing techniques are also commonly used for preconcentration prior to electrophoresis. For sample labeling, the sample is mixed with an appropriate dye and incubated for a certain period of time, usually at room temperature, before analysis. Though the integration of these sample preparation methods in microfluidic devices can be challenging, significant progress has been made.[152] Advantages of microfluidic sample preparation include automation and integration, which facilitate assays such as for point-of-care usage.[153]

### 1.4.2 Extraction and purification

Solid phase extraction is a useful purification and enrichment method wherein analytes are first retained on a solid support and then are subsequently eluted in a concentrated form.[154] SPE is a chromatographic technique which avoids many of the problems encountered in liquid-liquid extraction such as incomplete phase separations and reduced sample recoveries.[155] In this

technique, which is typically carried out in a cartridge, the sample is loaded on a stationary phase and the unattached sample is washed away. A suitable solvent is then used to elute the extracted analyte.[155] Implementation of this procedure in microfluidic systems is facilitated by the fact that it can be integrated with other processes like thermal cycling, separation and detection.[156] The most common SPE modes in microfluidics are reversed-phase, which works for non-polar to moderately polar compounds, and affinity, which provides greater specificity via interaction between target analyte and a complementary compound such as an antibody bound on the solid phase.

In reversed-phase extraction the stationary phase is non-polar while the analyte is dissolved in a polar matrix. Less polar analytes are attracted to the stationary phase due to chemical similarities. Elution of the sorbed analyte is achieved through a non-polar solvent which is capable of displacing the analyte from the stationary phase.[157] Silica-based columns (beads, particles, porous silica sol-gel, and bead/sol-gel hybrids) are the most common supports used for reversed-phase SPE and they have been shown to be both reproducible and reliable.[158] The hydrophilic silanol groups at the surface of the silica are generally coupled to hydrophobic alkyl or aryl functional groups by reaction with silanes, with C8 and C18 being some of the most widely used coatings.[159, 160] The use of monolithic columns is increasing, especially in the microchip format, because they can be easily prepared by UV polymerization without a need for forming retaining structures like frits.[76, 161] In addition, the porosity and surface area of monoliths can be tuned by varying the monomer and porogen composition.[74] Appropriate hydrophobicity for reversed-phase SPE is provided by monoliths made of butyl-, lauryl-, octadecyl-, or 2-hydroxyethyl methacrylates.[11, 154, 162, 163]

Affinity extraction techniques which are based on the strong interaction between an analyte and a receptor attached to the column are highly specific. In this method a ligand with high affinity for the analyte of interest is immobilized on the stationary phase and the sample is passed through the column. Molecular recognition of the analyte by the ligand then enables its extraction while the other components are not retained. Elution of the sample is achieved by changing the pH, temperature or polarity of the buffer, or by the use of a specific component which binds to the ligand more strongly than the analyte.[164] Affinity extraction is frequently used for sample pretreatment to isolate a specific component before analysis. This technique also purifies and concentrates that component. A wide variety of ligands have been implemented in both conventional and microfluidic formats. Anti-fluorescein isothiocyanate (FITC) was immobilized on monoliths in PMMA microdevices and used to selectively extract FITC-tagged proteins, followed by elution and μCE separation.[165] Biotinylated PCR products were selectively extracted on a streptavidin-modified bed fabricated in a PMMA microdevice; the purified material was subsequently eluted by thermal denaturation and analyzed by μCE.[166] Aptamers, which are short nucleic acid sequences that bind to target molecules with high specificity, are alternatives to antibody-based extraction. A PDMS-glass multilayer microfluidic device packed with aptamer-functionalized microbeads was used to selectivity extract and concentrate arginine vasopressin, with its temperature-dependent binding and release controlled by an integrated microheater and temperature sensor.[167] The binding of target nucleic acid sequences to their complementary immobilized probe nucleic acid molecules has also been investigated in microfluidic devices, particularly for DNA microarrays.[168]

### 1.4.3 Preconcentration

Preconcentration is frequently employed in sample analysis for the determination of low concentration analytes.[169] The simplest preconcentration method is filtration where the sample is passed through a membrane, usually made of cellulose, and the components separate on the basis of size. Another technique, LLE, is a straightforward method of sample preconcentration which requires two immiscible solvents. However, a large amount of solvent is required in this technique and it is gradually being replaced by newer variants such as homogeneous LLE and dispersive liquid-liquid microextraction. Other preconcentration techniques include chromatography-based SPE, discussed in Section 1.4.2, and methods based on electrophoretic mobility, like stacking or isotachophoresis. The volume of loaded sample in chromatography-based methods does not depend on the volume of the column, so large volumes can be loaded for improved enrichment.[170] Samples can be concentrated prior to (off-line) or after (on-line) injection. The on-line format is commonly used because it has a higher concentration efficiency than the off-line format.[171] Various on-line sample preconcentration techniques, utilizing analyte characteristics such as charge, affinity, mobility and size, have been applied to overcome the limited concentration detectability resulting from the short optical path lengths in microfluidic channels. An additional benefit of concentrating samples prior to analysis is improved detection of low concentration analytes typically encountered in real-world samples.[172]

In isotachophoresis (ITP) a leading electrolyte (the fastest moving ion), sample and trailing electrolyte (the slowest moving ion) are injected in that order into a separation column. The sample components separate according to their mobilities, with the fastest ion directly behind the leading electrolyte and the slowest near the trailing electrolyte, and a constant speed for all ions

in the sample zone is maintained. Advantages of ITP are large preconcentration factors and ease of coupling to separation techniques such as capillary zone electrophoresis, isoelectric focusing and gel electrophoresis.[173] However, its execution is complicated by the fact that it requires rigorous selection of buffers and mobility markers for each analyte.[174] For microchip ITP determination of bacterial urinary tract infections, 16S rRNA was monitored in bacterial lysates obtained from patient urine samples using molecular beacons. The combination of extraction, focusing, and detection of 16S rRNA was realized in a single step and clinically significant concentrations of *E. coli* were detected.[175]

Compared to free solution techniques, enrichment based on exclusion methods such as nanoporous filters generally offers a simpler analysis setup and can be employed in both electrophoretic and chromatographic methods. The filters, usually nanoporous monoliths or membranes, are integrated into the column and their properties enable selective trapping of certain components.[151] In the use of membranes for preconcentration analytes are selectively transported across the membrane.[176] Most of the membranes used in electrophoretic methods are anionic enabling ion-selectivity. With the application of voltage across these charged membranes analytes of a specific charge are concentrated on one side of the membrane and subsequently analyzed. Hydrogel membranes made from acrylic monomers can act as either neutral or charged nanoporous filters whose pore size and mechanical properties can be controlled by varying the polymerization conditions. Hatch et al.[177] integrated two neutral acrylic polymer hydrogel membranes in a glass device, one for size-based preconcentration and the other as a separation matrix for gel electrophoresis. Negatively charged acrylamide membranes can be formed by addition of an ionizable co-monomer, such as 2-acrylamido-2-methylpropanesulfonic acid

(AMPS), enabling the membrane to be ion-selective.[178] Chun et al.[178] showed preconcentration of anions with an ion-conductive membrane made entirely of crosslinked AMPS in glass microchips. Other membranes that have been employed include polycarbonate, titania, and Nafion. Polycarbonate nanopore membranes were integrated in PDMS microchips and used to concentrate labeled serum albumin.[179] Titania membranes fabricated at the intersection of two fluidic channels on a microfluidic device were used to electrokinetically enrich 2,7-dichlorofluorescein.[180] Proteins were also concentrated in a PDMS-glass microfluidic device having an integrated Nafion strip.[181]

### 1.4.4 Fluorescent labeling

Many samples do not fluoresce naturally and have to be derivatized to benefit from the low limits of detection of LIF. The fluorescent dyes used are usually small organic molecules with reactive groups that attach to specific sites on the analyte.[182] For labeling, a sample is mixed with the fluorescent dye and left to react between 1 – 24 h at room temperature.[183,184] The unconjugated dye is then removed before analysis.[183] Efficient labeling is obtained with original sample concentrations between 1 – 10 mg/mL,[185] though lower concentrations could be equally labeled with higher dye-to-sample molar ratios. One disadvantage of labeling samples at high concentration is that not all of the sample can be used and the rest will be wasted.

#### 1.4.4.1 On-chip labeling

On-chip labeling was developed to address some of the issues of conventional labeling such as lengthy label times and the necessity to label high concentrations of samples. In on-chip labeling lower sample concentrations are possible and the labeled samples are used immediately.

Moreover, there is a significant reduction in the time required for labeling. In addition, integration of labeling into microfluidic devices increases automation. On-chip labeling has been achieved both in pre-column and post-column formats. Pre-column labeling was initially shown in a glass microchip for on-chip labeling of amino acids with subsequent μCE and LIF detection.[186] To carry out parallel analysis of multiple unlabeled samples, a multilayer PMMA microfluidic device with integrated on-chip labeling and electrophoretic separation was demonstrated wherein one fluorescent label reservoir allowed parallel labeling and analysis of up to eight samples in different channels.[187] A long serpentine reaction channel was employed for online derivatization of reduced glutathione with ThioGlo-1. The system integrated derivatization, injection, separation and detection, enabling the study of glutathione reductase kinetics by continuously monitoring the concentration of the generated reduced glutathione.[188]

Post-column methods require the placement of an additional connection after separation but before detection. A cross design glass microchip with a post-column reactor positioned between the separation channel and the detection point was fabricated and used for derivatization of separated amino acids.[189] A similar post-column setup was employed to continuously monitor the on-chip release of neurotransmitters from immobilized PC 12 cells in a multilayer PDMS-glass device incorporating a cell reactor, continuous flow sampling and electrophoresis, with post-separation derivatization for fluorescent detection.[190] Though on-chip labeling provides automation and faster sample derivatization compared to off-chip labeling a major limitation is the presence of unreacted dye which in high concentration could conceal some analyte peaks. Separation of unreacted dye from sample prior to detection is therefore necessary. Another limitation is that the dynamic labeling usually employed has a lower labeling efficiency for more

dilute samples due to the elimination of incubation time. This could be alleviated by the incorporation of micromixers or by use of a solid support which allows more interaction between the sample and fluorescent dyes.

### 1.4.5 Integration

Integration is one of the key advantages of miniaturization,[191] and can facilitate assays such as for point-of-care usage.[153] Indeed, the objective of lab-on-a-chip (LOC) systems is to integrate all laboratory processes into a single device so that sample pre-treatment, chemical reaction, separation, detection and data analysis operations can be carried out in an automated manner.[192] Though important progress toward this goal has been made, most microfluidic systems typically perform only one or a few select steps on-chip.[193] The integration of complex functions on-chip can limit sample loss, reduce analysis time, and enable new detection methods for microfluidic analyses, as an example.[152,194] The extent of integration can be anywhere between a disposable chip in external equipment to complete integration of all laboratory functions.[195] Components such as pumps, valves and mixers, which enable functions such as sample preparation, separation, etc., are integral to creating LOC systems. Remaining challenges in making fully integrated LOC systems are the complexity of combining several different components in a single device[196] and interfacing with the macroscopic world.[197] Some examples of integrated microfluidic systems are discussed below.

Microfluidic systems that integrate sample preparation methods with separation offer automated analysis. Magnetic bead based immunoassays for immunoglobulin and prostate specific antigen were demonstrated in a multilayer PDMS-glass microfluidic device. In this technique, automated

parallel loading of capture antibody, wash buffer, antigen and magnetic bead-coated secondary antibody into patterned reaction wells was performed with the aid of integrated valves and pumps.[198] Both reversed-phase and affinity SPE modules have been integrated into microdevices. C18-coated magnetic particles have been used for in-line SPE-μCE to analyze mixtures of parabens and fluorescent dyes. The magnetic particles were trapped at the intersection of an offset-T microchip, and an additional side channel was connected to a syringe pump for elution.[199] An integrated PMMA microfluidic device with a monolithic affinity column coupled to μCE was used for the extraction and quantification of cancer biomarkers in human blood serum. The chip was designed with multiple reservoirs to enable uninterrupted movement of the different fluids required for loading, rinsing, eluting and separating the sample.[149] Immunoglobulin E and nuclear factor-κB were extracted and concentrated with an aptamer-functionalized size-exclusion membrane in an integrated glass microfluidic device that also enabled mixing and buffer exchange. The samples were eluted from the preconcentration membrane directly into a separation channel for gel electrophoresis and LIF detection.[200] Apart from increasing the level of automation, integration of sample preparation reduces cross contamination and decreases sample loss which occurs when transferring off-chip prepared samples to microdevices. However, a major difficulty in integration of sample preparation methods is coupling with analysis in a manner that does not decrease separation efficiency.

Though many advantages of integrated microfluidic systems have been demonstrated, as discussed above, they also have some limitations. The main disadvantage in integrated systems is the increase in complexity of design and analysis. For example, stacking techniques are commonly used to couple sample preconcentration with μCE because of their compatibility.

However, the execution of these techniques often requires complicated designs which render separation very challenging. In addition, the integration of components such as valves and pumps for efficient fluid manipulation requires complicated fabrication and operation processes. To address these challenges components with low levels of fabrication complexity should be integrated in microdevices and used to simultaneously perform a variety of sample preparation techniques such as analyte extraction, purification, concentration and derivatization.

## 1.5 OVERVIEW OF DISSERTATION

The analysis of specific analytes in complex biological samples requires purification and concentration of the desired analyte for improved sensitivity as discussed in Section 1.4. LIF detection offers low detection limits but conjugation with fluorescence dyes is required for samples to be detected by LIF. Most sample preparation methods are time consuming; for example, conventional sample labeling typically requires up to 24 h. Integration of these processes on-chip reduces the time required for overall analysis and improves the level of assay automation. In my dissertation, I describe efforts to develop new approaches for the integration of sample pretreatment with μCE. A brief overview of microfluidic materials, fabrication techniques, μCE and sample preparation methods has been given in this chapter.

In Chapter 2, I present protocols for the fabrication of polymeric microfluidic devices and affinity columns. I have adapted fabrication methods for hot embossing and thermal bonding that were developed by previous members of Prof. Woolley's research group. Affinity columns were prepared in these devices by *in situ* photopolymerization and used for protein extraction. Monomers used for the preparation of affinity columns had reactive epoxide groups which

allowed for functionalization with antibodies so that specific proteins could be extracted from a complex mixture. I also present protocols for fluorescent labeling of proteins and μCE. Experiments on the extraction of HSP90 with an anti-HSP90 functionalized column show specificity towards HSP90.

Chapter 3 focuses on the *in situ* preparation of ion-permeable membranes for on-chip preconcentration of proteins prior to μCE. The negatively charged membrane made from acrylamide, N,N'-methylene-bisacrylamide and 2-(acrylamido)-2-methylpropanesulfonate was photopolymerized near the injection intersection. Proteins excluded from this membrane based on both size and charge concentrated at the injection intersection and were subsequently separated by μCE. Forty-fold enrichment of BSA was achieved with 4 min of preconcentration while >10-fold enrichment was obtained for the biomarkers AFP and HSP90 with just 1 min of preconcentration.

In Chapter 4, I demonstrate the use of monolithic columns for on-chip preconcentration, fluorescence labeling and purification. Sample enrichment by reversed-phase SPE was realized with a butyl methacrylate monolith fabricated in cyclic olefin copolymer microdevices. Samples retained on the monolithic column were labeled with either Alexa Fluor 488 or Chromeo P503, and excess dye was rinsed off the column before elution. Application of this technique to HSP90 samples showed a linear relationship between eluted peak areas and sample concentration. This proves that a calibration curve can be obtained and used for quantification of analytes.

Conclusions reached from my work on the extraction of labeled proteins from affinity columns, preconcentration of proteins prior to μCE and on-chip extraction, preconcentration and derivatization of proteins are discussed in Chapter 5. Future work on the coupling of affinity with reversed phase columns for on-chip protein extraction, digestion, preconcentration, labeling and μCE with either LIF or MS detection is also discussed in Chapter 5.

## 1.6 REFERENCES


(1) Terry, S. C.; Jerman, J. H.; Angell, J. B. *IEEE Trans. Electron Devices* **1979**, *26*, 1880-1886.
(2) Reyes, D. R.; Iossifidis, D.; Auroux, P.-A.; Manz, A. *Anal. Chem.* **2002**, *74*, 2623-2636.
(3) Madou, M. J. *Fundamentals of microfabrication: the science of miniaturization*, 2nd ed.; CRC Press, 2002.
(4) Yeo, L. Y.; Chang, H.-C.; Chan, P. P. Y.; Friend, J. R. *Small* **2011**, *7*, 12-48.
(5) Effenhauser, C. S.; Bruin, G. J. M.; Paulus, A.; Ehrat, M. *Anal. Chem.* **1997**, *69*, 3451-3457.
(6) Roman, G. T.; Hlaus, T.; Bass, K. J.; Seelhammer, T. G.; Culbertson, C. T. *Anal. Chem.* **2005**, *77*, 1414-1422.
(7) Bodas, D.; Khan-Malek, C. *Microelectron. Eng.* **2006**, *83*, 1277-1279.
(8) Wang, D.; Oleschuk, R. D.; Horton, J. H. *Langmuir* **2008**, *24*, 1080-1086.
(9) Tsao, C. W.; Hromada, L.; Liu, J.; Kumar, P.; DeVoe, D. L. *Lab Chip* **2007**, *7*, 499-505.
(10) Zhang, J.; Das, C.; Fan, Z. *Microfluid. Nanofluid.* **2008**, *5*, 327-335.
(11) Liu, J.; Chen, C.-F.; Tsao, C.-W.; Chang, C.-C.; Chu, C.-C.; DeVoe, D. L. *Anal. Chem.* **2009**, *81*, 2545-2554.
(12) Faure, K.; Albert, M.; Dugas, V.; Crétier, G.; Ferrigno, R.; Morin, P.; Rocca, J.-L. *Electrophoresis* **2008**, *29*, 4948-4955.
(13) Martinez, A. W.; Phillips, S. T.; Whitesides, G. M.; Carrilho, E. *Anal. Chem.* **2009**, *82*, 3-10.
(14) Pelton, R. *TrAC, Trends Anal. Chem.* **2009**, *28*, 925-942.
(15) Nie, Z.; Deiss, F.; Liu, X.; Akbulut, O.; Whitesides, G. M. *Lab Chip* **2010**, *10*, 3163-3169.
(16) Dungchai, W.; Chailapakul, O.; Henry, C. S. *Analyst* **2011**, *136*, 77-82.
(17) Schilling, K. M.; Lepore, A. L.; Kurian, J. A.; Martinez, A. W. *Anal. Chem.* **2012**, *84*, 1579-1585.
(18) Martinez, A. W.; Phillips, S. T.; Whitesides, G. M. *Proc. Natl. Acad. Sci. U. S. A.* **2008**.
(19) Allen, P. B.; Chiu, D. T. *Anal. Chem.* **2008**, *80*, 7153-7157.
(20) Junwen, L.; Jintang, S.; Jieying, T.; Qing-An, H. *J. Microelectromech. Syst.* **2011**, *20*, 909-915.
(21) Yu, L.; Tay, F. E. H.; Xu, G.; Chen, B.; Avram, M.; Iliescu, C. *J. Phys.: Conf. Ser.* **2006**, *34*, 776.
(22) Iliescu, C.; Taylor, H.; Avram, M.; Miao, J.; Franssila, S. *Biomicrofluidics* **2012**, *6*, 016505-016516.
(23) Qin, D.; Xia, Y.; Whitesides, G. M. *Nat. Protoc.* **2010**, *5*, 491-502.
(24) Lalo, H.; Ayela, C.; Dague, E.; Vieu, C.; Haupt, K. *Lab Chip* **2010**, *10*, 1316-1318.
(25) Wang, Y.; Balowski, J.; Phillips, C.; Phillips, R.; Sims, C. E.; Allbritton, N. L. *Lab Chip* **2011**, *11*, 3089-3097.
(26) Abdelgawad, M.; Watson, M. W. L.; Young, E. W. K.; Mudrik, J. M.; Ungrin, M. D.; Wheeler, A. R. *Lab Chip* **2008**, *8*, 1379-1385.
(27) Kelly, R. T.; Woolley, A. T. *Anal. Chem.* **2003**, *75*, 1941-1945.
(28) Choi, S.; Kim, D.; Kwon, T. *Microsyst. Technol.* **2009**, *15*, 309-316.
(29) Kim, D. S.; Lee, S. H.; Ahn, C. H.; Lee, J. Y.; Kwon, T. H. *Lab Chip* **2006**, *6*, 794-802.
(30) Hansen, T. S.; Selmeczi, D.; Larsen, N. B. *J. Micromech. Microeng.* **2010**, *20*, 015020.

(31) Edwards, T. L.; Harper, J. C.; Polsky, R.; Lopez, D. M.; Wheeler, D. R.; Allen, A. C.; Brozik, S. M. *Biomicrofluidics* **2011**, *5*, 044115-044114.
(32) Qi, H.; Wang, X.; Chen, T.; Ma, X.; Zuo, T. *Microsyst. Technol.* **2009**, *15*, 1027-1030.
(33) Tsao, C.-W.; DeVoe, D. *Microfluid. Nanofluid.* **2009**, *6*, 1-16.
(34) Koesdjojo, M. T.; Koch, C. R.; Remcho, V. T. *Anal. Chem.* **2009**, *81*, 1652-1659.
(35) Ng, S.; Tjeung, R.; Wang, Z.; Lu, A.; Rodriguez, I.; de Rooij, N. *Microsyst. Technol.* **2008**, *14*, 753-759.
(36) Kelly, R. T.; Li, Y.; Woolley, A. T. *Anal. Chem.* **2006**, *78*, 2565-2570.
(37) Fuentes, H. V.; Woolley, A. T. *Anal. Chem.* **2008**, *80*, 333-339.
(38) Koesdjojo, M. T.; Tennico, Y. H.; Remcho, V. T. *Anal. Chem.* **2008**, *80*, 2311-2318.
(39) Tennico, Y. H.; Koesdjojo, M. T.; Kondo, S.; Mandrell, D. T.; Remcho, V. T. *Sens. Actuators, B* **2010**, *143*, 799-804.
(40) Park, T.; Song, I.-H.; Park, D. S.; You, B. H.; Murphy, M. C. *Lab Chip* **2012**, *12*, 2799-2802.
(41) Johnson, T. J.; Ross, D.; Locascio, L. E. *Anal. Chem.* **2002**, *74*, 45-51.
(42) Zhuang, Z.; Mitra, I.; Hussein, A.; Novotny, M. V.; Mechref, Y.; Jacobson, S. C. *Electrophoresis* **2011**, *32*, 246-253.
(43) Ohlsson, P. D.; Ordeig, O.; Mogensen, K. B.; Kutter, J. P. *Electrophoresis* **2009**, *30*, 4172-4178.
(44) Felhofer, J. L.; Blanes, L.; Garcia, C. D. *Electrophoresis* **2010**, *31*, 2469-2486.
(45) Henry, C. S. Microchip capillary electrophoresis: An introduction. In *Methods Mol. Biol.,* Henry, C. S., Ed. Humana Press: 2006; Vol. 339, pp 1-9.
(46) Breadmore, M. C. *J. Chromatogr. A* **2012**, *1221*, 42-55.
(47) Yang, W.; Woolley, A. T. *JALA* **2010**, *15*, 198-209.
(48) Copper, C. L. *J. Chem. Educ.* **1998**, *75*, 343.
(49) Zhang, H.; Hassanali, A. A.; Shin, Y. K.; Knight, C.; Singer, S. J. *J. Chem. Phys.* **2011**, *134*, 024705.
(50) Gilman, S. D.; Chapman, P. J. Measuring Electroosmotic Flow in Microchips and Capillaries. In *Methods Mol. Biol.,* Henry, C. S., Ed. Humana Press: 2006; Vol. 339, pp 187-201.
(51) Wang, W.; Zhou, F.; Zhao, L.; Zhang, J.-R.; Zhu, J.-J. *J. Chromatogr. A* **2007**, *1170*, 1-8.
(52) Dossi, N.; Toniolo, R.; Susmel, S.; Pizzariello, A.; Bontempelli, G. *Electrophoresis* **2010**, *31*, 2541-2547.
(53) Sinton, D.; Ren, L.; Li, D. *J. Colloid Interface Sci.* **2003**, *266*, 448-456.
(54) Chen, P.; Feng, X.; Sun, J.; Wang, Y.; Du, W.; Liu, B.-F. *Lab Chip* **2010**, *10*, 1472-1475.
(55) Yang, S.; Liu, J.; DeVoe, D. L. *Lab Chip* **2008**, *8*, 1145-1152.
(56) Shihabi, Z. K. *J. Chromatogr. A* **2005**, *1066*, 205-210.
(57) Du, W.-B.; Fang, Q.; He, Q.-H.; Fang, Z.-L. *Anal. Chem.* **2005**, *77*, 1330-1337.
(58) Price, A. K.; Culbertson, C. T. *Anal. Chem.* **2009**, *81*, 8942-8948.
(59) Chang, C.-L.; Hou, H.-H.; Fu, L.-M.; Tsai, C.-H. *Electrophoresis* **2008**, *29*, 3135-3144.
(60) Ermakov, S. V.; Jacobson, S. C.; Ramsey, J. M. *Anal. Chem.* **2000**, *72*, 3512-3517.
(61) Sun, X.; Kelly, R. T.; Danielson, W. F.; Agrawal, N.; Tang, K.; Smith, R. D. *Electrophoresis* **2011**, *32*, 1610-1618.
(62) Luo, Y.; Wu, D.; Zeng, S.; Gai, H.; Long, Z.; Shen, Z.; Dai, Z.; Qin, J.; Lin, B. *Anal. Chem.* **2006**, *78*, 6074-6080.

(63) Obubuafo, A.; Balamurugan, S.; Shadpour, H.; Spivak, D.; McCarley, R. L.; Soper, S. A. *Electrophoresis* **2008**, *29*, 3436-3445.
(64) Zhu, Z.; Lu, J. J.; Liu, S. *Anal. Chim. Acta.* **2012**, *709*, 21-31.
(65) Han, J.; Singh, A. K. *J. Chromatogr. A* **2004**, *1049*, 205-209.
(66) Brahmasandra, S. N.; Ugaz, V. M.; Burke, D. T.; Mastrangelo, C. H.; Burns, M. A. *Electrophoresis* **2001**, *22*, 300-311.
(67) Xu, Z.; Ando, T.; Nishine, T.; Arai, A.; Hirokawa, T. *Electrophoresis* **2003**, *24*, 3821-3827.
(68) Augustin, V.; Jardy, A.; Gareil, P.; Hennion, M.-C. *J. Chromatogr. A* **2006**, *1119*, 80-87.
(69) Slentz, B. E.; Penner, N. A.; Regnier, F. E. *J. Chromatogr. A* **2002**, *948*, 225-233.
(70) Peters, E. C.; Petro, M.; Svec, F.; Fréchet, J. M. J. *Anal. Chem.* **1997**, *69*, 3646-3649.
(71) Jacobson, S. C.; Hergenroeder, R.; Koutny, L. B.; Ramsey, J. M. *Anal. Chem.* **1994**, *66*, 2369-2373.
(72) Jemere, A. B.; Oleschuk, R. D.; Harrison, D. J. *Electrophoresis* **2003**, *24*, 3018-3025.
(73) Fonverne, A.; Ricoul, F.; Demesmay, C.; Delattre, C.; Fournier, A.; Dijon, J.; Vinet, F. *Sens. Actuators, B* **2008**, *129*, 510-517.
(74) Ladner, Y.; Crétier, G.; Faure, K. *J. Chromatogr. A* **2010**, *1217*, 8001-8008.
(75) Gustafsson, O.; Mogensen, K. B.; Kutter, J. P. *Electrophoresis* **2008**, *29*, 3145-3152.
(76) Hua, Y.; Jemere, A. B.; Harrison, D. J. *J. Chromatogr. A* **2011**, *1218*, 4039-4044.
(77) Karenga, S.; El Rassi, Z. *Electrophoresis* **2010**, *31*, 3192-3199.
(78) Angelescu, D. E. *Highly Integrated Microfluidics Design*; Artech House, 2011.
(79) Myers, F. B.; Lee, L. P. *Lab Chip* **2008**, *8*, 2015-2031.
(80) Mitra, I.; Zhuang, Z.; Zhang, Y.; Yu, C.-Y.; Hammoud, Z. T.; Tang, H.; Mechref, Y.; Jacobson, S. C. *Anal. Chem.* **2012**, *84*, 3621-3627.
(81) Mainz, E. R.; Gunasekara, D. B.; Caruso, G.; Jensen, D. T.; Hulvey, M. K.; Fracassi da Silva, J. A.; Metto, E. C.; Culbertson, A. H.; Culbertson, C. T.; Lunte, S. M. *Anal. Methods* **2012**, *4*, 414-420.
(82) García-Campaña, A. M.; Lara, F. J.; Gámiz-Gracia, L.; Huertas-Pérez, J. F. *TrAC, Trends Anal. Chem.* **2009**, *28*, 973-986.
(83) Schulze, P.; Belder, D. *Anal. Bioanal. Chem.* **2009**, *393*, 515-525.
(84) Holcomb, R. E.; Kraly, J. R.; Henry, C. S. *Analyst* **2009**, *134*, 486-492.
(85) Vazquez, M.; Frankenfeld, C.; Coltro, W. K. T.; Carrilho, E.; Diamond, D.; Lunte, S. M. *Analyst* **2010**, *135*, 96-103.
(86) Šolínová, V.; Kašička, V. *J. Sep. Sci.* **2006**, *29*, 1743-1762.
(87) Baker, C. A.; Duong, C. T.; Grimley, A.; Roper, M. G. *Bioanalysis* **2009**, *1*, 967-975.
(88) Coltro, W. K. T.; Lima, R. S.; Segato, T. P.; Carrilho, E.; de Jesus, D. P.; do Lago, C. L.; da Silva, J. A. F. *Anal. Methods* **2012**, *4*, 25-33.
(89) Wu, J.; Gu, M. *J. Biomed. Opt.* **2011**, *16*, 080901-080912.
(90) Gunasekara, D. B.; Hulvey, M. K.; Lunte, S. M. *Electrophoresis* **2011**, *32*, 832-837.
(91) Ibanez-Garcia, N.; Mercader, M. B.; Mendes da Rocha, Z.; Seabra, C. A.; Góngora-Rubio, M. R.; Chamarro, J. A. *Anal. Chem.* **2006**, *78*, 2985-2992.
(92) Almeida, S. A. A.; Arasa, E.; Puyol, M.; Martinez-Cisneros, C. S.; Alonso-Chamarro, J.; Montenegro, M. C. B. S. M.; Sales, M. G. F. *Biosens. Bioelectron.* **2011**, *30*, 197-203.
(93) Jang, A.; Zou, Z.; Lee, K. K.; Ahn, C. H.; Bishop, P. L. *Talanta* **2010**, *83*, 1-8.
(94) Baker, C. A.; Roper, M. G. *Anal. Chem.* **2012**, *84*, 2955-2960.

(95) Tsao, C.-W.; Tao, S.; Chen, C.-F.; Liu, J.; DeVoe, D. *Microfluid. Nanofluid.* **2010**, *8*, 777-787.
(96) Fritzsche, S.; Ohla, S.; Glaser, P.; Giera, D. S.; Sickert, M.; Schneider, C.; Belder, D. *Angew. Chem., Int. Ed.* **2011**, *50*, 9467-9470.
(97) Jebrail, M. J.; Yang, H.; Mudrik, J. M.; Lafreniere, N. M.; McRoberts, C.; Al-Dirbashi, O. Y.; Fisher, L.; Chakraborty, P.; Wheeler, A. R. *Lab Chip* **2011**, *11*, 3218-3224.
(98) Prensner, J. R.; Rubin, M. A.; Wei, J. T.; Chinnaiyan, A. M. *Sci. Transl. Med.* **2012**, *4*, 127rv123.
(99) Rusling, J. F.; Kumar, C. V.; Gutkind, J. S.; Patel, V. *Analyst* **2010**, *135*, 2496-2511.
(100) Huang, C.-S.; Chaudhery, V.; Pokhriyal, A.; George, S.; Polans, J.; Lu, M.; Tan, R.; Zangar, R. C.; Cunningham, B. T. *Anal. Chem.* **2011**, *84*, 1126-1133.
(101) Pan, S.; Chen, R.; Brand, R. E.; Hawley, S.; Tamura, Y.; Gafken, P. R.; Milless, B. P.; Goodlett, D. R.; Rush, J.; Brentnall, T. A. *J. Proteome Res.* **2012**, *11*, 1937-1948.
(102) Mishra, A.; Verma, M. *Cancers* **2010**, *2*, 190-208.
(103) Polanski, M.; Anderson, N. L. *Biomarker Insights* **2006**, *1*, 1-48.
(104) Uversky, V. N.; Narizhneva, N. V.; Ivanova, T. V.; Kirkitadze, M. D.; Tomashevski, A. Y. *FEBS Lett.* **1997**, *410*, 280-284.
(105) De Masi, S.; Tosti, M. E.; Mele, A. *Dig. Liver Dis.* **2005**, *37*, 260-268.
(106) Personeni, N.; Bozzarelli, S.; Pressiani, T.; Rimassa, L.; Tronconi, M. C.; Sclafani, F.; Carnaghi, C.; Pedicini, V.; Giordano, L.; Santoro, A. *J. Hepatol.* **2012**, *57*, 101-107.
(107) Brugge, W. R.; Lewandrowski, K.; Lee-Lewandrowski, E.; Centeno, B. A.; Szydlo, T.; Regan, S.; del Castillo, C. F.; Warshaw, A. L. *Gastroenterology* **2004**, *126*, 1330-1336.
(108) Yamamoto, M.; Baba, H.; Kakeji, Y.; Endo, K.; Ikeda, Y.; Toh, Y.; Kohnoe, S.; Okamura, T.; Maehara, Y. *Oncology* **2004**, *67*, 19-26.
(109) Cook, G. B.; Neaman, I. E.; Goldblatt, J. L.; Cambetas, D. R.; Hussain, M.; Luftner, D.; Yeung, K. K.; Chan, D. W.; Schwartz, M. K.; Allard, W. J. *Anticancer Res.* **2001**, *21*, 1465-1470.
(110) Mian, C.; Lodde, M.; Haitel, A.; Egarter, V. E.; Marberger, M.; Pycha, A. *Urology* **2000**, *56*, 228-231.
(111) Lima, N.; Cavaliere, H.; Tomimori, E.; Knobel, M.; Medeiros-Neto, G. *J. Endocrinol. Invest.* **2002**, *25*, 110-115.
(112) Gann, P. H.; Hennekens, C. H.; Stampfer, M. J. *JAMA* **1995**, *273*, 289-294.
(113) Skates, S. J.; Menon, U.; MacDonald, N.; Rosenthal, A. N.; Oram, D. H.; Knapp, R. C.; Jacobs, I. J. *Journal of Clinical Oncology* **2003**, *21*, 206-210.
(114) Yamaguchi, K.; Nakamura, M.; Shirahane, K.; Konomi, H.; Torata, N.; Hamasaki, N.; Kawakita, M.; Tanaka, M. *Dig. Liver Dis.* **2005**, *37*, 190-194.
(115) Ciambellotti, E.; Coda, C.; Lanza, E. *Minerva Med* **1993**, *84*, 107-112.
(116) Mor, G.; Visintin, I.; Lai, Y.; Zhao, H.; Schwartz, P.; Rutherford, T.; Yue, L.; Bray-Ward, P.; Ward, D. C. *Proc. Natl. Acad. Sci. U. S. A.* **2005**, *102*, 7677-7682.
(117) Xiao, T.; Ying, W.; Li, L.; Hu, Z.; Ma, Y.; Jiao, L.; Ma, J.; Cai, Y.; Lin, D.; Guo, S.; Han, N.; Di, X.; Li, M.; Zhang, D.; Su, K.; Yuan, J.; Zheng, H.; Gao, M.; He, J.; Shi, S.; Li, W.; Xu, N.; Zhang, H.; Liu, Y.; Zhang, K.; Gao, Y.; Qian, X.; Cheng, S. *Mol. Cell. Proteomics* **2005**, *4*, 1480-1486.
(118) Lemech, C.; Arkenau, H.-T. *Cancers* **2011**, *3*, 1844-1860.
(119) Tan, E.; Gouvas, N.; Nicholls, R. J.; Ziprin, P.; Xynos, E.; Tekkis, P. P. *Surg. Oncol.* **2009**, *18*, 15-24.

(120) Parkhurst, M. R.; Yang, J. C.; Langan, R. C.; Dudley, M. E.; Nathan, D.-A. N.; Feldman, S. A.; Davis, J. L.; Morgan, R. A.; Merino, M. J.; Sherry, R. M.; Hughes, M. S.; Kammula, U. S.; Phan, G. Q.; Lim, R. M.; Wank, S. A.; Restifo, N. P.; Robbins, P. F.; Laurencot, C. M.; Rosenberg, S. A. *Mol. Ther.* **2011**, *19*, 620-626.
(121) Li, Y.; Chen, Y.; Dilley, J.; Arroyo, T.; Ko, D.; Working, P.; Yu, D.-C. *Mol. Cancer Ther.* **2003**, *2*, 1003-1009.
(122) Graham, B.; Curry, J.; Smyth, T.; Fazal, L.; Feltell, R.; Harada, I.; Coyle, J.; Williams, B.; Reule, M.; Angove, H.; Cross, D. M.; Lyons, J.; Wallis, N. G.; Thompson, N. T. *Cancer Sci.* **2012**, *103*, 522-527.
(123) Yi, F.; Regan, L. *ACS Chem. Biol.* **2008**, *3*, 645-654.
(124) Biamonte, M. A.; Van de Water, R.; Arndt, J. W.; Scannevin, R. H.; Perret, D.; Lee, W.-C. *J. Med. Chem.* **2010**, *53*, 3-17.
(125) Sawai, A.; Chandarlapaty, S.; Greulich, H.; Gonen, M.; Ye, Q.; Arteaga, C. L.; Sellers, W.; Rosen, N.; Solit, D. B. *Cancer Res.* **2008**, *68*, 589-596.
(126) Wayne, N.; Mishra, P.; Bolon, D. N. Hsp90 and Client Protein Maturation. In *Molecular Chaperones: Methods and Protocols,* Calderwood, S. K.; Prince, T. L., Eds. Humana Press: 2011; Vol. 787, pp 33-44.
(127) Bagatell, R.; Whitesell, L. *Mol. Cancer Ther.* **2004**, *3*, 1021-1030.
(128) Alegre, M. M.; Robison, R. A.; O'Neill, K. L. *J. Oncol.* **2012**, Article ID 575647, pp. 1-5
(129) Munch-Petersen, B. *FEBS Journal* **2009**, *276*, 571-580.
(130) Brockenbrough, J. S.; Morihara, J. K.; Hawes, S. E.; Stern, J. E.; Rasey, J. S.; Wiens, L. W.; Feng, Q.; Vesselle, H. *J. Histochem. Cytochem.* **2009**, *57*, 1087-1097.
(131) Welin, M.; Kosinska, U.; Mikkelsen, N.-E.; Carnrot, C.; Zhu, C.; Wang, L.; Eriksson, S.; Munch-Petersen, B.; Eklund, H. *Proc. Natl. Acad. Sci. U. S. A.* **2004**, *101*, 17970-17975.
(132) Lin, J.; Roy, V.; Wang, L.; You, L.; Agrofoglio, L. A.; Deville-Bonne, D.; McBrayer, T. R.; Coats, S. J.; Schinazi, R. F.; Eriksson, S. *Bioorg. Med. Chem.* **2010**, *18*, 3261-3269.
(133) O'Neill, K. L.; Zhang, F.; Li, H.; Fuja, D. G.; Murray, B. K. *Leukemia (08876924)* **2007**, *21*, 560-563.
(134) He, Q.; Fornander, T.; Johansson, H.; Johansson, U.; Hu, G. Z.; Rutqvist, L.-E.; Skog, S. *Anticancer Res.* **2006**, *26*, 4753-4759.
(135) Olteanu, A.; Patel, C. N.; Dedmon, M. M.; Kennedy, S.; Linhoff, M. W.; Minder, C. M.; Potts, P. R.; Deshmukh, M.; Pielak, G. J. *Biochem. Biophys. Res. Commun.* **2003**, *312*, 733-740.
(136) Bertini, I.; Grassi, E.; Luchinat, C.; Quattrone, A.; Saccenti, E. *Genomics* **2006**, *88*, 669-672.
(137) Barczyk, K.; Kreuter, M.; Pryjma, J.; Booy, E. P.; Maddika, S.; Ghavami, S.; Berdel, W. E.; Roth, J.; Los, M. *Int. J. Cancer* **2005**, *116*, 167-173.
(138) Osaka, A.; Hasegawa, H.; Yamada, Y.; Yanagihara, K.; Hayashi, T.; Mine, M.; Aoyama, M.; Sawada, T.; Kamihira, S. *J. Cancer Res. Clin. Oncol.* **2009**, *135*, 371-377.
(139) Ambrosi, A.; Airò, F.; Merkoçi, A. *Anal. Chem.* **2009**, *82*, 1151-1156.
(140) Zangar, R. C.; Daly, D. S.; White, A. M. *Expert Rev. Proteomics* **2006**, *3*, 37-44.
(141) Ang, C.-S.; Nice, E. C. *J. Proteome Res.* **2010**, *9*, 4346-4355.
(142) Gonzalez, R. M.; Seurynck-Servoss, S. L.; Crowley, S. A.; Brown, M.; Omenn, G. S.; Hayes, D. F.; Zangar, R. C. *J. Proteome Res.* **2008**, *7*, 2406-2414.
(143) Armenta, J. M.; Dawoud, A. A.; Lazar, I. M. *Electrophoresis* **2009**, *30*, 1145-1156.
(144) Wulfkuhle, J. D.; Liotta, L. A.; Petricoin, E. F. *Nat. Rev. Cancer* **2003**, *3*, 267-275.

(145) Ongay, S.; Martín-Álvarez, P. J.; Neusüß, C.; de Frutos, M. *Electrophoresis* **2010**, *31*, 3314-3325.
(146) Wang, Q.; Chaerkady, R.; Wu, J.; Hwang, H. J.; Papadopoulos, N.; Kopelovich, L.; Maitra, A.; Matthaei, H.; Eshleman, J. R.; Hruban, R. H.; Kinzler, K. W.; Pandey, A.; Vogelstein, B. *Proc. Natl. Acad. Sci. U. S. A.* **2011**.
(147) Zeng, X.; Hood, B. L.; Sun, M.; Conrads, T. P.; Day, R. S.; Weissfeld, J. L.; Siegfried, J. M.; Bigbee, W. L. *J. Proteome Res.* **2010**, *9*, 6440-6449.
(148) Wang, S.; Zhao, X.; Khimji, I.; Akbas, R.; Qiu, W.; Edwards, D.; Cramer, D. W.; Ye, B.; Demirci, U. *Lab Chip* **2011**, *11*, 3411-3418.
(149) Yang, W.; Yu, M.; Sun, X.; Woolley, A. T. *Lab Chip* **2010**, *10*, 2527-2533.
(150) Malhotra, R.; Patel, V.; Chikkaveeraiah, B. V.; Munge, B. S.; Cheong, S. C.; Zain, R. B.; Abraham, M. T.; Dey, D. K.; Gutkind, J. S.; Rusling, J. F. *Anal. Chem.* **2012**, *84*, 6249-6255.
(151) Zhang, J. Y.; Do, J.; Premasiri, W. R.; Ziegler, L. D.; Klapperich, C. M. *Lab Chip* **2010**, *10*, 3265-3270.
(152) Kovarik, M. L.; Gach, P. C.; Ornoff, D. M.; Wang, Y.; Balowski, J.; Farrag, L.; Allbritton, N. L. *Anal. Chem.* **2011**, *84*, 516-540.
(153) Schumacher, S.; Nestler, J.; Otto, T.; Wegener, M.; Ehrentreich-Forster, E.; Michel, D.; Wunderlich, K.; Palzer, S.; Sohn, K.; Weber, A.; Burgard, M.; Grzesiak, A.; Teichert, A.; Brandenburg, A.; Koger, B.; Albers, J.; Nebling, E.; Bier, F. F. *Lab Chip* **2012**, *12*, 464-473.
(154) Kang, Q.-S.; Li, Y.; Xu, J.-Q.; Su, L.-J.; Li, Y.-T.; Huang, W.-H. *Electrophoresis* **2010**, *31*, 3028-3034.
(155) www.sigmaaldrich.com/Graphics/Supelco/objects/4600/4538.pdf.
(156) Reedy, C. R.; Hagan, K. A.; Strachan, B. C.; Higginson, J. J.; Bienvenue, J. M.; Greenspoon, S. A.; Ferrance, J. P.; Landers, J. P. *Anal. Chem.* **2010**, *82*, 5669-5678.
(157) Cakal, C.; Ferrance, J. P.; Landers, J. P.; Caglar, P. *Anal. Chim. Acta.* **2011**, *690*, 94-100.
(158) Wen, J.; Legendre, L. A.; Bienvenue, J. M.; Landers, J. P. *Anal. Chem.* **2008**, *80*, 6472-6479.
(159) Wan Ibrahim, W. A.; Veloo, K. V.; Sanagi, M. M. *J. Chromatogr. A* **2012**, *1229*, 55-62.
(160) Perman, C. A.; Telepchak, M. *LC-GC North America* **2011**, *29*, 516-524.
(161) Woodward, S. D.; Urbanova, I.; Nurok, D.; Svec, F. *Anal. Chem.* **2010**, *82*, 3445-3448.
(162) Li, Y. Y.; Tolley, H. D.; Lee, M. L. *Anal. Chem.* **2009**, *81*, 9416-9424.
(163) Karenga, S.; El Rassi, Z. *J. Sep. Sci.* **2008**, *31*, 2677-2685.
(164) Tetala, K. K. R.; van Beek, T. A. *J. Sep. Sci.* **2010**, *33*, 422-438.
(165) Sun, X.; Yang, W.; Pan, T.; Woolley, A. T. *Anal. Chem.* **2008**, *80*, 5126-5130.
(166) Njoroge, S. K.; Witek, M. A.; Battle, K. N.; Immethun, V. E.; Hupert, M. L.; Soper, S. A. *Electrophoresis* **2011**, *32*, 3221-3232.
(167) Nguyen, T.; Pei, R.; Landry, D. W.; Stojanovic, M. N.; Lin, Q. *Sens. Actuators, B* **2011**, *154*, 59-66.
(168) Wang, L.; Li, P. C. H. *Anal. Chim. Acta.* **2011**, *687*, 12-27.
(169) Foote, R. S.; Khandurina, J.; Jacobson, S. C.; Ramsey, J. M. *Anal. Chem.* **2004**, *77*, 57-63.
(170) Faure, K.; Delaunay, N.; Alloncle, G.; Cotte, S.; Rocca, J.-L. *J. Chromatogr. A* **2007**, *1149*, 145-150.
(171) Simpson Jr, S. L.; Quirino, J. P.; Terabe, S. *J. Chromatogr. A* **2008**, *1184*, 504-541.

(172) Giordano, B. C.; Burgi, D. S.; Hart, S. J.; Terray, A. *Anal. Chim. Acta.* **2012**, *718*, 11-24.
(173) Bottenus, D.; Hossan, M. R.; Ouyang, Y.; Dong, W.-J.; Dutta, P.; Ivory, C. F. *Lab Chip* **2011**, *11*, 3793-3801.
(174) El Rassi, Z.; Nashabeh, W. High Performance Capillary Electrophoresis of Carbohydrates and Glycoconjugates. In *J. Chromatogr. Libr.*, Ziad El, R., Ed. Elsevier: 1995; Vol. 58, pp 267-360.
(175) Bercovici, M.; Kaigala, G. V.; Mach, K. E.; Han, C. M.; Liao, J. C.; Santiago, J. G. *Anal. Chem.* **2011**, *83*, 4110-4117.
(176) Bishop, E. J.; Mitra, S. *J. Pharmaceut. Biomed. Anal.* **2005**, *37*, 81-86.
(177) Hatch, A. V.; Herr, A. E.; Throckmorton, D. J.; Brennan, J. S.; Singh, A. K. *Anal. Chem.* **2006**, *78*, 4976-4984.
(178) Chun, H.; Chung, T. D.; Ramsey, J. M. *Anal. Chem.* **2010**, *82*, 6287-6292.
(179) Wu, D.; Steckl, A. J. *Lab Chip* **2009**, *9*, 1890-1896.
(180) Hoeman, K. W.; Lange, J. J.; Roman, G. T.; Higgins, D. A.; Culbertson, C. T. *Electrophoresis* **2009**, *30*, 3160-3167.
(181) Shen, M.; Yang, H.; Sivagnanam, V.; Gijs, M. A. M. *Anal. Chem.* **2010**, *82*, 9989-9997.
(182) Modesti, M. *Methods Mol. Biol. (N. Y., NY, U. S.)* **2011**, *783*, 101-120.
(183) *Labeling protocol obtained from manual by Molecular Probes: http://tools.invitrogen.com/content/sfs/manuals/mp20180.pdf* **accessed October 26, 2012**.
(184) Yang, W.; Sun, X.; Wang, H.-Y.; Woolley, A. T. *Anal. Chem.* **2009**, *81*, 8230-8235.
(185) *Labeling protocol obtained from manual by Molecular Probes: http://www.probes.invitrogen.com/media/pis/mp06434.pdf* **accessed October 26, 2012**.
(186) Jacobson, S. C.; Hergenroder, R.; Moore, A. W., Jr.; Ramsey, J. M. *Anal. Chem.* **1994**, *66*, 4127-4132.
(187) Yu, M.; Wang, Q.; Patterson, J. E.; Woolley, A. T. *Anal. Chem.* **2011**, *83*, 3541-3547.
(188) Wu, J.; Ferrance, J. P.; Landers, J. P.; Weber, S. G. *Anal. Chem.* **2010**, *82*, 7267-7273.
(189) Jacobson, S. C.; Koutny, L. B.; Hergenroeder, R.; Moore, A. W., Jr.; Ramsey, J. M. *Anal. Chem.* **1994**, *66*, 3472-3476.
(190) Li, M. W.; Martin, R. S. *Analyst* **2008**, *133*, 1358-1366.
(191) Johnson, A. S.; Selimovic, A.; Martin, R. S. *Electrophoresis* **2011**, *32*, 3121-3128.
(192) Malic, L.; Brassard, D.; Veres, T.; Tabrizian, M. *Lab Chip* **2010**, *10*, 418-431.
(193) Wu, A.; Wang, L.; Jensen, E.; Mathies, R.; Boser, B. *Lab Chip* **2010**, *10*, 519-521.
(194) Rivet, C.; Lee, H.; Hirsch, A.; Hamilton, S.; Lu, H. *Chem Eng Sci* **2011**, *66*, 1490-1507.
(195) Gervais, L.; de Rooij, N.; Delamarche, E. *Adv Mater* **2011**, *23*, H151-H176.
(196) Sin, M.; Gao, J.; Liao, J.; Wong, P. *J. Biol. Eng.* **2011**, *5*, 6.
(197) Sen, A. K.; Darabi, J.; Knapp, D. *Microsyst. Technol.* **2010**, *16*, 617-623.
(198) Kim, J.; Jensen, E. C.; Megens, M.; Boser, B.; Mathies, R. A. *Lab Chip* **2011**, *11*, 3106-3112.
(199) Tennico, Y. H.; Remcho, V. T. *Electrophoresis* **2010**, *31*, 2548-2557.
(200) Hecht, A. H.; Sommer, G. J.; Durland, R. H.; Yang, X.; Singh, A. K.; Hatch, A. V. *Anal. Chem.* **2010**, *82*, 8813-8820.

## 2. INTEGRATED AFFINITY AND ELECTROPHORESIS SYSTEMS FOR BIOMARKER ANALYSIS*

### 2.1 INTRODUCTION

Biomarkers can be used in non-invasive early stage disease detection and in assessing patient response to treatments.[1] Present methods for biomarker detection, in prostate cancer for example, are neither sensitive nor specific enough to enable early stage detection,[2] such that improvements are needed. A promising route to probing trace target analytes in complex mixtures entails integrating components capable of performing sample preparation, separation, and detection into a single device.[3] Affinity columns have strong potential to provide selective analysis of desired components in a complex matrix.[4, 5] Monolithic supports are an emerging method for chromatographic assays;[6, 7] importantly, these columns can easily be prepared in microfluidic devices by in-situ photopolymerization.[8] Integration of affinity preparation with miniaturized separation offers the advantages of sample extraction and preconcentration coupled with the portability, speed, automation, and reduction of sample volume[9, 10] provided by methods such as microchip electrophoresis (μ-CE).

Here I describe the fabrication of poly(methyl methacrylate) microfluidic devices by the processes of photolithography, hot embossing and thermal bonding and demonstrate an approach for the preparation and application of affinity columns in these devices. The use of monomers with reactive epoxide groups allowed for direct functionalization with antibodies,[11-14] which is more straightforward than a multistep process. Application of these columns to biomarker

---

* This Chapter is modified from Chapter 18 in: *Methods in Molecular Biology: Clinical Applications of Capillary Electrophoresis*, Nge, P. N.; Pagaduan, J. V.; Yang, W.; Woolley, A. T., Vol. 919, Phillips, T. M.; Kalish, H., Eds.; pp 189-201. Copyright Humana Press, 2013

analysis has multiple requirements. The biomarkers need to be labeled to enable laser-induced fluorescence detection. Biomarkers must be bound to their corresponding antibodies on the column followed by washing to remove unwanted low-affinity components. Captured biomarkers are eluted into a μ-CE system. These integrated devices offer efficient sample pretreatment and preconcentration. Simultaneous quantification of multiple biomarkers in complex mixtures such as blood serum can also be carried out with more complex device designs.

## 2.2 MATERIALS

### 2.2.1 PMMA device fabrication

A silicon template was prepared by the photolithographic procedure shown in Figure 2.1. Briefly, a thermally oxidized silicon <100> wafer was coated with photoresist and exposed to UV radiation. Silicon wafers cleave according to their crystalline orientation; to obtain square templates when the wafer is cleaved, silicon <100> is preferred since it cleaves at 90° angles. The wafer was developed to remove exposed photoresist and then etched in 10% buffered HF solution to remove the oxide layer. This was followed by wet etching in 40% aqueous KOH solution to yield raised channel features of ~15 μm height.[15] PMMA sheets (1.5- and 3-mm thickness) for device fabrication were obtained from Cyro Industries, Rockaway, NJ, USA. The thinner layer (1.5 mm) facilitates embossing of the pattern from a silicon template while the thicker layer (3.0 mm) used for the cover plate enables a larger volume (up to 20 μL) of solution to fit into the reservoir. This ensures that solution does not easily evaporate away during the analysis process. Other necessary materials include glass microscope slides (75 mm × 50 mm × 1 mm), C-clamps, acetone, isopropyl alcohol (IPA), a laser cutter (Universal Laser Systems,

Scottsdale, AZ, USA), canned compressed gas for dust removal (GUST, Quarryville, PA, USA), copper plates, and a precision convection oven (Thermo Scientific, Asheville, NC, USA).

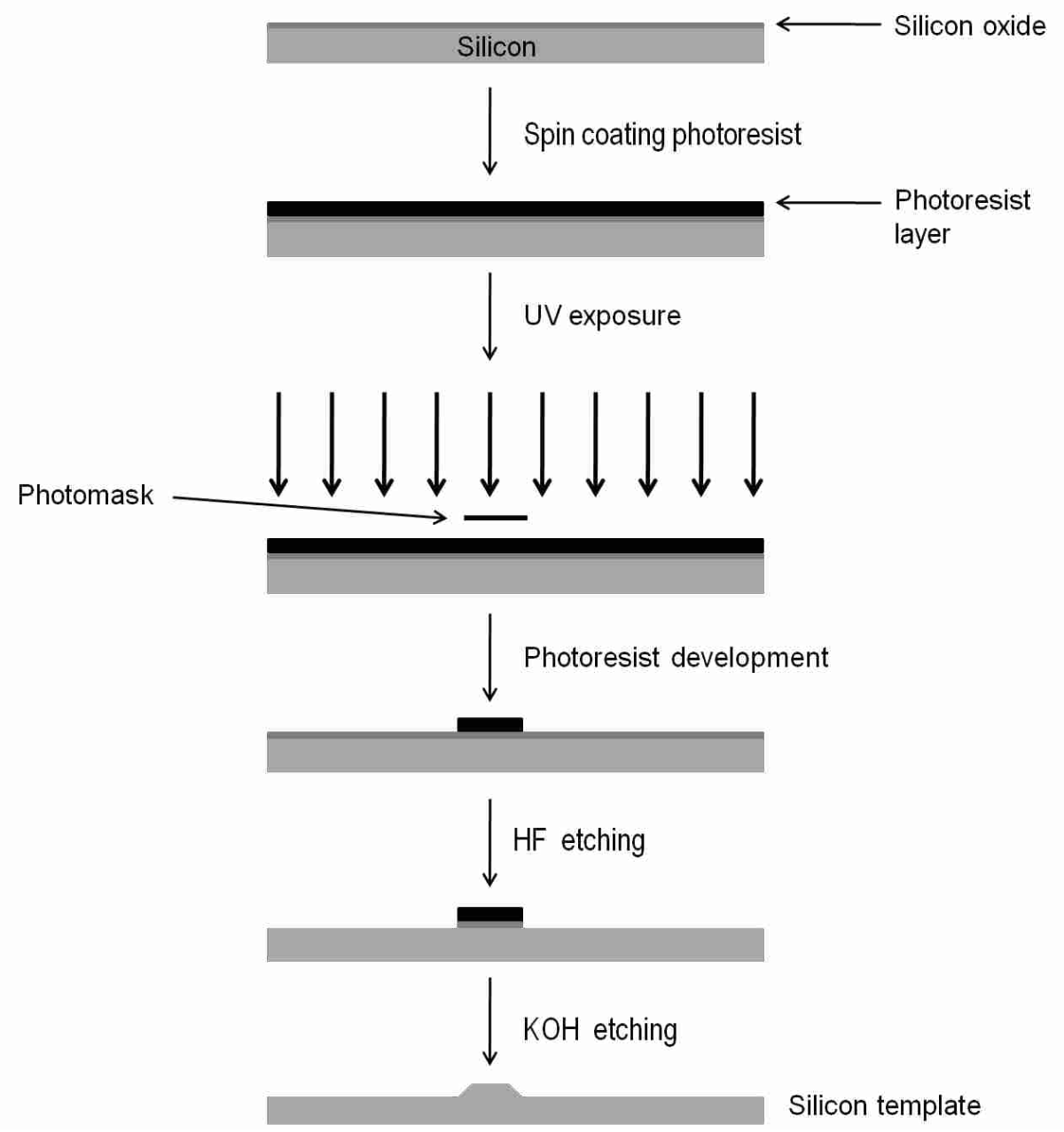


**Figure 2.1.** Photolithographic procedure for the fabrication of a silicon template.

### 2.2.2 Affinity columns

Glycidyl methacrylate (GMA, 97%), ethylene glycol dimethacrylate (EGDMA, 98%), 2,2-dimethoxy-2-phenylacetophenone (DMPA, 98%), 1-dodecanol (98%), and cyclohexanol were obtained from Sigma-Aldrich, (St Louis, MO, USA). Tween 20 was from Mallinckrodt Baker (Paris, KY, USA). Borate buffer (0.1 M, pH 8.6) was prepared as follows: 3.81 g (10 mmol) of sodium tetraborate decahydrate was dissolved in 100 mL water in one flask and 0.62 g (10 mmol) of boric acid was dissolved in 100 mL water in another flask. The boric acid solution was added to the tetraborate solution until pH 8.6 was reached. Tris buffer (0.1 M) was prepared as follows: 0.65 g (5.4 mmol) Tris base and 0.72 g (4.6 mmol) Tris-HCl was weighed, transferred to a 100 mL volumetric flask containing ~20 mL water and mixed until the solid dissolved completely. Water was then added up to the 100 mL mark. The solution was stored at 4 °C. Carbonate buffer (0.1 M, pH 9.3) was prepared as follows: 0.69 g (8.1 mmol) sodium bicarbonate and 0.20 g (1.9 mmol) anhydrous sodium carbonate was weighed, transferred to a 100 mL volumetric flask containing ~20 mL water and mixed until the solid dissolved completely. Water was added up to the 100 mL mark and the buffer was stored at 4 °C. Monoclonal anti-AFP antibody in phosphate buffered saline (PBS, pH 7.2) was from Sigma-Aldrich while monoclonal anti-HSP90 in PBS pH 7.2, containing 50% glycerol and 0.09% sodium azide was from Stressgen (Ann Arbor, MI, USA). Other materials included 1.5 dram glass vials, a syringe pump (Harvard Apparatus, Holliston, MA, USA), a UV lamp (SunRay from Uvitron International, West Springfield, MA, USA), a photomask and black electrical tape.

### 2.2.3 Biomarker analysis

Carbonate buffer (0.1 M, pH 9.3) was prepared as in Section 2.2.2, and 0.1 M phosphate buffer, pH 7.0 was prepared as follows: ~20 mL water was added to a 100 mL volumetric flask. 0.52 g (3.8 mmol) monosodium phosphate monohydrate and 0.88 g (6.2 mmol) anhydrous disodium phosphate was weighed, transferred to the flask and mixed until the solid dissolved completely. Water was added up to the 100 mL mark and the buffer was stored at 4 °C. This buffer was made into PBS by adding 0.88 g (15 mmol) NaCl once the flask was filled to the mark. Amicon Ultra-0.5 centrifugal filters (30 kDa MWCO) were from Millipore (Billerica, MA). AFP (1.75 mg/mL in 0.1 M PBS pH 7.4, containing 15 mM sodium azide) was obtained from Lee Biosolutions (St. Louis, MO). The AFP buffer was exchanged with PBS, pH 7.2 - 7.4 using an Amicon Ultra-0.5 centrifugal filter. This step is essential because buffers containing primary amines such as Tris or buffers containing sodium azide interfere with the labeling process since they compete for conjugation with the amine-reactive dye. It is therefore important to exchange such buffers for nonreactive ones like PBS, carbonate or borate. This buffer exchange process also concentrates the sample to ~2 mg/mL. HSP90 (2.1 mg/mL in Dulbecco's PBS containing 2.7 mM potassium chloride, 1.5 mM potassium phoshate, 137 mM sodium chloride, 8.1 mM sodium phosphate, and 10% glycerol) was obtained from Stressgen. TK1 (0.91 mg/mL in PBS pH 7.4 containing 10% glycerol) was from GenScript (Piscataway, NJ, USA). Alexa Fluor 488 TFP ester and fluorescein isothiocyanate (FITC) were obtained from Invitrogen (Carlsbad, CA, USA), while dimethyl sulfoxide (DMSO) and hydroxypropyl cellulose (HPC, average MW 100 kDa) were from Sigma-Aldrich. High voltage power supplies were from Stanford Research Systems (Sunnyvale, CA, USA).

## 2.3 METHODS

### 2.3.1 Hot embossing and bonding

A laser cutter was used to section the PMMA sheets into 54 mm × 38 mm pieces and to form 2.5-mm-diameter holes in the 3-mm-thick PMMA to make the buffer reservoirs. The silicon template was rinsed with acetone and IPA, and then blow dried with compressed air or nitrogen. These solvents remove oil and organic residues from surfaces. Since solvents like acetone leave residues on surfaces, a two-solvent method is used. The silicon template was placed, with the patterned side facing upwards, on a glass microscope slide. A 1.5-mm-thick piece of PMMA was set on the template, with another glass slide atop the PMMA (Fig. 2.2A). The glass slides were sandwiched with copper plates and the assembly held together with C-clamps. The clamps were not over tightened as this could break the glass slides or template, causing the hot embossing step to fail. The assembly was placed in the convection oven at 140 °C for 30 min and the elevated features on the template were transferred onto the PMMA substrate (Fig. 2.2B). The assembly was removed from the oven and allowed to cool for a few minutes before removing the clamps and copper plates. The template was then placed against a cooler surface so the imprinted PMMA pulled away from the template (Fig. 2.2C). Removing the embossed PMMA when the assembly is totally cooled is not usually a problem. However, detachment after partial cooling prevents melted PMMA from sticking to the sides of the patterns on the silicon template, which can affect subsequent patterning.

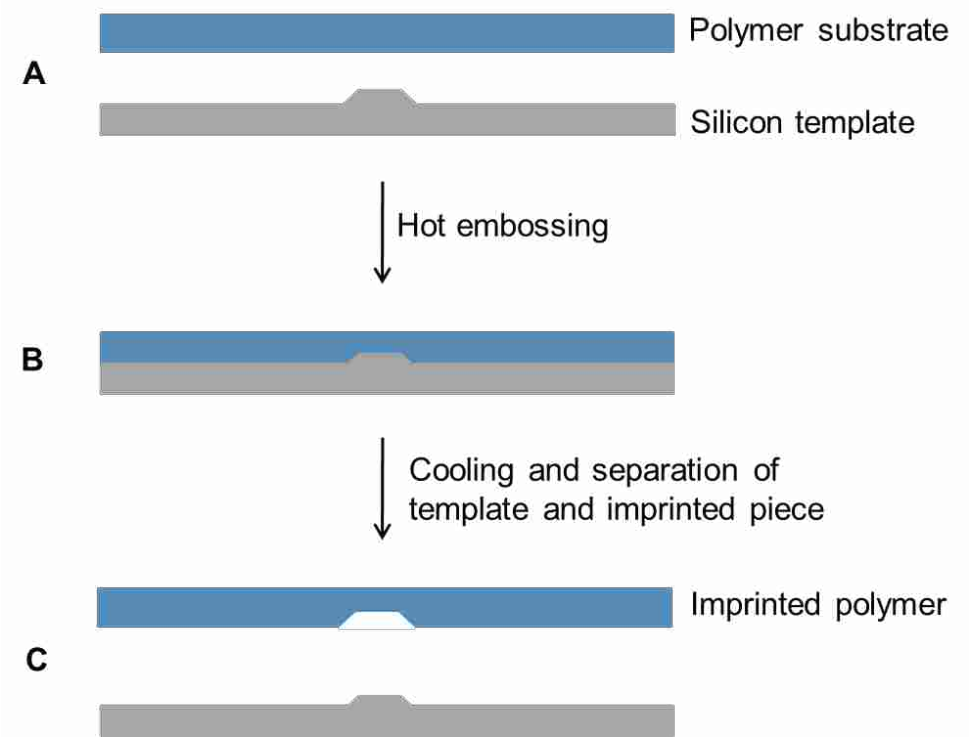


**Figure 2.2.** Schematic overview of the hot embossing procedure. a) Polymer substrate placed on the silicon template. b) Application of temperature and pressure to transfer pattern from the template to the substrate. c) Separation of imprinted substrate from the template.

Both the patterned PMMA and the 3-mm-thick cover plate were cleaned with canned compressed gas for dust removal, and the cover plate was placed on the imprinted PMMA. This ensured that no particles were trapped in between these plates during bonding, where they could block the channels. Compressed air can also be used, but canned dust removal with compressed gas was found to be more effective. The two PMMA pieces were sandwiched with glass slides and copper plates and then held together with C-clamps as in the imprinting process (Fig. 2.3A). The C-clamps were the same type and size so uniform pressure was applied to the substrates, since uneven pressure can cause one side of the device to be over-bonded with the other side being under-bonded. The assembly was placed in the convection oven at 110 °C for ~25 min to bond the two pieces together (Fig. 2.3B). Bonding time depended on the number of devices

being bonded simultaneously. More than two assemblies placed in the oven at the same time required longer than 25 min. The assembly was removed from the oven and allowed to cool completely before taking off the C-clamps. The device was then checked to ensure complete bonding. Schematics of completed device layouts are shown in Figures 2.3C-D.

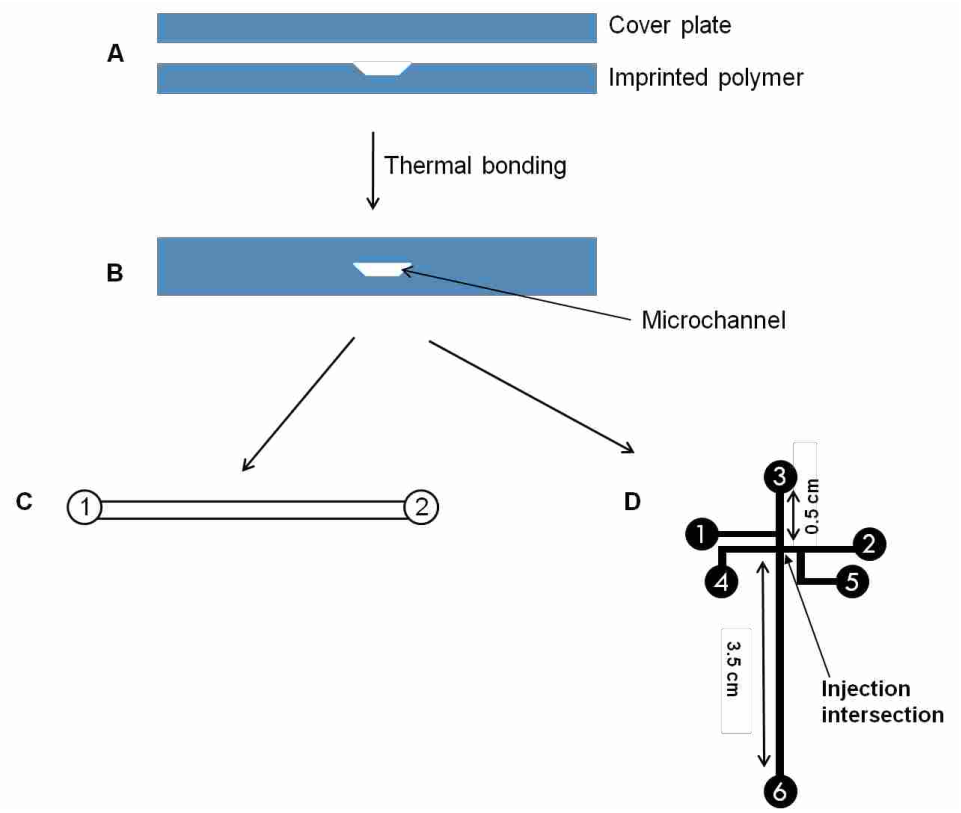


**Figure 2.3.** Schematic overview of thermal bonding procedure and completed devices. a) Imprinted polymer and cover plate placed between glass slides and copper plates, and held together by C-clamps. b) Thermal bonding of the two pieces. c) Simple two-reservoir device. d) Multichannel device for automated experiments.

### 2.3.2 Preparation of porous monolithic columns

To prepare the porous monolithic column 400 mg 1-dodecanol, 300 mg cyclohexanol, 200 mg GMA, 100 mg EGDMA and 20 mg DMPA were mixed in a glass vial, vortexed briefly and sonicated until the DMPA was completely dissolved. GMA is the monomer, EGDMA serves as

the crosslinker, and DMPA functions as the photoinitiator. Half (500 mg) of this solution was transferred into a clean glass vial and 200 mg of Tween 20 was added to it. The solution was sonicated for 5 min and immediately purged with $N_2$ for 5 min. The vial containing the remaining solution was capped and kept in the dark at room temperature to avoid polymerization. This solution was used within 10 h. It was necessary to repeat the $N_2$ purging before filling the channel with any stored solution. A small amount of the purged solution was immediately transferred into reservoir 1 **(**Fig. 2.3C**)**, and allowed to fill the channel by capillary flow. A fill time of 2-3 min was allowed to ensure that the channel was completely filled and that the solution had stopped flowing. The channel can also be viewed under a microscope to ensure that it is completely filled and that the solution has stopped flowing. Polymerization may be incomplete or absent if the solution is still flowing during UV exposure. Excess solution was then removed from the reservoir. This step was important to minimize polymerization in the reservoir, which resulted in a blocked channel. A schematic procedure for *in situ* preparation of the porous monolith is shown in Figure 2.4. A photomask or black tape was used to cover the regions around the affinity column to make a window for UV exposure **(**Fig. 2.4B**)**. When black tape was used the backside of the device, except for the window for exposure, was also covered. The device was exposed to UV light for 12-14 min at room temperature using the SunRay lamp. Using a glass mask reduced spurious polymerization but also increased the polymerization time. With black tape, 12 min was sufficient to polymerize the monolith, but with a photomask 14 min was needed. Placing a white object under the device to reflect the UV light was also helpful in obtaining complete polymerization. The tape or photomask was removed and vacuum immediately applied to remove unpolymerized solution. Then, IPA was flowed through the channel until the monolithic column became white in color. Immediate removal of

unpolymerized solution was essential to prevent further polymerization and potential channel blockage. The channel was flushed with deionized water until the IPA was completely removed, and then filled with water. If IPA was not completely removed an alcohol-water interface was formed which could be observed under a microscope. Vacuum was then applied to remove the water from the device. The monolith appeared black under optical microscope viewing when the water was removed **(**Fig. 2.4C**)**. The monolith can be stored dry at room temperature until it is ready to be functionalized. An electron micrograph of a monolith can be seen in Figure 2.5.

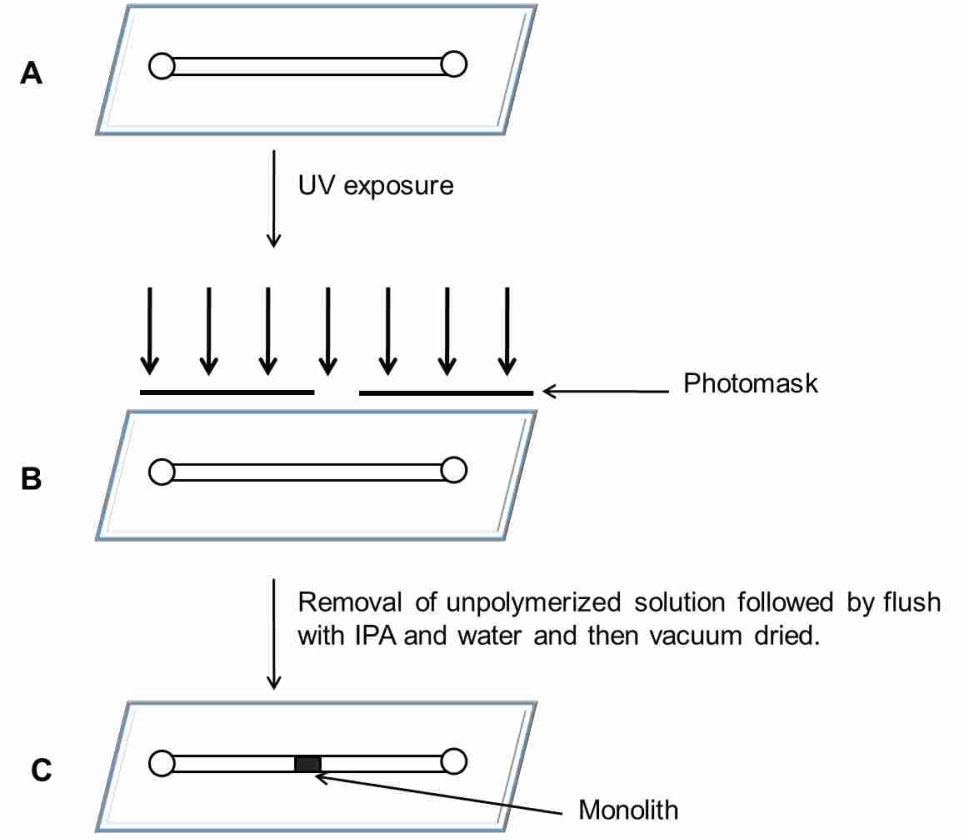


**Figure 2.4.** Schematic procedure for preparation of a monolith. a) Device filled with prepolymer mixture. b) Exposure of device to UV radiation through a photomask. c) Monolith formed in the microchannel.

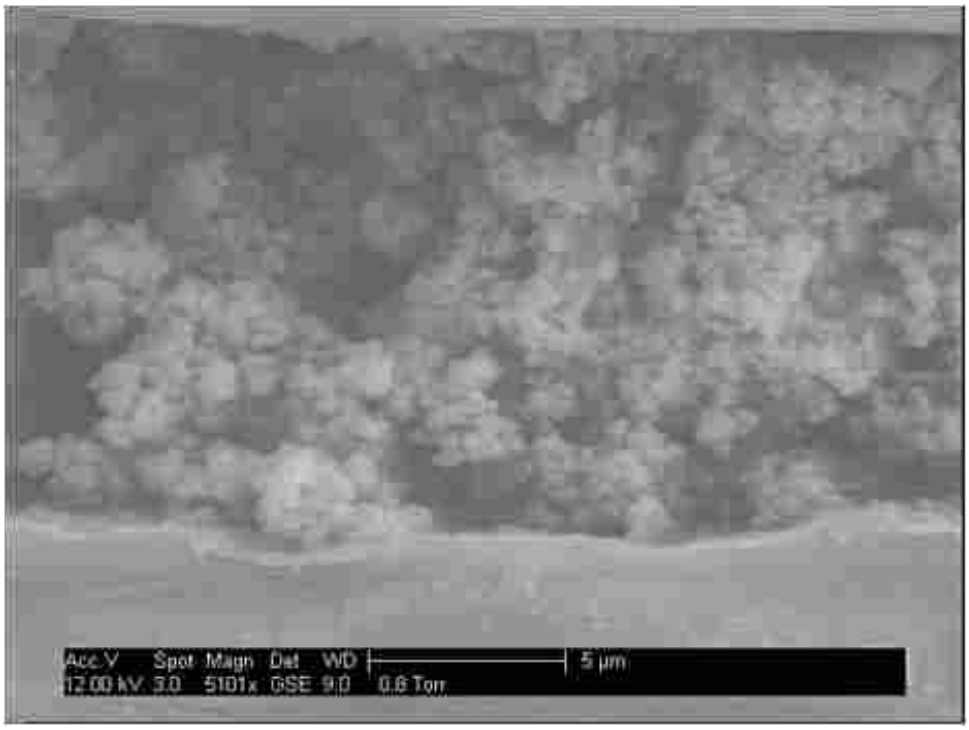


**Figure 2.5.** Electron micrograph of a porous monolithic column formed in a microfluidic channel. The monolithic structure consists of small globular nodules that offer high surface area, with an average through pore size of ~2 µm.

### 2.3.3 Attaching antibodies to the columns

An antibody solution was diluted to 0.5 mg/mL in 50 mM borate buffer (pH 8.6), pipetted into reservoir 1 (Fig. 2.3C), and allowed to fill the column by capillary action. Tris buffer was avoided at this stage, because it contains amine groups that react with the epoxy groups on the monolith. Borate buffer was placed in all other reservoirs to maintain liquid in the channels during the reaction. The entire chip was sealed with clear adhesive tape and left to react at 37 °C for 24 h in the dark. When the reaction was completed, the device was flushed with 100 mM Tris buffer (pH 8.3) for 30 min to deactivate any remaining epoxy groups on the column. The entire chip was then rinsed with carbonate buffer (pH 9.3) before use.

### 2.3.4 Fluorescence labeling of proteins

Proteins were diluted to 1 mg/mL with carbonate buffer, pH 9.3. All but one of the proteins listed in Section 2.2.3 label efficiently at pH ~9.3; TK1, with a pI of 8.75, did not. The average number of dye molecules coupled to each TK1 was 0.5 at pH 9.3, 1 at pH 9.8, and ~2 at pH 10.6. This indicates that TK1 may not be reactive enough at pH 9.3 for efficient labeling. Higher pHs favor deprotonation of amine groups, resulting in a greater likelihood of reaction between amine-reactive dyes and the protein. For FITC labeling, 2 mg of FITC was dissolved in 100 μL of anhydrous DMSO. Part of this solution (10 μL) was added to 250 μL of protein sample and incubated in the dark for 3 h at room temperature and then overnight at 4 $^{o}$C. Any unused label was discarded as degradation occurred rapidly once the fluorophore was dissolved in solvent. Unconjugated dye was separated from the protein samples by diafiltration, using an Amicon Ultra-0.5 centrifugal filter (30 kDa MWCO) and 10 mM PBS, pH 7.4. This step was not necessary when affinity purification was done on-chip. For labeling with Alexa Fluor 488 TFP ester, the fluorescent tag was dissolved in DMSO to a concentration of 10 mg/mL. The Alexa Fluor 488 TFP ester solution (5 μL) and protein sample (200 μL) were mixed and incubated in the dark for 1 h at room temperature. Sodium azide was added to the labeled proteins to a final concentration of 2 mM. The fluorescently labeled samples were stored in the dark at 4 $^{o}$C until used. For long-term storage, the sample was divided into small portions before freezing. Then, one portion was removed and used when needed. This avoided repeated freezing and thawing which could break down the sample.

### 2.3.5 Electrophoresis without affinity extraction

Separation buffer was prepared by adding HPC to 10 mM carbonate to a final concentration of ~0.5% to suppress electroosmotic flow and prevent adsorption of proteins to the channel walls. This buffer was loaded into the device and all reservoirs except reservoir 1 (Fig. 2.3D). Platinum electrodes were placed in reservoirs 1, 2, 3 and 6 (Fig. 2.3D) and connected to the high voltage power supplies. Electrophoresis was performed using "pinched injection".[15, 16] For pinched injection, reservoirs 1, 3, and 6 were grounded while +600 V was applied to reservoir 2. For separation, reservoir 3 was grounded, +600 V was applied to reservoirs 1 and 2, and +1600 V was applied to reservoir 6. Fluorescence was detected in the separation channel near reservoir 6 (Fig. 2.3D). An inverted microscope coupled with LIF equipment was used (see Figure 1.6). Briefly, a 488 nm laser was focused within the separation channel using a 20× 0.45 NA objective. Fluorescence was collected via the same objective, filtered spectrally and spatially, and detected at a photomultiplier tube. Detector signal was amplified, filtered and recorded on a computer. Data points were obtained at 20 Hz.

### 2.3.6 Affinity extraction

The separation buffer was loaded into the two-reservoir device (Fig. 2.3C). The buffer in the sample reservoir (reservoir 1) was replaced with protein solution which was loaded on the affinity column by applying +400 V for 5 min between reservoirs 1 and 2. The sample in reservoir 1 was then replaced with PBS and the affinity column was rinsed by applying +400 V for 5 min between reservoirs 1 and 2. For elution, phosphoric acid/dihydrogen phosphate, pH 2.1, replaced PBS in reservoir 1. The low pH was needed to disrupt the protein-antibody

interaction and elute the protein sample. The retained analyte was then eluted from the column by application of +400 V between reservoirs 1 and 2.

## 2.4 RESULTS AND DISCUSSION

Efficient labeling of most of the proteins discussed above occurred at pH ~9 except for TK1. However, TK1 was better labeled at a higher pH of 10.6. Figure 2.6 shows electropherograms of TK1 labeled at pH 10.6 before (Fig. 2.6A) and after (Fig. 2.6B) removal of the unreacted label. μCE of Alexa Fluor 488-labeled TK1 showed complete separation of the unreacted dye and the labeled protein.

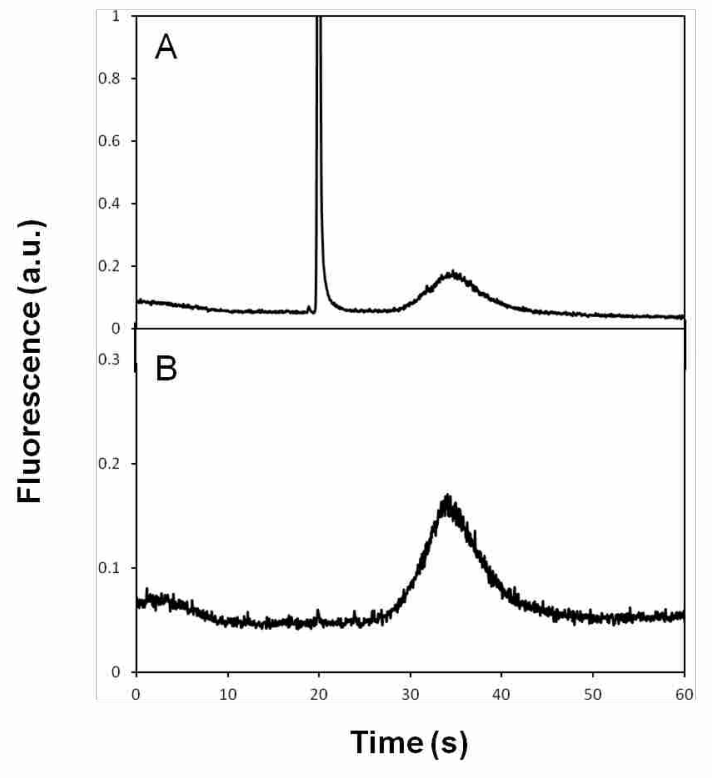


**Figure 2.6.** Electropherograms of 500 ng/mL Alexa Fluor 488-labeled TK1 (A) before and (B) after removal of dye.

Proteins were fluorescently labeled and extracted on an affinity monolith. I have studied the use of porous monoliths for the extraction of HSP90 in a device like the one in Figure 2.3C. The monolith was prepared and functionalized with anti-HSP90 as described above. To test the specificity of the anti-HSP90 column, the fluorescent dye Alexa Fluor 488 TFP ester was loaded on a functionalized and unfunctionalized column by the application of voltage (see Figure 2.7). Elution was carried out with phosphoric acid/dihydrogen phosphate buffer, pH 2.1, and the fluorescence intensity was measured with a PMT. When Alexa Fluor 488 was flowed through an unfunctionalized column, a significant amount was extracted and subsequently eluted (Fig. 2.7A), since there is increased non-specific sorption of dye when antibody is not bound to the affinity column. When the column was functionalized with anti-HSP90 very little Alexa Fluor 488 was eluted from the column as evidenced by the small eluted peak (Fig. 2.7B). The limited amount of dye eluted could be the result of its reaction with the protein on the column which could cause it to remain attached to the column.

Figure 2.8 shows the elution of Alexa Fluor 488-labeled HSP90 from a functionalized column. The labeled HSP90 attached to anti-HSP90 by the specific antibody-antigen interaction as it flowed through the column. The elution intensity can give an indication of the amount of protein that was attached to the column. The elution profile in this case showed that a significant amount of HSP90 was extracted, even though the fluorescent intensity is partially quenched by the low pH of the elution buffer. These results demonstrate that prior removal of unreacted label is not necessary with the use of these affinity columns. Functionalized columns could be used to extract other proteins in a similar manner, and extraction of multiple proteins could be achieved by immobilizing their respective antibodies on a single column.

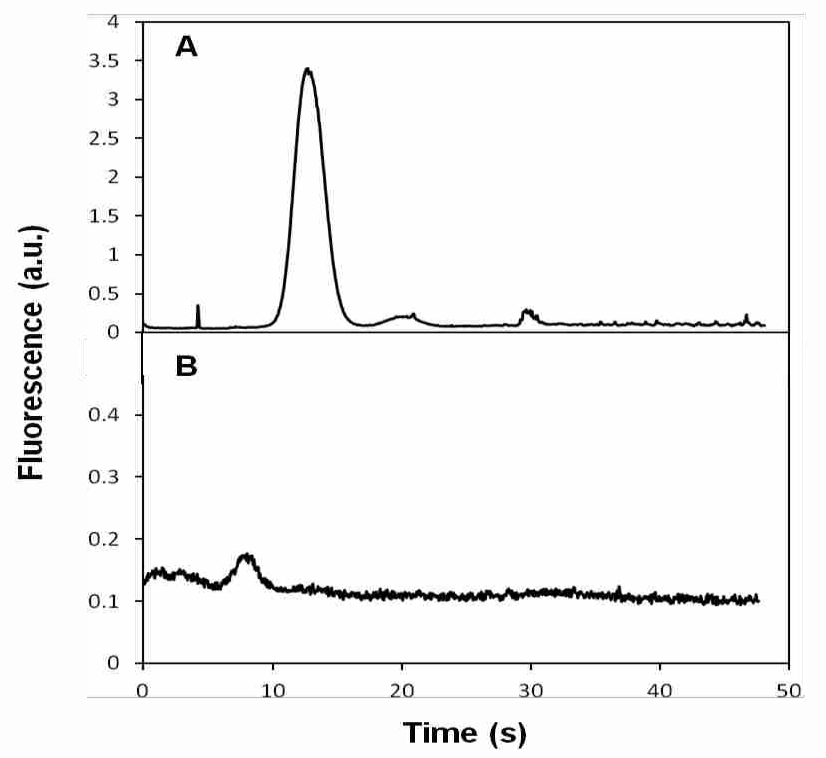


**Figure 2.7.** Elution profiles of 0.5 µg/mL Alexa Fluor 488 TFP ester from an affinity column that was a) unfunctionalized, and b) functionalized with anti-HSP90.

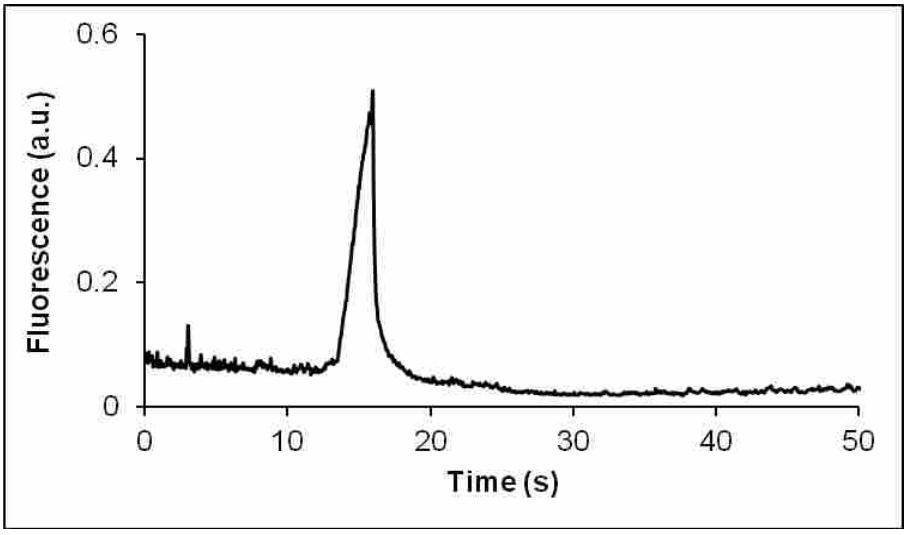


**Figure 2.8.** Elution profile of 1 µg/mL HSP90 from an affinity column that was functionalized with anti-HSP90.

## 2.5 REFERENCES


(1) Tainsky, M. A. *Biochim. Biophys. Acta* **2009**, *1796*, 176-193.

(2) Makarov, D. V.; Loeb, S.; Getzenberg, R. H.; Partin, A. W. *Annu. Rev. Med.* **2009**, *60*, 139-151.

(3) Bani-Yaseen, A.; Kawaguchi, T.; Price, A.; Culbertson, C.; Jankowiak, R. *Analytical and Bioanalytical Chemistry* **2011**, *399*, 519-524.

(4) Jmeian, Y.; El Rassi, Z. *J. Proteome Res.* **2009**, *8*, 4592-4603.

(5) Vizioli, N. M.; Rusell, M. L.; Carbajal, M. L.; Carducci, C. N.; Grasselli, M. *Electrophoresis* **2005**, *26*, 2942-2948.

(6) Cakal, C.; Ferrance, J. P.; Landers, J. P.; Caglar, P. *Anal. Chim. Acta.* **2011**, *690*, 94-100.

(7) Svec, F. *J. Chromatogr. A* **2010**, *1217*, 902-924.

(8) He, M.; Zeng, Y.; Sun, X.; Harrison, D. J. *Electrophoresis* **2008**, *29*, 2980-2986.

(9) Dossi, N.; Toniolo, R.; Pizzariello, A.; Susmel, S.; Bontempelli, G. *Electrophoresis* **2011**, *32*, 906-912.

(10) Felhofer, J. L.; Blanes, L.; Garcia, C. D. *Electrophoresis* **2010**, *31*, 2469-2486.

(11) Yang, W.; Sun, X.; Wang, H.-Y.; Woolley, A. T. *Anal. Chem.* **2009**, *81*, 8230-8235.

(12) Yang, W.; Yu, M.; Sun, X.; Woolley, A. T. *Lab Chip* **2010**, *10*, 2527-2533.

(13) Sun, X.; Yang, W.; Pan, T.; Woolley, A. T. *Anal. Chem.* **2008**, *80*, 5126-5130.

(14) Zhang, L.-Y.; Wang, H.; Liang, Z.; Shan, Y.-C.; Zhang, L.-H.; Zhang, Y.-K. *Se Pu* **2010**, *38*, 659-662.

(15) Kelly, R. T.; Woolley, A. T. *Anal. Chem.* **2003**, *75*, 1941-1945.

(16) Jacobson, S. C.; Hergenroder, R.; Koutny, L. B.; Warmack, R. J.; Ramsey, J. M. *Anal. Chem.* **1994**, *66*, 1107-1113.

# 3. ION-PERMEABLE MEMBRANE FOR ON-CHIP PRECONCENTRATION AND SEPARATION OF CANCER MARKER PROTEINS*

## 3.1 INTRODUCTION

Cancer, a malignant and invasive growth of cells in the body, is the second most common cause of death in the US.[1] Survival rates in some cancer types have improved over the years, due in part to detection at an early stage when the cancer can be easily treated.[2-4] The development of cost-effective techniques that are sensitive and specific enough to diagnose cancer at an earlier stage than is currently possible will further improve cancer survivability. Cancer biomarkers have been shown to enable early detection, and facilitate the prognosis and monitoring of the response to cancer therapy.[2] However, of the numerous proteins proposed as cancer biomarkers only nine have been approved by the FDA,[5] one of which is α-fetoprotein (AFP), a diagnostic marker for hepatocellular carcinoma. AFP is a 67 kDa glycoprotein which has high levels in fetal sera.[6] Its concentration decreases to trace levels soon after birth; therefore, raised AFP levels in adult serum usually indicate a disease state. Another biomarker of interest is heat shock protein 90 (HSP90), a 90 kDa molecular chaperone that oversees the proper folding of newly formed proteins. Many HSP90 clients are proteins whose mutation or overproduction promotes cancer, making HSP90 inhibition a target in cancer therapy.[7, 8] Even though HSP90 is presently not FDA approved, its elevated levels in many human cancer types indicate potential utility for diagnosis and the monitoring of response to treatment.[9] Enhanced detection of these and other biomarkers is thus important in early detection of cancer and follow-up of cancer therapy.

---

* This chapter is reproduced with permission from Electrophoresis, Nge, P. N.; Yang, W.; Pagaduan, J. V.; Woolley, A.T., *Electrophoresis* 2011, 32, 1133-1140. Copyright 2011 Wiley-VCH Verlag GmbH & Co.

A diagnostic technique that is applicable to point-of-care (POC) settings needs to be fast, sensitive and quantitative.[10] The method commonly used for protein detection is ELISA, which is effective for a large number of samples and thus best suited for clinical settings rather than POC analysis.[10] Microfluidic devices are attractive for POC analysis because they offer the benefits of portability, minimal solvent and reagent consumption, and speed.[11] Microchip capillary electrophoresis (μ-CE) in particular has been successfully applied to the analysis of different types of molecules, including cancer biomarkers.[12-14] An appealing aspect of miniaturization is integration: various components can easily be combined in these devices to perform multiple tasks including analyte extraction, control of fluidic movement and sample preconcentration. While microfluidics improves on the slower analysis times offered by ELISA,[10] the small volumes and pathlengths can lead to reduced sensitivity. Therefore, microfluidic assays could benefit considerably from integrated methods to improve the limits of detection.[15]

Several stacking procedures have been successfully used for sample preconcentration in a microfluidic format including field amplified sample stacking,[16] field amplified sample injection,[17] isotachophoresis (ITP),[18, 19] electric field gradient focusing,[20] temperature gradient focusing (TGF),[21] isoelectric focusing (IEF),[22] electrokinetic supercharging,[23] and sweeping.[24] Sometimes two of these techniques can be combined for improved results. Munson, et al.[21] combined a form of sample stacking, field amplified continuous sample injection, with TGF. The combination of electrokinetic injection with transient ITP has also been coupled with gel electrophoresis.[18] While methods like ITP and IEF may be compatible with μ-CE, they often require two or three different buffers, which complicate execution in a microchip format.

Moreover, the required coupling of many of these techniques with microchip gel electrophoresis renders the overall separation process more challenging. A technique known as electrophoretic exclusion has recently been used to achieve both selectivity and enrichment of proteins by manipulating voltage in combination with hydrodynamic flow.[25] The simplicity of this method promises potential for future application in a microchip format.

Other preconcentration methods for microfluidic systems involve affinity techniques like solid phase extraction (SPE),[26] and exclusion methods based on nanogaps[27, 28] or nanoporous filters.[15, 29-35] In affinity methods the analyte is generally made to adsorb to a column, and a different solution is used to elute the retained components. Affinity techniques are effective but are complicated by the need for different buffers to be used in pretreatment and analysis. Enrichment based on exclusion generally offers a simpler analysis setup, but a more complex device fabrication process. Nanogaps can be formed via photolithography[29] or by applying a high voltage to a PDMS-glass device to cause dielectric breakdown.[27, 28] In nanogap devices, preconcentration without subsequent separation has been done, but the process was lengthy (30-60 min).[28] In contrast, membrane-based preconcentration methods are generally faster than with nanogaps, and the fabrication methods have a range of complexity. Some materials used to fabricate these membranes are polycarbonate (PC),[33] track-etched PC,[32, 36] titania,[29] nafion,[37] and silica gel.[31] These membrane materials were anionic to concentrate analytes based on charge exclusion. For several device arrangements preconcentration only, without protein separation, was done.[29, 32, 33, 37] Long et al.[36] used a track-etched PC membrane to concentrate Rhodamine 123 and FITC-labeled ephedrine samples 1000-fold by SPE-μCE; however, the technique required careful timing of online injection after the SPE process. Foote et al.[31] used a porous

silica membrane in a glass microchip to obtain signal enhancement of ~600-fold by on-chip preconcentration followed by sodium dodecyl sulfate (SDS) – microchip gel electrophoresis separation. However, the use of glass devices and the coupling of a preconcentration membrane with gel-based separation require a more complicated fabrication process.

Hydrogel membranes involving acrylic monomers offer a special type of preconcentration system and can be either neutral or charged.[15, 30, 34, 35] The pore size of these membranes and their mechanical properties can be controlled by varying the ratio of cross-linking agent to acrylamide. Hatch et al.[15] integrated two acrylic polymer hydrogel structures in a glass device: one for size-based preconcentration (up to 1000-fold) and the other to separate the preconcentrated sample by SDS-gel electrophoresis. However, the fabrication of two different gels in a microdevice was somewhat complicated, and the proteins analyzed had to be denatured to achieve separation. Addition of an ionic comonomer, such as 2-acrylamido-2-methylpropanesulfonic acid (AMPS), to acrylamide imparts a negative charge and enables the membrane to be ion-selective.[38] This type of polymer membrane has been used for the preconcentration of model proteins,[30] but in that work preconcentration was not coupled to separation. In addition, Chun et al.[35] fabricated a glass microchip with a hydrogel made entirely of crosslinked AMPS; however, protein separation was not performed in conjunction with preconcentration. Yamamoto et al.[34] made a polymer membrane combining acrylamide and AMPS, and used it to couple $10^5$-fold preconcentration with μ-CE of separate samples of oligosaccharides, α1-acid glycoprotein, and glycopeptides, but not to analyze a mixture of proteins. Their monomer and crosslinker concentrations were high at 26% T and 20% C; moreover, the standard device layout did not make it easy to remove monomer solution after membrane polymerization. In summary,

hydrogel-based microchip preconcentration systems show promise in their ability to be fine-tuned easily, but simplifying fabrication procedures and application to the separation of proteins still needs further effort.

In this chapter, a polymer membrane was fabricated *in situ* and used for on-line preconcentration prior to separation of cancer marker proteins. The membrane consisted of acrylamide, N,N'-methylene-bisacrylamide and AMPS, and was photopolymerized in the microdevice near the injection intersection region. Negatively charged proteins were excluded from the porous membrane, enabling their enrichment. Initial characterization of the device with bovine serum albumin (BSA) led to a 40-fold enrichment in the μ-CE peak with 4 min of preconcentration time. Fine-tuning of the buffer pH provided baseline resolution of model cancer marker proteins, and careful control of preconcentration time kept peak broadening to a minimum. More than 10-fold enhancement of μ-CE signal in a protein mixture was achieved with just 1 min of preconcentration, and the entire analysis was completed in <5 min. Our approach provides a simple and fast route to the analysis of low-concentration samples.

## 3.2 EXPERIMENTAL SECTION

### 3.2.1 Reagents and materials

The monomers acrylamide and AMPS, as well as the cross-linking agent N,N'-methylene-bisacrylamide were purchased from Sigma-Aldrich (St. Louis, MO). Riboflavin was obtained from Eastman (Rochester, NY), tetramethylethylenediamine (TEMED) was from Invitrogen (Carlsbad, CA), and ammonium persulfate (APS) was obtained from EMD Chemicals (Gibbstown, NJ). Bovine serum albumin (BSA) was purchased from New England Biolabs

(Ipswich, MA), heat shock protein 90 (HSP90) was from Sigma-Aldrich and alpha-fetoprotein (AFP) was from Lee Biosolutions (St Louis, MO). The proteins were labeled with fluorescein isothiocyanate (FITC) or Alexa Fluor 488 TFP ester purchased from Invitrogen. Dimethyl sulfoxide (DMSO) was purchased from Sigma-Aldrich. Hydroxypropyl cellulose (HPC, average MW 100 000) was from Aldrich (Milwaukee, WI). PBS buffer (10 X, pH 7.4), anhydrous sodium carbonate, sodium bicarbonate, and sodium azide were purchased from EMD Chemicals. Amicon Ultra-0.5 centrifugal filter devices were obtained from Millipore (Billerica, MA).

### 3.2.2 Device fabrication

The microchips were made from poly(methyl methacrylate), PMMA, using a combination of photolithographic techniques, hot embossing and thermal bonding as previously described in Section 2.3.1.[39] The microchip design, shown in Figure 3.1A, is similar to an offset-T device, except for the addition of two reservoirs (4 and 6) and the channels leading to them. The channel connected to reservoir 4 helped to empty monomer solution from the channel leading to reservoir 2 after polymerization of the membrane. The channel leading to reservoir 6 provided for cross-injection, as an alternative to offset-T injection. The channels were ~15 μm deep and ~50 μm wide.

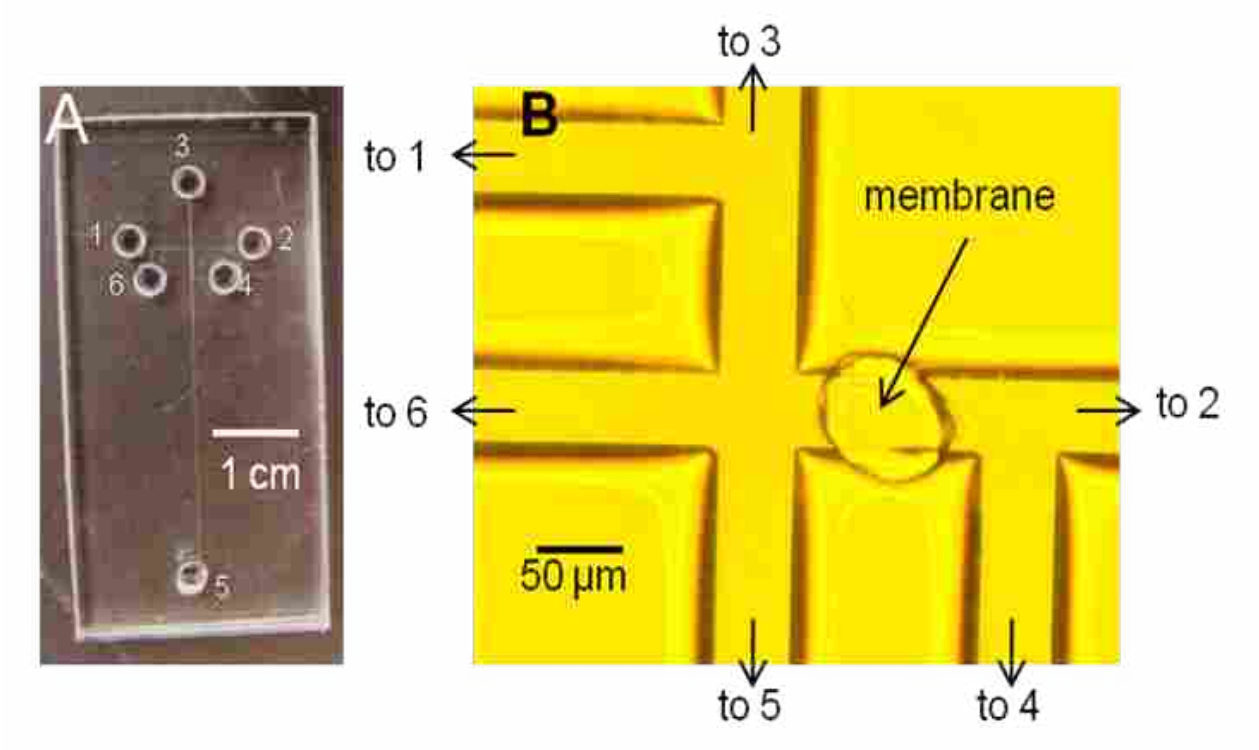


**Figure 3.1.** Photograph of a microfluidic device and zoom view of a preconcentration membrane. (A) Photograph of the microfluidic device used for sample preconcentration. Reservoir labels are 1, sample; 2, sample waste; and 3-6, buffer. The channel connected to reservoir 4 helped to empty the monomer solution from the channel leading to reservoir 2 after polymerization of the gel. The channel leading to reservoir 6 provides cross-T injection while the channel connected to reservoir 1 provides offset-T injection. (B) Photomicrograph of microchannel intersection region showing position of the polymerized membrane, indicated by the black arrow.

Before gel polymerization the microchannels were conditioned sequentially with 0.1 M HCl and 0.1 M NaOH, rinsed with deionized water and dried with vacuum. This made the channel surface more hydrophilic and improved adhesion of the membrane to the channel walls.[40, 41] The pore size of the membrane depends on the total amount of acrylamide present (%T), and the amount of cross-linker (%C), where T is percentage of acrylamide, bisacrylamide and AMPS, expressed in grams per 100 mL of mixture, and C is the percentage of bisacrylamide in the total monomer content. To fabricate the membrane, an 8% T and 5% C monomer solution was prepared. The

mass percent of AMPS in the total mixture was 0.5%. The solution was filtered with a 0.2 μm syringe filter and degassed. To initiate polymerization, riboflavin and APS were added to a final mass percent of 0.004% and 0.008%, respectively, followed by addition of 1.5 μL of TEMED per mL of monomer solution. A 10 μL aliquot of the monomer solution was immediately placed in reservoir 3 and left for a few seconds to fill the microchip by capillary action, after which the remaining solution in reservoir 3 was removed to prevent hydrodynamic flow during photopolymerization. A 488 nm laser beam (1 mW) was focused on the membrane location for ~45 s to produce a polymer membrane with diameter of ~60 μm (Figure 3.1B). The unpolymerized monomer solution was then removed from the chip using vacuum, and the channels were rinsed with deionized water.

### 3.2.3 Fluorescent labeling

The protein solutions were prepared in carbonate buffer, pH 9.2, at a concentration of 2 mg/mL. FITC solution was prepared by dissolving 2 mg of FITC in 100 μL of anhydrous DMSO. This FITC solution (10 μL) was added to 250 μL of protein sample and incubated in the dark, first for 3 h at room temperature and then overnight at 4 ºC. For labeling with Alexa Fluor 488 TFP ester, the dye was dissolved in DMSO to a concentration of 10 mg/mL. Dye solution (5 μL) was added to 250 μL of sample and incubated in the dark for 1 h at room temperature. The unconjugated dye in each case was separated from the protein samples by diafiltration, using an Amicon Ultra-0.5 centrifugal filter device (30 kDa MWCO) and 10 mM PBS, pH 7.4. The labeled protein was collected, and sodium azide was added to a final concentration of 2 mM. The fluorescently labeled samples were stored in the dark at 4 ºC until used.

### 3.2.4 Electrophoresis experiments

The separation buffer for single-component samples was 10 mM carbonate (pH 9.2) containing 0.1% HPC, while that for the protein mixture was 10 mM phosphate (pH 7.0) containing 0.05% HPC. Buffer solution was filled in the channels and all reservoirs, except reservoir 1 which was filled with the sample solution (20 μL). Platinum electrodes were placed in reservoirs 1, 2, 3 and 5. The electrodes were connected to high voltage power supplies (Stanford Research Systems, Sunnyvale, CA) via a custom-built switch. Electrophoresis involved a standard "pinched injection" with an offset-T layout.[42, 43] For injection, reservoirs 1, 3, and 5 were grounded while 600 V were applied to reservoir 2. For separation, reservoir 3 was grounded, 600 V were applied to reservoirs 1 and 2, and 1600 V were applied to reservoir 5.

The laser-induced fluorescence system used to detect the analytes has been described previously.[44] Briefly, sample excitation was done with a 488 nm laser (Ar ion) focused at a spot in the channel close to reservoir 5 using a 20× 0.45 NA objective. Emitted photons were detected (after spectral and spatial filtering) with a photomultiplier tube, then amplified and filtered, and finally recorded on a computer. The data sampling rate was 20 Hz.

### 3.2.5 Data analysis

Calculation of concentrations was based on peak areas, obtained by subtracting the background individual signal values from a given peak and then summing the results. For comparison, the peak height was obtained by subtracting the baseline from the peak maximum. For preconcentration of HSP90 and AFP, control data were obtained from similar chips without a preconcentration membrane. The peak areas or heights obtained after preconcentration were then

divided by the corresponding areas or heights before preconcentration to determine the amount of preconcentration that occurred.

### 3.3 RESULTS AND DISCUSSION

The devices used for these experiments were designed to provide a good yield during polymerization of the preconcentration membrane. When a simple offset T design was used, it was difficult to empty the channel arm of the microchip leading to reservoir 2 (Figure 3.1A) after polymerization of the gel. Therefore, a channel connected to reservoir 4 was added to facilitate the flushing process after polymerization. Our device layout can also be used for either cross-injection (sample in reservoir 6) or offset-T injection (sample in reservoir 1). In the experiments reported here, offset-T injection was used to increase sample plug volume.

The membrane was photopolymerized in the injection channel just beyond the intersection region (Figure 3.1B). The properties of acrylamide gels were found to depend not only on the monomer composition but also on polymerization conditions. When riboflavin only was used as the initiator, polymerization was much slower (5-10 min), and the resulting membrane was more porous and less stable. Addition of APS decreased polymerization time and made the process more reproducible. In addition, when these two initiators were combined the total amount of initiator was lower, decreasing undesirable side effects caused by excess initiator concentration.[45] The diameter of our membrane was ~60 μm. Larger membranes increased the electrical resistance, leading to a higher voltage drop across the membrane, which negatively affected separation efficiency.[15] The apparent pore radius for a 10.5% T, 5% C gel was reported

to be 21 nm,[46] so our 8% T, 5% C gel is estimated to have a pore radius somewhat larger than that.

BSA was used initially to test the effectiveness of the preconcentration membrane. The buffer was 10 mM carbonate, pH 9.2 with 0.1% HPC added to suppress electroosmotic flow (EOF). Previous experiments had shown that 0.5% HPC was effective in suppressing EOF to yield reproducible results;[39] however, 0.5% HPC was found to block the membrane, resulting in poor separation. Thus, lower HPC concentrations were used (0.05-0.1%) which did not block the membrane but still provided adequate separation efficiency.

Electropherograms of increasing concentrations of BSA (Figure 3.2A) show corresponding increases in peak area. Figure 3.2B shows μ-CE of 5 nM BSA without preconcentration, along with other electropherograms after on-chip preconcentration times of 30 s to 4 min. Preconcentration times of 30 s to 1 min produce ~10-fold enhancement of signal without compromising the peak shape. A larger, 20-fold enhancement was produced with 2 min preconcentration, but peak tailing was beginning to be evident. By 4 min of preconcentration a significant degree of peak tailing occurred with the ~40-fold enrichment. Thus, enrichment factors of at least 10 can be obtained quickly and without distortion of peak shape; even higher factors (~40) can be achieved if some peak shape distortion can be tolerated.

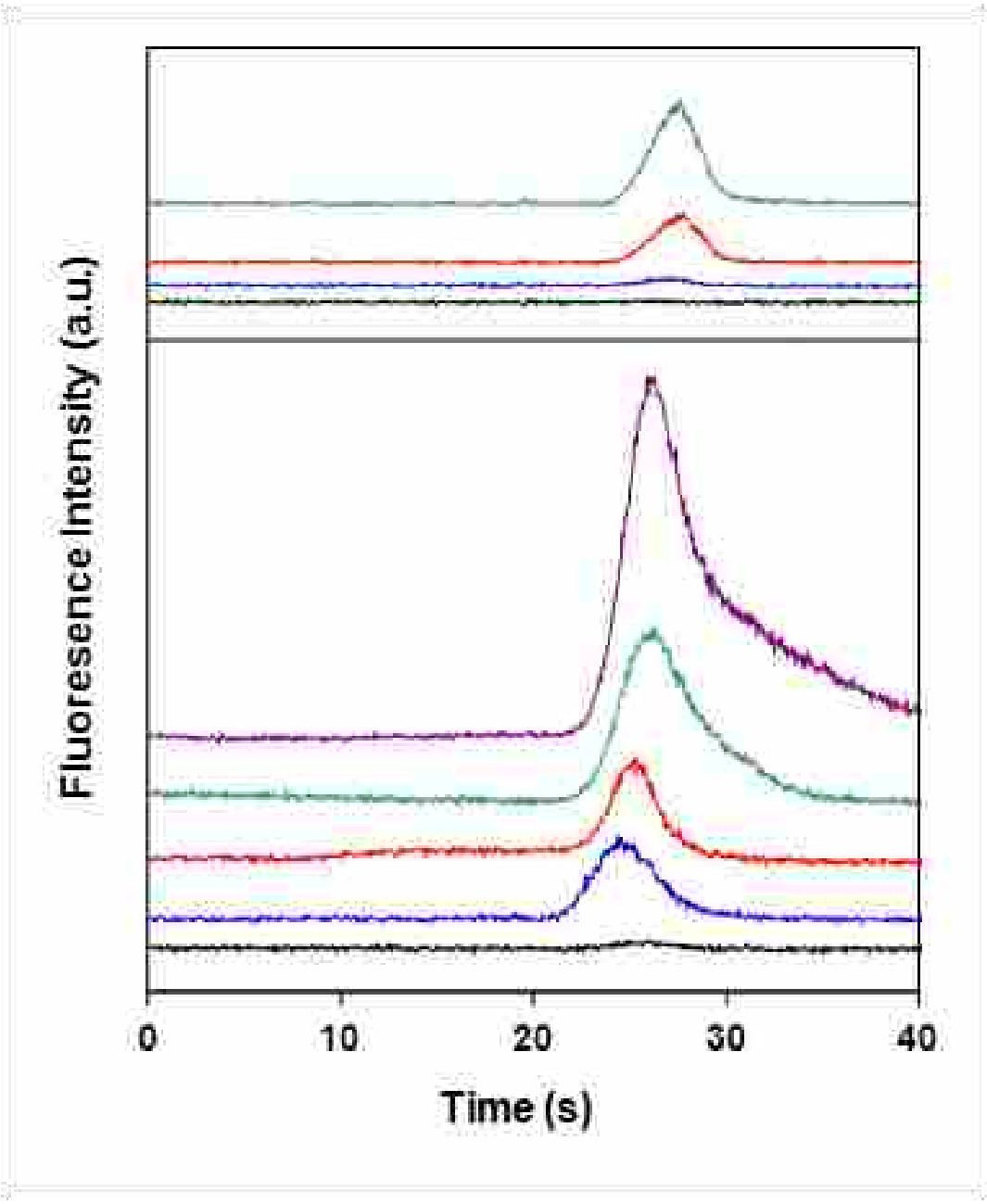


**Figure 3.2.** Dependence of peak width on sample concentration and preconcentration effects on peak width. (A) Dependence of peak shape on injected BSA concentration during μ-CE. BSA concentrations are: 1 nM, black; 5 nM, blue; 20 nM, red; 50 nM, green. (B) Effect of preconcentration time on BSA signal during μ-CE; all traces are for 5 nM initial BSA concentration. The preconcentration times for the curves are: 0 min (no preconcentration), black; 0.5 min, blue; 1 min, red; 2 min, green; 4 min, violet. All electropherograms are offset vertically for clarity.

Peak tailing at longer preconcentration times could be caused by concentration polarization (CP), which occurs when current traverses an ion-selective membrane.[47] Increased cation and anion concentrations on alternate sides of the membrane make a concentration gradient that increases the electrical resistance across the membrane, resulting in a local voltage drop.[48] This voltage drop reduces the effectiveness of the potentials applied to reservoirs 1 and 2 during separation to prevent sample leakage and pull remaining analyte out from the intersection,[49] leading to peak tailing. Since this CP-induced voltage drop increases as a function of preconcentration time,[15, 48] most of our experiments were carried out with a preconcentration time of ~1 min to limit these tailing issues.

Quantitation of the BSA samples was done on the basis of peak area, which increased linearly as a function of concentration, as seen in Figure 3.3A. Figure 3.3B similarly shows a linear increase in BSA peak area with preconcentration time for the range of 0.5 to 4 min. A 5 min preconcentration time (result not shown) resulted in a peak with severe tailing and a height that was lower than that in the 4 min result. At this point the negative factors associated with a long preconcentration time became apparent. This tailing puts an upper limit of ~4 min on the preconcentration time, to allow for adequate separation performance in μ-CE.

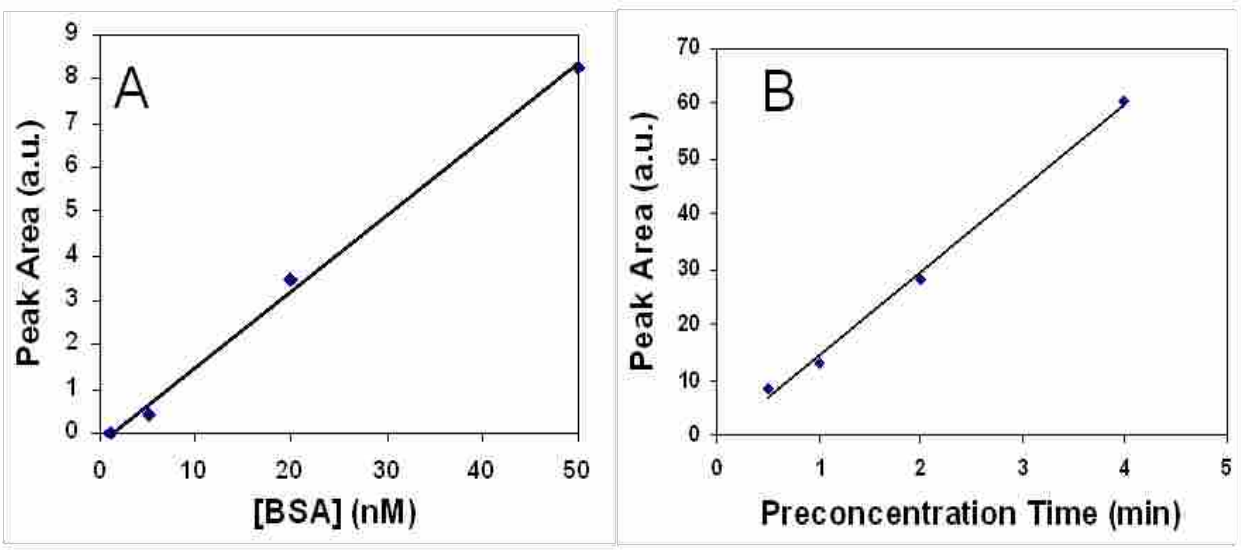


**Figure 3.3.** Dependence of μ-CE peak area on BSA concentration and preconcentration time. (A) Plot of peak area as a function of BSA concentration. The slope is 0.71 ±0.02, and the intercept is -0.21 ± 0.16, with $R^2$ = 0.9972. (B) Plot of peak area as a function of preconcentration time. The slope is 15.10 ±0.60, and the intercept is -0.7 ± 1.5, with $R^2$ = 0.9959.

The preconcentration and separation conditions optimized for BSA were next applied to AFP and HSP90. Preconcentration of 5 nM HSP90 having a small amount of FITC (Figure 3.4A) was done for 4 min, resulting in ~80-fold enrichment of the HSP90 peak in the electropherogram. The enriched peak was symmetrical, but its migration time was somewhat slower than in the separation without preconcentration. The slower migration time was likely due to some CP occurring during this longer preconcentration time, as noted above. The FITC peak in the separation without enrichment was almost undetectable; however, the peak became readily observable after preconcentration, with ~20 fold enhancement. Even though the pore size of the membrane was large enough to allow the passage of FITC, electrostatic repulsion between FITC and the AMPS in the membrane allowed some preconcentration. The preconcentration of 10 nM AFP for 1 min in Figure 3.4B yielded a symmetrical peak with an enrichment factor of 16. The

AFP peak was somewhat broader and migrated slower than the HSP90 peak in the separation without preconcentration.[12]

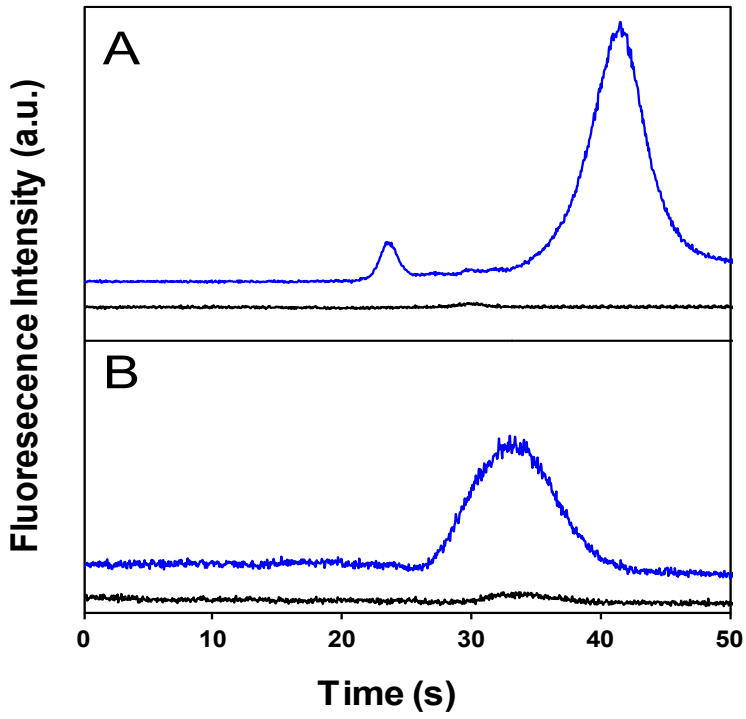


**Figure 3.4.** Preconcentration and μ-CE of cancer-related proteins. (A) Preconcentration of 5 nM HSP90. The peak at ~23 s is FITC. HSP90 (peak at ~42 s) is concentrated ~80-fold with the 4 min preconcentration time. (B) Preconcentration of 10 nM AFP. AFP is concentrated ~15-fold in 1 min. In both (A) and (B) the trace in black represents μ-CE without preconcentration, while the blue trace denotes preconcentration followed by μ-CE separation.

To determine if the peak width of AFP was influenced by the FITC tags, AFP was also labeled with Alexa Fluor 488. The μ-CE peak produced by Alexa Fluor 488-labeled AFP was ~2 s narrower than that of FITC-labeled AFP (Figure 3.5), most likely due to reduced impacts of multiple site labeling. However, the electrophoretic mobility of Alexa Fluor 488-labeled AFP was slightly faster than FITC-labeled AFP, so when run with HSP90 there was a higher degree of peak overlap. In these experiments the chip-to-chip reproducibility in migration time for

the same sample under the same conditions was ±1s while the reproducibility in peak height depended on the channel heights. Chips fabricated from the same template had good peak height reproducibility of ±0.2 units (on a scale of 0-5). The peak height variability for chips made from different templates was as much as ±1 unit on this same scale.

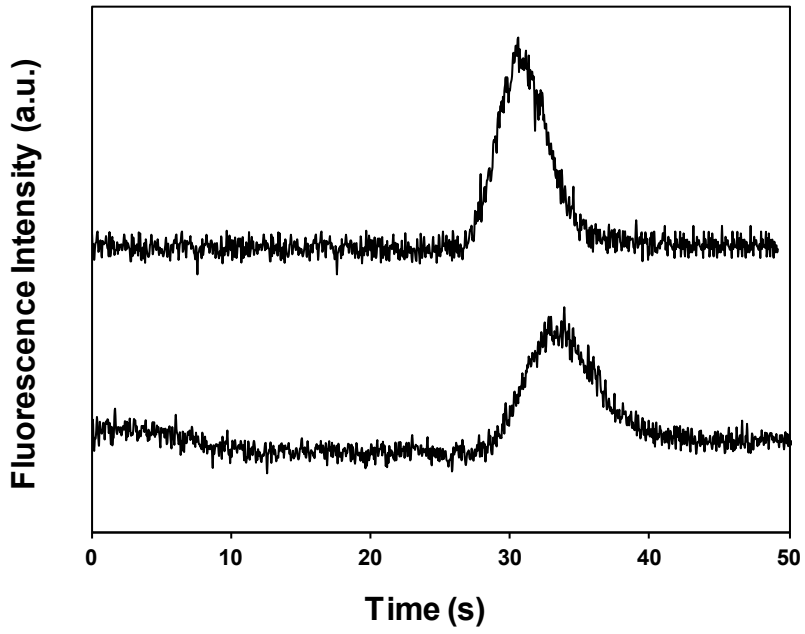


**Figure 3.5.** Electropherograms of 50 nM AFP labeled with FITC (bottom) and Alexa Fluor 488 TFP ester (top). Traces are offset vertically. AFP labeled with FITC was about ~2 s broader than that labeled with Alexa Fluor 488. Peak intensity was ~2-fold higher with Alexa Fluor 488-labeled AFP than the FITC-tagged protein, and this peak also had a higher electrophoretic mobility.

I found that the resolution of AFP and HSP90 depended on the pH. Poor resolution was obtained when electrophoresis was carried out in 10 mM carbonate buffer (pH 10.5) but resolution improved to near baseline at pH 9.2, with baseline resolution being achieved with a pH of ~7 (Figure 3.6). Liu et al.[50] likewise noticed an improvement in protein resolution at lower pH,

which they believed was caused by an increase in the charge difference between proteins at pH values near the pI.

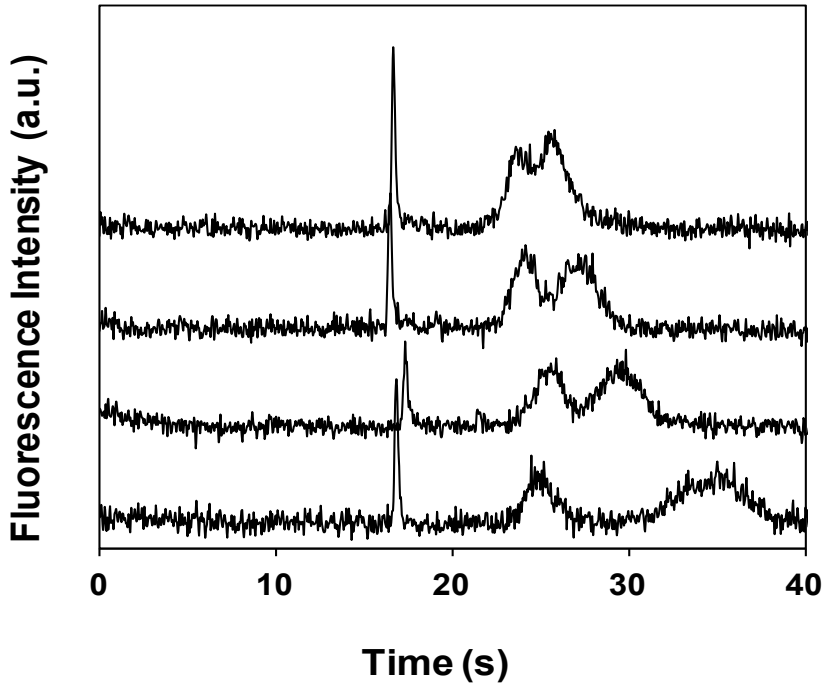


**Figure 3.6.** Effect of pH on resolution of a mixture of HSP90 and AFP. The pHs were from bottom to top: 7.0, 9.2, 10.0, and 10.5. Resolution is improved at lower pHs.

Preconcentration and separation of mixtures of different concentrations of HSP90 and AFP (Figure 3.7) show well-resolved peaks with 1 min preconcentration time. The enrichment factors for HSP90 and AFP in the 10 nM mixture were 10- and 16-fold, respectively, while those for the 20 nM mixture were 7- and 13-fold, respectively. Thus, a slightly higher enrichment factor was achieved with lower sample concentrations. AFP also showed a higher level of preconcentration compared to HSP90, which could be attributed to factors such as size, charge, or mobility. The diagnostic threshold has been reported to be 20 ng/mL (0.3 nM) for AFP[12] and ~20 ng/mL (0.2 nM) for HSP90.[51, 52] Detection limits achieved with this preconcentration technique are ~42 ng/mL for AFP and ~6 ng/mL for HSP90. Though the limit of detection for AFP is above the

diagnostic threshold, it can be easily improved by a slight increase in preconcentration time. An additional enrichment factor of 10-fold or more could be achieved by optimizing the pore size and charge of the membrane such that longer preconcentration times could be used without compromising separation efficiency. Importantly, these results demonstrate a rapid and simple procedure by which multiple cancer biomarkers can be concentrated ~10-fold or more with a straightforward, 1 min process prior to μ-CE analysis.

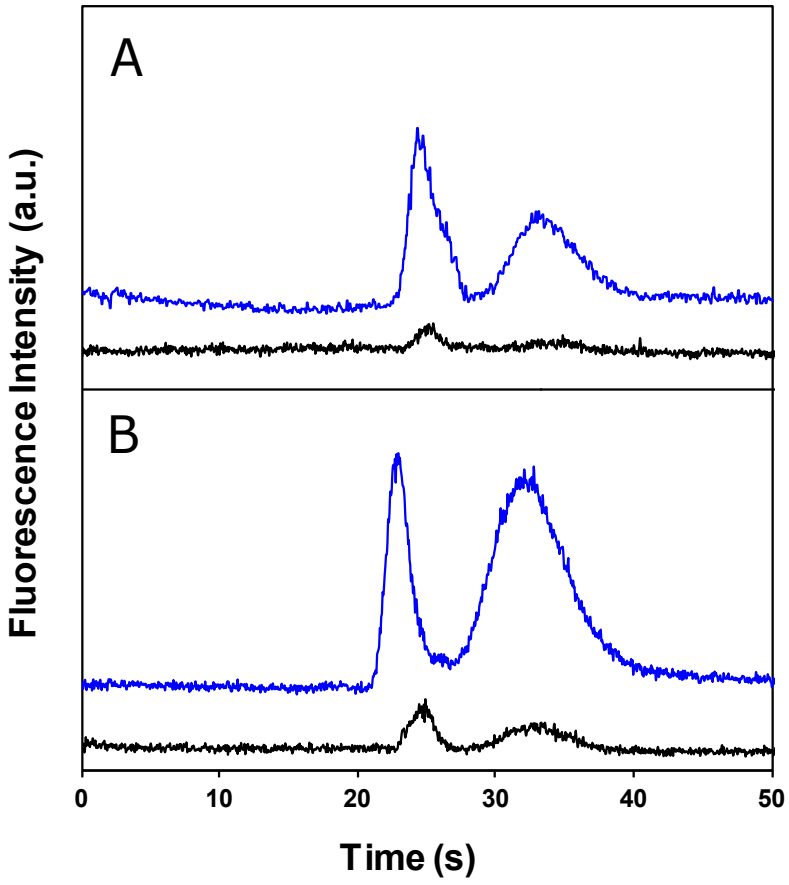


**Figure 3.7.** Preconcentration and μ-CE of cancer-related proteins. Mixture of HSP90 and AFP; (A) 10 nM and (B) 20 nM. Preconcentration time was 1 min. The black traces represent μ-CE without preconcentration, while the blue traces denote preconcentration followed by separation. Enrichment factors are given in the text.

## 3.4 REFERENCES


(1) Statistic *provided by the American Cancer Society at http://www.cancer.org/Research/CancerFactsFigures/CancerFactsFigures/cancer-facts-and-figures-2010* **Accessed 12/02/2010**.
(2) Tainsky, M. A. *Biochim. Biophys. Acta* **2009**, *1796*, 176-193.
(3) Tchagang, A. B.; Tewfik, A. H.; DeRycke, M. S.; Skubitz, K. M.; Skubitz, A. P. N. *Mol. Cancer Ther.* **2008**, *7*, 27-37.
(4) Gromov, P.; Gromova, I.; Bunkenborg, J.; Cabezon, T.; Moreira, J. M. A.; Timmermans-Wielenga, V.; Roepstorff, P.; Rank, F.; Celis, J. E. *Mol. Oncol.* **2010**, *4*, 65-89.
(5) Polanski, M.; Anderson, N. L. *Biomarker Insights* **2006**, *1*, 1-48.
(6) Uversky, V. N.; Narizhneva, N. V.; Ivanova, T. V.; Kirkitadze, M. D.; Tomashevski, A. Y. *FEBS Lett.* **1997**, *410*, 280-284.
(7) Yi, F.; Regan, L. *ACS Chem. Biol.* **2008**, *3*, 645-654.
(8) Biamonte, M. A.; Van de Water, R.; Arndt, J. W.; Scannevin, R. H.; Perret, D.; Lee, W.-C. *J. Med. Chem.* **2010**, *53*, 3-17.
(9) Bagatell, R.; Whitesell, L. *Mol. Cancer Ther.* **2004**, *3*, 1021-1030.
(10) Heath, J. R.; Davis, M. E. *Annu. Rev. Med.* **2008**, *59*, 251-265.
(11) Zhang, J. Y.; Do, J.; Premasiri, W. R.; Ziegler, L. D.; Klapperich, C. M. *Lab Chip* **2010**, *10*, 3265-3270.
(12) Yang, W.; Yu, M.; Sun, X.; Woolley, A. T. *Lab Chip* **2010**, *10*, 2527-2533.
(13) Minarik, M.; Gassman, M.; Belsanova, B.; Pesek, M.; Schouten, J.; Chudoba, R.; Gas, B.; Benesova, L. *Electrophoresis* **2010**, *31*, 3518-3524.
(14) Zhang, S.; Cao, W.; Li, J.; Su, M. *Electrophoresis* **2009**, *30*, 3427-3435.
(15) Hatch, A. V.; Herr, A. E.; Throckmorton, D. J.; Brennan, J. S.; Singh, A. K. *Anal. Chem.* **2006**, *78*, 4976-4984.
(16) Shiddiky, M. J. A.; Park, H.; Shim, Y.-B. *Anal. Chem.* **2006**, *78*, 6809-6817.
(17) Gong, M.; Wehmeyer, K. R.; Limbach, P. A.; Arias, F.; Heineman, W. R. *Anal. Chem.* **2006**, *78*, 3730-3737.
(18) Wainright, A.; Nguyen, U. T.; Bjornson, T.; Boone, T. D. *Electrophoresis* **2003**, *24*, 3784-3792.
(19) Wang, J.; Zhang, Y.; Mohamadi, M. R.; Kaji, N.; Tokeshi, M.; Baba, Y. *Electrophoresis* **2009**, *30*, 3250-3256.
(20) Sun, X.; Farnsworth, P. B.; Woolley, A. T.; Tolley, H. D.; Warnick, K. F.; Lee, M. L. *Anal. Chem.* **2008**, *80*, 451-460.
(21) Munson, M. S.; Danger, G.; Shackman, J. G.; Ross, D. *Anal. Chem.* **2007**, *79*, 6201-6207.
(22) Shimura, K.; Takahashi, K.; Koyama, Y.; Sato, K.; Kitamori, T. *Anal. Chem.* **2008**, *80*, 3818-3823.
(23) Xu, Z.; Ando, T.; Nishine, T.; Arai, A.; Hirokawa, T. *Electrophoresis* **2003**, *24*, 3821-3827.
(24) Pan, Q.; Zhao, M.; Liu, S. *Anal. Chem.* **2009**, *81*, 5333-5341.
(25) Meighan, M. M.; Vasquez, J.; Dziubcynski, L.; Hews, S.; Hayes, M. A. *Anal. Chem.* **2010**, Article ASAP, 10.1021/ac1025495.
(26) Yu, C.; Davey, M. H.; Svec, F.; Fréchet, J. M. J. *Anal. Chem.* **2001**, *73*, 5088-5096.
(27) Kim, S. M.; Burns, M. A.; Hasselbrink, E. F. *Anal. Chem.* **2006**, *78*, 4779-4785.
(28) Lee, J. H.; Chung, S.; Kim, S. J.; Han, J. *Anal. Chem.* **2007**, *79*, 6868-6873.

(29) Hoeman, K. W.; Lange, J. J.; Roman, G. T.; Higgins, D. A.; Culbertson, C. T. *Electrophoresis* **2009**, *30*, 3160-3167.
(30) Song, S.; Singh, A. K.; Kirby, B. J. *Anal. Chem.* **2004**, *76*, 4589-4592.
(31) Foote, R. S.; Khandurina, J.; Jacobson, S. C.; Ramsey, J. M. *Anal. Chem.* **2005**, *77*, 57-63.
(32) Long, Z.; Liu, D.; Ye, N.; Qin, J.; Lin, B. *Electrophoresis* **2006**, *27*, 4927-4934.
(33) Wu, D.; Steckl, A. J. *Lab Chip* **2009**, *9*, 1890-1896.
(34) Yamamoto, S.; Hirakawa, S.; Suzuki, S. *Anal. Chem.* **2008**, *80*, 8224-8230.
(35) Chun, H.; Chung, T. D.; Ramsey, J. M. *Anal. Chem.* **2010**, *82*, 6287-6292.
(36) Long, Z.; Shen, Z.; Wu, D.; Qin, J.; Lin, B. *Lab Chip* **2007**, *7*, 1819-1824.
(37) Shen, M.; Yang, H.; Sivagnanam, V.; Gijs, M. A. M. *Anal. Chem.* **2010**, *82*, 9989-9997.
(38) Travas-Sejdic, J.; Easteal, A. *Polym. Gels Networks* **1997**, *5*, 481-502.
(39) Sun, X.; Yang, W.; Pan, T.; Woolley, A. T. *Anal. Chem.* **2008**, *80*, 5126-5130.
(40) Diaz-Quijada, G. A.; Peytavi, R.; Nantel, A.; Roy, E.; Bergeron, M. G.; Dumoulin, M. M.; Veres, T. *Lab Chip* **2007**, *7*, 856-862.
(41) Chen, R.; Guo, H.; Shen, Y.; Hu, Y.; Sun, Y. *Sens. Actuators, B* **2006**, *114*, 1100-1107.
(42) Jacobson, S. C.; Hergenroder, R.; Koutny, L. B.; Ramsey, J. M. *Anal. Chem.* **1994**, *66*, 1114-1118.
(43) Yang, W.; Sun, X.; Pan, T.; Woolley, A. T. *Electrophoresis* **2008**, *29*, 3429-3435.
(44) Kelly, R. T.; Woolley, A. T. *Anal. Chem.* **2003**, *75*, 1941-1945.
(45) Menter, P. *Bio-Rad Bulletin1156* **2000**, Bio-Rad Laboratories, Hercules, CA 94547 USA.
(46) Stellwagen, N. C. *Electrophoresis* **1998**, *19*, 1542-1547.
(47) Nischang, I.; Reichl, U.; Seidel-Morgenstern, A.; Tallarek, U. *Langmuir* **2007**, *23*, 9271-9281.
(48) Dhopeshwarkar, R.; Crooks, R. M.; Hlushkou, D.; Tallarek, U. *Anal. Chem.* **2008**, *80*, 1039-1048.
(49) Currie, C. A.; Heineman, W. R.; Halsall, H. B.; Seliskar, C. J.; Limbach, P. A.; Arias, F.; Wehmeyer, K. R. *J. Chromatogr. B* **2005**, *824*, 201-205.
(50) Liu, Y.; Foote, R. S.; Culbertson, C. T.; Jacobson, S. C.; Ramsey, R. S.; Ramsey, J. M. *J. Microcolumn Sep.* **2000**, *12*, 407-411.
(51) Sun, Y.; Zang, Z.; Xu, X.; Zhang, Z.; Zhong, L.; Zan, W.; Zhao, Y.; Sun, L. *Int. J. Mol. Sci.* **2010**, *11*, 1423–1433.
(52) Szerafin, T.; Hoetzenecker, K.; Hacker, S.; Horvath, A.; Pollreisz, A.; Arpad, P.; Mangold, A.; Wliszczak, T.; Dworschak, M.; Seitelberger, R.; Wolner, E.; Ankersmit, H. J. *Ann. Thorac. Surg.* **2008**, *85*, 80-87.

# 4. MICROFLUIDIC CHIPS WITH REVERSED-PHASE MONOLITHS FOR SOLID PHASE EXTRACTION AND ON-CHIP LABELING*

## 4.1 INTRODUCTION

The integration of multiple functions in a single device can result in faster, cheaper and improved analysis compared to traditional laboratory methods.[1] Many such processes have been integrated in microfluidic devices, including extraction/purification,[2-6] labeling,[7, 8] preconcentration,[9, 10] microdialysis,[11, 12] and detection.[13, 14] One of the greatest difficulties in achieving completely miniaturized and integrated analysis has been the step of sample preparation,[15] although important progress is being made in selected areas as noted below. Importantly, solid phase extraction (SPE) has been used in integrated sample processing, including extraction, purification and preconcentration.[2, 5, 6]

SPE is a common sample preparation method wherein analytes are retained on a solid support and are subsequently eluted in a concentrated form.[16] The most common SPE modes in microfluidics are affinity[4, 17, 18] and reversed-phase.[6, 19, 20] Affinity SPE in microchips has been used to extract and quantify four cancer biomarkers in blood,[4] to preconcentrate and purify PCR products,[17] and to extract thiazole orange-conjugated adenosine monophosphate.[18] Reversed-phase columns are useful in the extraction of non-polar to moderately polar compounds. Silica-based materials are common reversed-phase SPE supports, having been used for the extraction of parabens and fluorescent dyes,[6] the preconcentration of peptides and cytochrome c,[19] and the concentration and separation of Rhodamine 123 and fluorescein isothiocyanate (FITC)-labeled

---

* This chapter is reproduced with permission from Journal of Chromatography A, Nge, P. N.; Pagaduan, J. V.; Yu, M; Woolley, A. T., *J. Chromatogr. A* 2012, 1261, 129-135. Copyright 2012, Elsevier.

ephedrine.[20] Monolithic columns are seeing increased usage because they can be easily prepared on-chip without the need for retaining structures like frits,[5, 21] and the porosity and surface area can be tuned by varying the monomer/porogen composition.[22] Neutral methacrylates are generally hydrophobic enough for reversed-phase SPE.[23, 24] Cyclic olefin copolymer (COC) is a preferred polymer material for SPE microchips because of its stability in organic solvents such as acetonitrile that are used for elution.[24, 25] Though photografting is generally used to modify the microchannel for enhanced monolith/wall adhesion,[24] it has also been shown that monoliths fabricated in COC devices can be stable without surface pretreatment.[26]

The integration of SPE with capillary electrophoresis or microchip electrophoresis (μCE) offers the advantages of improved sensitivity and sample cleanup, along with shorter analysis times, reduced sample loss and increased automation.[20, 27] Typically, when SPE is coupled to μCE, an interface is used to control the transfer of analytes from the SPE column to the separation channel. In the analysis of dopamine by SPE-μCE, polydimethylsiloxane (PDMS) microvalves were used to segregate the processes of extraction, rinsing, sample elution and separation.[23] In a different setup, a nanoporous membrane sandwiched between two PDMS layers was used as an electrokinetic valve to separate the processes of SPE and electrophoretic separation.[20] In these PDMS SPE-μCE systems, separation of small molecules was done, which is less complicated since they typically do not bind as much as proteins to the device walls.[28]

Many samples do not fluoresce naturally and have to be derivatized to take advantage of the superior sensitivity of laser-induced fluorescence detection. Labeling is often performed off-chip, but on-chip labeling has been achieved both in pre-column[7, 8, 29] and post-column[30-32] formats.

Conventional dyes with high quantum yield, such as Alexa Fluor and fluorescein, are often used to label analytes. Additionally, fluorogenic reagents,[7, 8, 33] which are weakly fluorescent until they react with a primary amine, have been used for on-chip derivatization because they produce lower background fluorescence, their reaction kinetics are fast, and they do not change the electrical charge of the sample.[34] The fluorogenic reagents, CE dye 503,[7] ThioGlo-1,[8] and naphthalene-2,3-dicarboxaldehyde,[35] have been used for on-chip derivatization. While acceptable results were obtained from these integrated systems, lower limits of detection, avoiding on-line mixing of high concentrations of fluorescent dyes, and addressing system peaks and background fluorescence are all areas where improvement is desirable.

In this chapter I demonstrate a novel approach combining SPE with on-chip labeling and purification to improve over previous methods. I show that samples retained on a solid support can be concentrated and labeled on-chip prior to elution. Reversed-phase butyl methacrylate (BMA) porous polymer monoliths were formed in COC microdevices and used to study the retention of fluorophores, amino acids and proteins. The retained and concentrated samples were then labeled on-chip with Alexa Fluor 488 TFP ester or Chromeo P503. Subsequent rinsing to remove unreacted dye and selective elution of labeled sample relative to unconjugated fluorophore helped to greatly reduce the background fluorescence typically observed in on-chip labeling. On-chip labeling of heat shock protein 90 (HSP90) resulted in a concentration-dependent area of the eluted peak, demonstrating the ability of this method to quantify on-chip labeled samples. This chapter thus offers improved capabilities in on-chip labeling for miniaturized analysis.

## 4.2 EXPERIMENTAL

### 4.2.1 Reagents and materials

Zeonor 1020R (COC) was purchased from Zeon Chemicals (Louisville, KY, USA). Methyl methacrylate (MMA), BMA, lauryl methacrylate (LMA), 2,2-dimethoxy-2-phenylacetophenone (DMPA), 1-dodecanol, cyclohexanol, Tween 20, ethylene dimethacrylate (EDMA), and isopropyl alcohol were obtained from Sigma-Aldrich (St. Louis, MO, USA). Bovine serum albumin (BSA) was purchased from New England Biolabs (Ipswich, MA, USA) and HSP90 was from Sigma-Aldrich. The amino acids glycine, aspartic acid, phenylalanine and arginine were obtained from Sigma-Aldrich. The amino acids were labeled with FITC, while the proteins were labeled with Alexa Fluor 488 TFP ester. Both fluorophores were from Invitrogen (Carlsbad, CA, USA). Chromeo P503 was obtained from Active Motif (Carlsbad, CA, USA). Fluorescein (sodium salt) and dimethyl sulfoxide (DMSO) were purchased from Sigma-Aldrich. Hydroxypropyl cellulose (HPC, 100 kDa average molecular weight) was from Aldrich (Milwaukee, WI, USA). Sodium dodecyl sulfate (SDS) was obtained from Fisher Scientific (Pittsburgh, PA, USA). Buffer solutions were made from anhydrous sodium carbonate, sodium bicarbonate, acetonitrile (ACN), and sodium azide, all from EMD Chemicals (Gibbstown, NJ, USA). Amicon Ultra-0.5 centrifugal filter devices were obtained from Millipore (Billerica, MA, USA). All solutions were prepared with deionized water (18.3 MΩ cm) purified by a Barnstead EASYpure UV/UF system (Dubuque, IA, USA).

### 4.2.2 Device fabrication

COC plates were obtained by cutting the sheets into 2" x 1" pieces with a bandsaw. Holes in the cover plate were then drilled to serve as reservoirs in the bonded devices. The microdevices were

fabricated using a combination of photolithographic patterning, etching, hot embossing and thermal bonding as described in Section 2.3.1.[36] Bonding of COC was done at 110 ºC for 20 min. Two different microchip designs were used for these experiments. A simple, two-reservoir layout (Fig. 4.1A) was used for initial testing while the design in Figure 4.1B was used for integrated experiments where no exchange of liquids in reservoirs was required. The channels in both designs were ~15 µm deep and ~50 µm wide. Before polymerization of a monolith, the channels were rinsed with isopropyl alcohol.

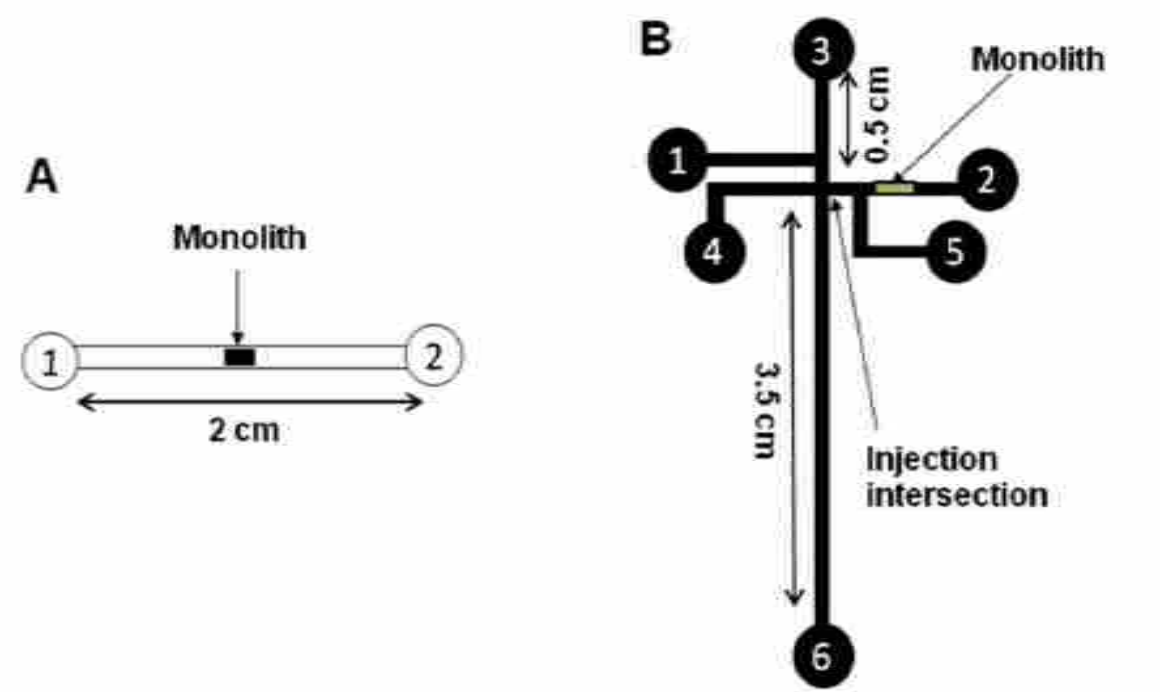


**Figure 4.1.** Schematic of microfluidic devices used for on-chip labeling. a) Simple, two reservoir design used for initial testing. b) Layout used for integrated experiments. The reservoirs are: 1 – sample, 3 – fluorescent dye, 4 – rinse buffer, 5 – eluent, and 2 and 6 – buffer. The lengths from reservoirs 1, 2, 4 and 5 to the injection intersection are all 0.5 cm.

### 4.2.3 Preparation of SPE monoliths

Monoliths were made from a solution consisting of 25% BMA (or MMA or LMA), 15% EDMA, 25% (w/w) dodecanol, 10% cyclohexanol, and 25% Tween 20. 1% DMPA was added to the

mixture as photoinitiator. The solution was sonicated for 10 min and degassed for 5 min. It was then filled into the device, and a mask was used to expose only the desired portion of the chip to UV radiation. Exposure was carried out with the use of a SunRay 600 UV floodlight from Uvitron International (West Springfield, MA, USA) at 50 mW/cm$^2$ for 10 min. A 2 mm long monolith was formed in each microdevice in the location indicated in Figure 4.1. After polymerization, devices were rinsed with isopropyl alcohol followed by buffer (10 mM carbonate, pH 9.3). The morphology of the monoliths was characterized using a Philips XL30 FEG environmental scanning electron microscope (SEM) from FEI (Hillsboro, OR, USA).

To determine the loading capacity of the monoliths, increasing concentrations of BSA were loaded on column using a syringe pump (Harvard Apparatus, Holliston, MA, USA) operating at 20 μL/min. First, the column was preconditioned with carbonate buffer containing 30% ACN, and then each BSA solution was loaded for 10 min (200 μL total volume), followed by a 5 min rinse with aqueous carbonate buffer. BSA retention was monitored via the background-subtracted fluorescent intensity at the CCD detector.

### 4.2.4 Off-chip labeling

Amino acids were separately mixed with FITC at a 4:1 molar ratio and incubated at room temperature for 24 h. This ratio ensures that almost no unreacted dye is left at the end of the labeling process. BSA and HSP90 were labeled with Alexa Fluor 488 TFP ester as described in Section 3.2.3.[9] The labeled samples were analyzed by μCE as described in Section 3.2.4[9] to confirm the lack of free dye, before loading into the monolithic column. A stock solution of Chromeo P503 was made by dissolving the dye in DMSO to a concentration of 0.8 mg/mL. For

off-chip labeling of BSA with Chromeo P503, the protein and dye were mixed to final concentrations of 5 μg/mL and 70 μg/mL, respectively, and incubated for 30 min at room temperature.

### 4.2.5 Microdevice operation

Before sample loading, monolithic columns were preconditioned with different solutions to find the most favorable conditions for sample sorption. The different pretreatments included rinsing the monolith with aqueous carbonate buffer (10 mM, pH 9.3), with carbonate buffer containing 30% ACN just prior to sample loading, or with carbonate buffer containing 30% ACN followed by thorough rinsing with aqueous carbonate buffer. I used pH 9.3 for all buffers except the eluent, because at pH values above 9 the ε-amino groups on proteins are mainly deprotonated,[37] facilitating labeling.

After column preconditioning, device operation for the simple design (Fig. 4.1A) was as follows. For retention and preconcentration studies, labeled sample in carbonate buffer was loaded on the monolithic column by applying +400 V to reservoir 2 and grounding reservoir 1 for 5 min. Rinsing was done by replacing the sample in reservoir 1 with carbonate buffer and applying the same voltages as before for 2 min. For elution, the rinse buffer in reservoir 1 was replaced with eluent consisting of 85% ACN, 15% carbonate buffer (7.5 mM, pH 9.6), 0.05% HPC, and 0.05% SDS. Elution was accomplished by grounding reservoir 1 and applying +1000 V to reservoir 2. On-chip labeling with Alexa Fluor 488 (TFP ester) was done by transferring protein solution into reservoir 1 and applying the same column loading voltages as above for 10 min. Next, 50 μg/mL of labeling solution was placed in reservoir 1, which was grounded, and +400 V were applied to

reservoir 2 for 15 min. This was followed by rinsing and elution as above. For on-chip labeling with Chromeo P503 the voltage polarity was reversed during loading of the dye and the rinse because of the positive charge on the label. The polarity was restored to positive for elution.

Experiments with the design in Figure 4.1B were done as follows (reservoirs not having a potential applied were allowed to float). Labeled sample was loaded by applying +400 V to reservoir 2 and grounding reservoir 1 for 5 min. Rinsing was achieved by applying the same potential to reservoir 2 and grounding reservoir 4. Elution was accomplished by applying +1000 V between reservoirs 5 and 2. For on-chip labeling with this design, unlabeled sample was loaded as before, then the dye was driven through the column by applying +400 V between reservoirs 3 and 2. This was followed by rinse and elution as above.

### 4.2.6 Instrumentation

The laser induced fluorescence system has been described previously.[34, 36] A Nikon Eclipse TE300 inverted microscope equipped with a CCD camera (Coolsnap HQ, Roper Scientific, Sarasota, FL, USA) was used. A 10x expander was used to increase the laser beam diameter, which was directed to a 20x, 0.45 NA objective on the microscope. For fluorescence monitoring, the detection point was positioned either just to the left of reservoir 2 (Fig. 4.1A or B), or directly on the monolith. The collected CCD images were analyzed using V++ Precision Digital Imaging software (Auckland, New Zealand).

### 4.2.7 Data analysis

To evaluate the extent to which different samples sorbed on the monolith, amino acids, fluorescent dyes and two proteins (BSA and HSP90) were loaded. Their retention was monitored

via CCD detection by measuring the background-subtracted fluorescent intensity on the monolith after rinsing.

For protein preconcentration, the background-subtracted steady state fluorescent intensity before the sample reached the monolith, which is the signal without preconcentration, was compared to the elution intensity, obtained by subtracting the baseline from the peak maximum. The calculation of HSP90 concentration for the calibration curve was based on the eluted peak area.

## 4.3 RESULTS AND DISCUSSION

### 4.3.1 Preparation of monoliths

I fabricated thermally bonded COC microdevices[38] with reversed-phase monolithic columns for SPE. COC was chosen because of its resistance to common organic solvents like acetonitrile[25] that are normally used for elution in SPE. Fabrication of a 2 mm long monolith in these microchips was done with a ternary porogenic solvent system consisting of dodecanol, cyclohexanol, and Tween 20.[39] Optimization of these porogens was carried out by Pagaduan et al.[39] who found that the monoliths formed were porous enough for water and buffer to flow through by capillary action. The monolith was made from a mixture consisting of a 60:40 porogen-to-monomer ratio, which provided more surface area and hence sample binding sites than monoliths with a higher ratio.[40] Importantly, experiments carried out in my monoliths showed that the application of voltage did not cause movement of the monolith, in agreement with Ladner et al.[26] Thus, pretreatment methods like photografting[24, 26] that complicate fabrication, adsorb sample and cause channel clogging were avoided. The monolithic structure

seen in Figure 4.2 showed clusters of globules with irregular through-pores, typical of high surface area monoliths.

**Figure 4.2.** SEM image of a BMA monolith showing detailed morphology.

BMA was chosen over other monomers such as MMA and LMA, which formed monoliths with morphologies shown in Figure 4.3. While MMA showed even packing and large pores, LMA produced a monolith with small through-pores. Even when the LMA monomer concentration was reduced to 25%, the very small through-pore dimensions were not favorable for flow. MMA was the least hydrophobic while LMA was the most hydrophobic of the monoliths fabricated. When LMA columns were used for protein extraction, elution was difficult because of the strong hydrophobic interactions with proteins. BMA, therefore, with intermediate properties between

MMA and LMA, was best suited for selective retention and elution in these experiments. Monoliths prepared with BMA and EDMA have been shown to have comparable hydrophobicity to C18 beads;[41] indeed, BMA monoliths have been used for SPE of proteins.[5, 42]

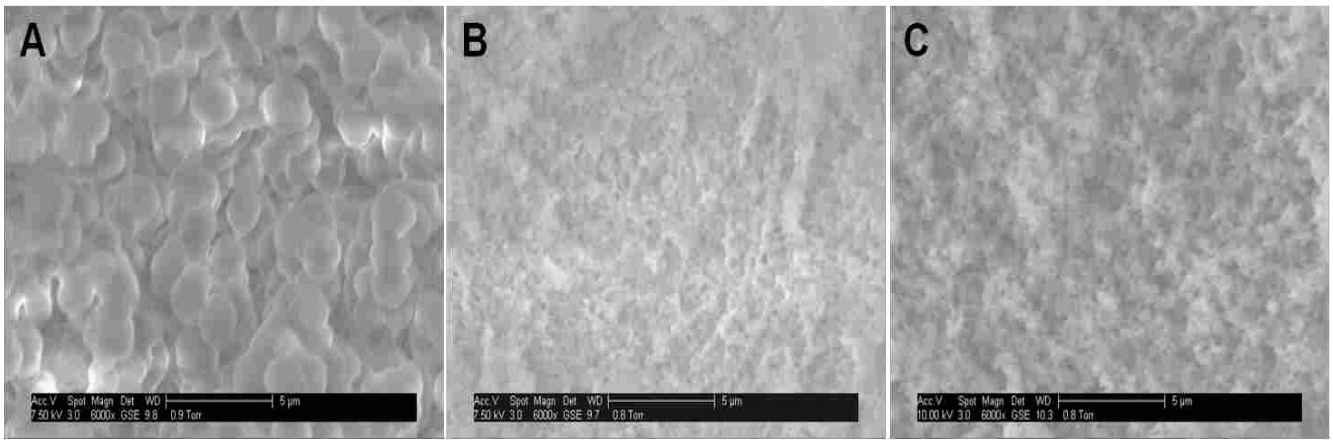


**Figure 4.3.** Comparison of monolithic structures with different carbon chain lengths: a) MMA (40%), b) LMA (40%), and c) LMA (25%). Porosity decreases while surface area increases with a longer carbon chain. See Figure 4.2 for BMA monolith morphology.

### 4.3.2 Retention of samples on BMA monoliths

An initial study of column preparation and sample loading conditions for BMA monoliths is summarized in Figure 4.4. Retention was greatest when the monolith was rinsed with carbonate buffer containing 30% ACN just before sample loading. It was also observed that samples dissolved in aqueous carbonate buffer or buffer having ≤0.5% ACN showed the best retention, while samples dissolved in carbonate buffer containing 2% ACN were retained less on the column. Rinsing reversed-phase monoliths with an ACN-aqueous buffer mixture has been shown to be necessary for preconditioning,[43] removing impurities that may interfere with sorption. Preconditioning with ACN also helps to activate and/or hydrate the monolith surface to provide adequate contact with the liquid sample.[44]

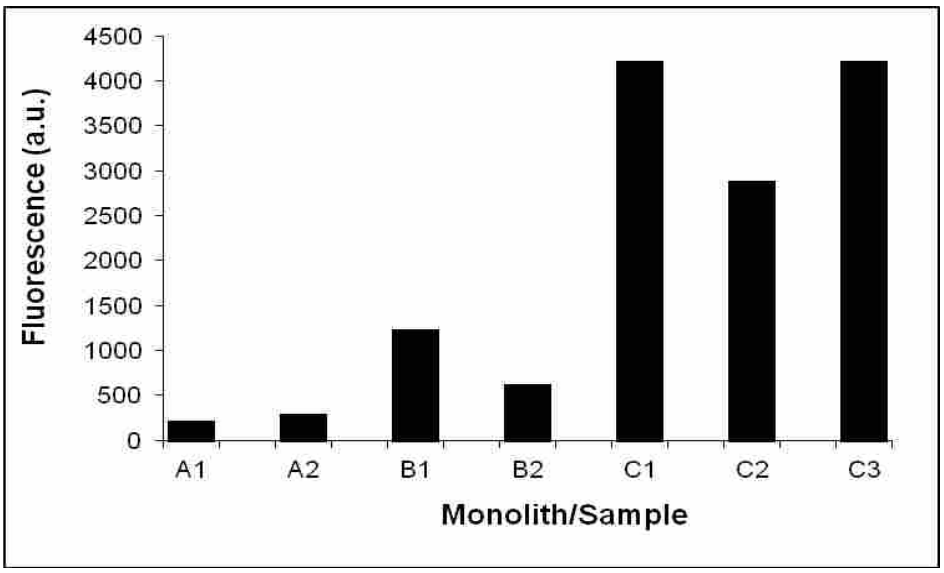


**Figure 4.4.** Effect of column preparation and sample loading conditions on retention for BMA monoliths. Sample was 1 μg/mL BSA. (A) Monolith rinsed with buffer (10 mM carbonate, pH 9.3) before loading. (B) Monolith rinsed with buffer solution containing 30% ACN followed by a thorough rinse with buffer. (C) Monolith rinsed with 30% ACN in buffer just before loading. (1) Sample dissolved in buffer containing no ACN, (2) sample dissolved in buffer containing 2% ACN, and (3) sample dissolved in buffer containing 0.5% ACN. Best retention was observed when the monolith was rinsed with ACN-containing buffer just before sample loading. ACN concentrations up to 0.5% in buffer did not significantly affect retention.

Figure 4.5 shows the normalized retention of fluorescent dyes, amino acids and proteins on BMA monoliths. Retention of the fluorescent dyes (Fig. 4.5A) on the column was relatively low. Unreacted (free) Chromeo P503 has a low fluorescence signal,[45] which explains its limited retention. The ionic sodium salt of fluorescein used does not partition significantly into the hydrophobic BMA column, accounting for its low retention. The slightly higher fluorescent intensities observed for Alexa Fluor 488 TFP ester and FITC are likely due to small differences in experimental conditions.

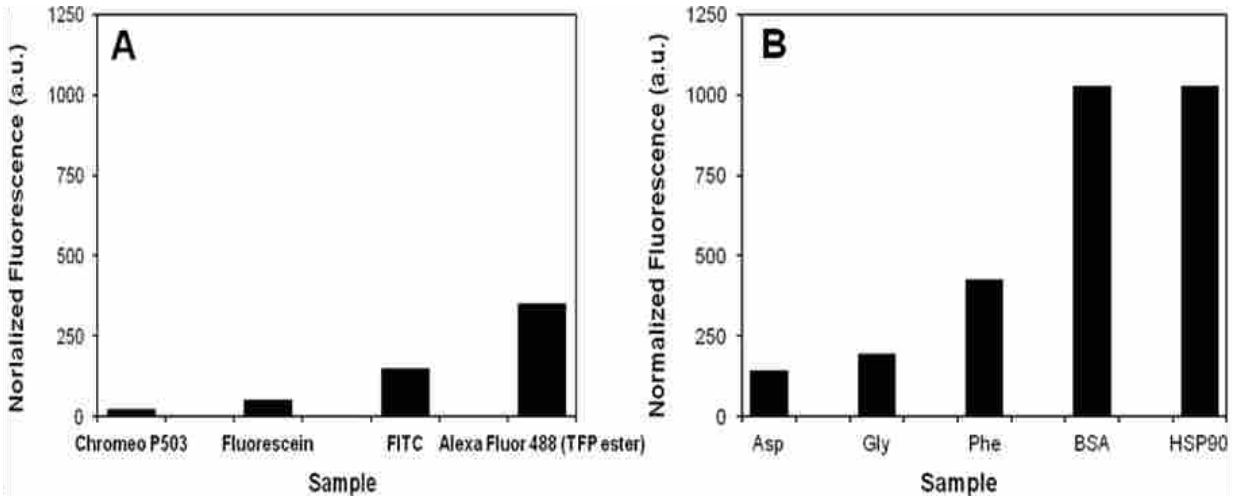


**Figure 4.5.** Normalized retention of a) fluorescent dyes, and b) amino acids and proteins on an on-chip BMA column. Loading was the same for all samples, except the polarity was reversed for Chromeo P503. Values were normalized to 100 nM dye concentration in (a) and 100 ng/mL amino acid or protein concentration in (b).

Retention of amino acids (Fig. 4.5B) on my BMA monolith depended on their hydrophobicity. Hydropathicity index, a measure of hydrophobicity of amino acids and proteins,[46] can predict their expected interaction with the monolith. More hydrophobic compounds have a more positive index value. Low retention was observed for aspartic acid and glycine, which have hydrophilic values of -3.5 and -0.4, respectively. As expected, phenylalanine, with an index of 2.8, was retained more. The two proteins in Figure 4.5B were more highly retained on BMA monoliths than any amino acids. Protein binding comes from the average surface hydrophobicity, which combines the contributions of all the amino acids present on the surface.[47] Some of these amino acids, such as phenylalanine, alanine, and methionine, are hydrophobic and form hydrophobic regions or "patches" on protein surfaces.[48, 49] The non-specific sorption of proteins like BSA to hydrophobic surfaces has been shown to be the result of interactions between these hydrophobic patches and surface.[50] These more extensive hydrophobic surface interactions for the two

proteins studied (relative to the free amino acids) result in their greater retention on these monoliths. I determined the protein loading capacity of our 2 mm long monoliths to be 2 μg (30 pmol) of BSA.

### 4.3.3 Elution of samples

Figure 4.6 shows elution profiles of fluorescent dyes on a BMA column. The areas of the eluted peaks were correlated with the amount retained (see Fig. 4.5A). The elution profiles of some amino acids and the proteins, BSA and HSP90, from a BMA monolith can be seen in Figure 4.7. The areas of the eluted amino acid peaks (Figure 4.7A) followed the order of the amount retained (Fig. 4.5B) with aspartic acid having the lowest elution intensity and phenylalanine the highest. The earlier elution of HSP90 compared to BSA (Fig. 4.7B) is likely due to the fact that HSP90 has a greater negative charge density,[51] and is not only more hydrophilic but also migrates faster in an electric field, both factors in electrochromatography.[52] A comparison of the intensities of the peaks at elution (Fig. 4.7B) to the signal before the sample reached the monolithic column gave the degree of preconcentration of each protein. The calculated enrichment factors were 11-fold for HSP90 and 6-fold for BSA, demonstrating that these proteins were concentrated on the reversed-phase column. The degree of preconcentration of HSP90 was higher than for BSA because it eluted in a ~2-fold narrower band, since it was less retained than BSA. It is expected that with longer columns and loading times the degree of preconcentration could be even greater.

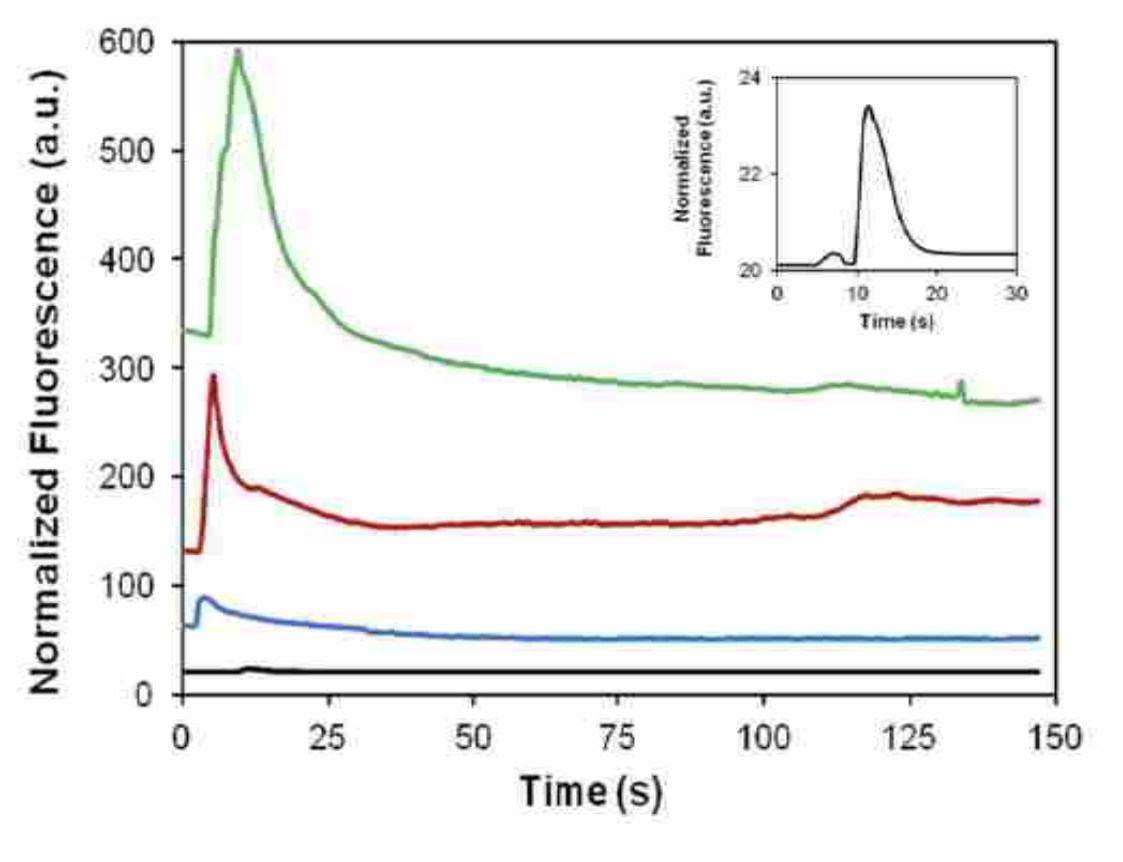


**Figure 4.6.** Elution profiles of fluorescent dyes from an on-chip BMA column. All signals were normalized to 100 nM dye concentration, as in Figure 4.5. Dyes (from bottom to top) are: Chromeo P503, fluorescein, FITC, and Alexa Fluor 488 TFP. Chromatograms are offset vertically for clarity. Positively charged Chromeo P503 dye was eluted with application of a negative voltage, while all others (negatively charged) required a positive voltage. The first 30 s of Chromeo P503 dye elution is expanded in the inset.

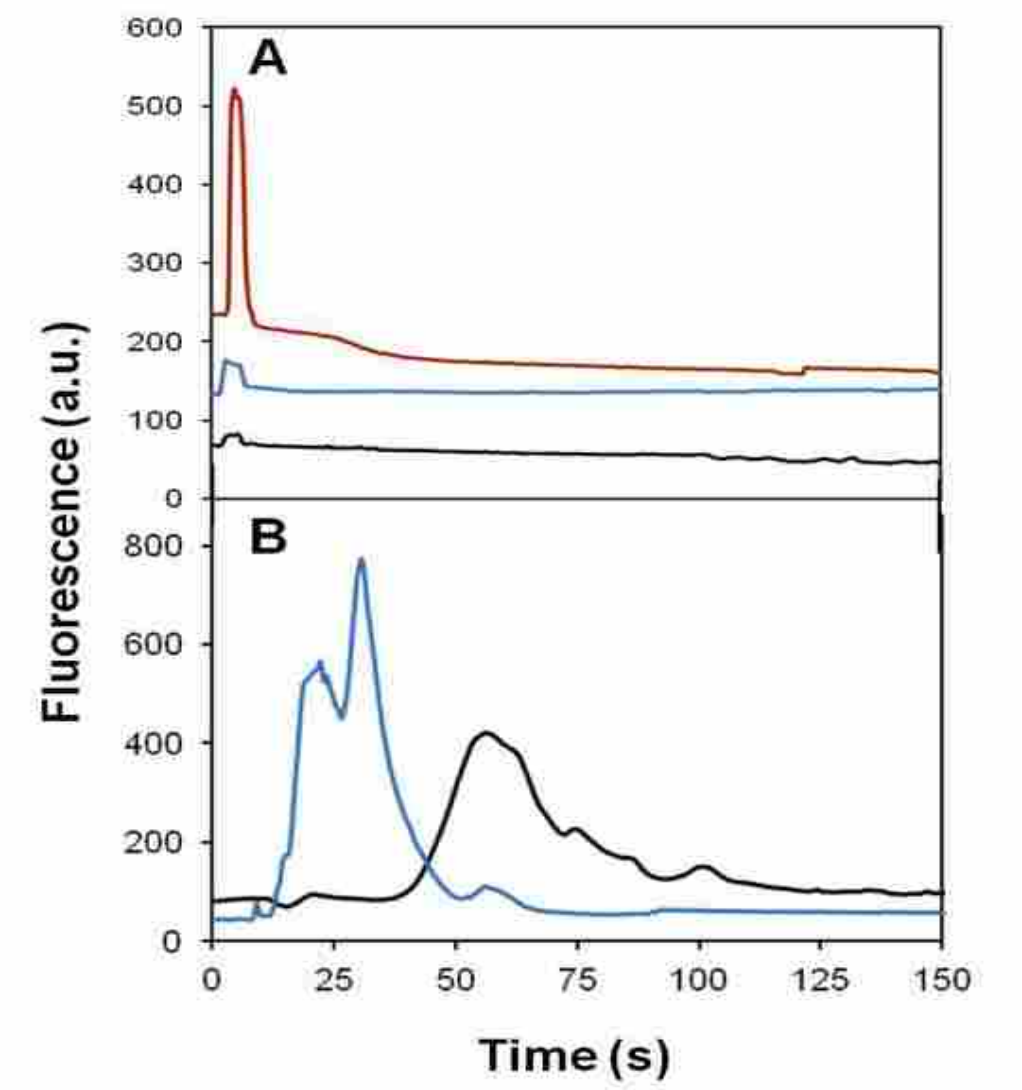


**Figure 4.7.** Elution profiles of amino acids and two proteins (BSA and HSP90) from an on-chip BMA monolith. a) Chromatograms of amino acids (100 ng/mL) from bottom to top are: aspartic acid, glycine, and phenylalanine. Chromatograms are offset vertically for clarity. b) Elution of 1 µg/mL proteins (BSA – maximum around 55 s, and HSP90 – maximum around 30 s).

### 4.3.4 Off- and on-chip labeling with Chromeo P503

Figure 4.8 shows elution profiles for BSA labeled off- and on-chip with Chromeo P503 dye. Although Chromeo P503 dye is positively charged, after reaction with BSA the labeled protein is negatively charged at pH 9.3. Elution of Chromeo P503-labeled BSA from the column (Fig. 4.8A) is slower than Alexa Fluor 488-labeled BSA (Fig. 4.7B) because Chromeo P503-labeled

protein has less negative charge.[53, 54] Figure 4.8B shows that the elution of BSA labeled on-chip with Chromeo P503 is similar to that for protein labeled off-chip. For on-chip labeling, the oppositely charged Chromeo P503 and labeled protein migrate in opposite directions under the elution voltage, simplifying purification. This use of charge to selectively elute proteins relative to dye makes on-chip labeling of protein samples with Chromeo P503 appealing.

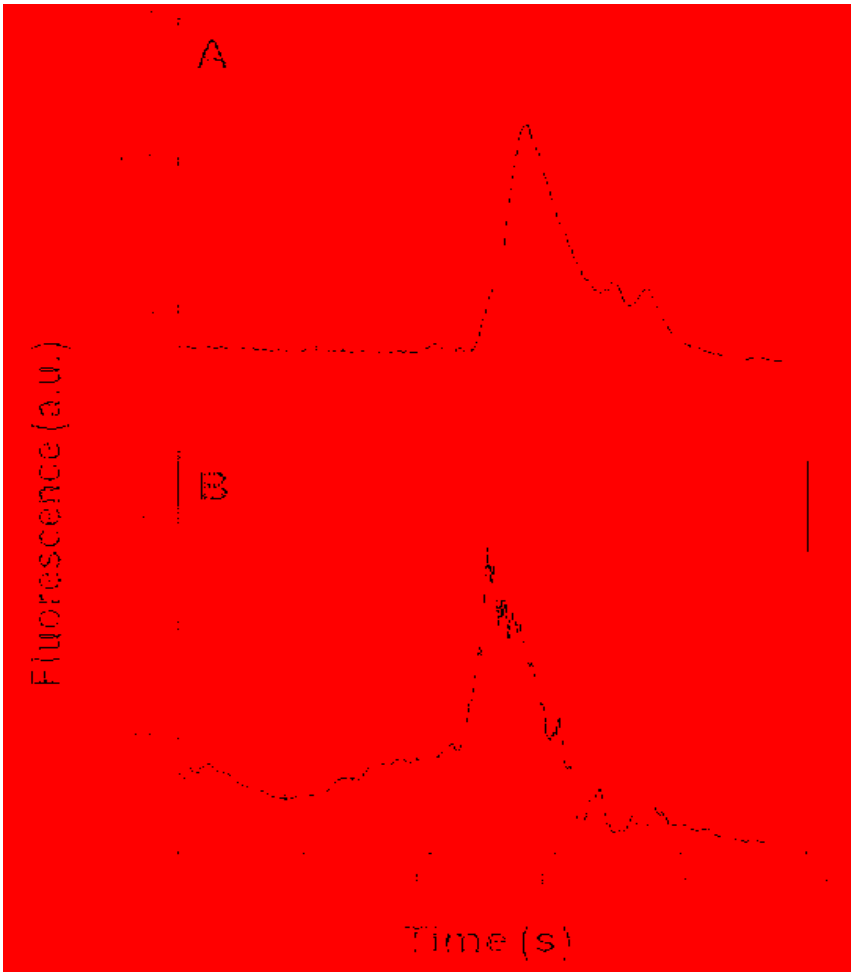


**Figure 4.8.** Elution profiles of 1 µg/mL BSA labeled a) off-chip and b) on-chip with Chromeo P503 dye.

### 4.3.5 On-chip labeling with Alexa Fluor 488 TFP ester

Alexa Fluor 488, which produces very bright and photostable conjugates,[55, 56] was used with HSP90 to demonstrate proof of principle of on-chip preconcentration, labeling and purification of protein from label within an integrated microfluidic platform. Figure 4.9 shows the elution of different concentrations of on-chip labeled HSP90 from a BMA column. A 15 min on-chip labeling of 1 µg/mL HSP90 with Alexa Fluor 488 TFP ester in Fig. 4.9A showed two peaks, the dye followed by HSP90. On-chip labeling of different concentrations of HSP90 retained on a BMA monolith showed increasing peak areas with concentration. A plot of peak area against HSP90 concentration (Fig. 4.9B) was linear, showing that concentration and signal can easily be correlated for an unknown sample after on-chip labeling. I note that these systems could be used to concentrate and label other proteins in a similar manner. Retention of more sample could be attained by increasing the surface area of the monolith through adjustment of polymerization conditions or usage of different branched crosslinkers, as demonstrated by Lee's group.[57, 58]

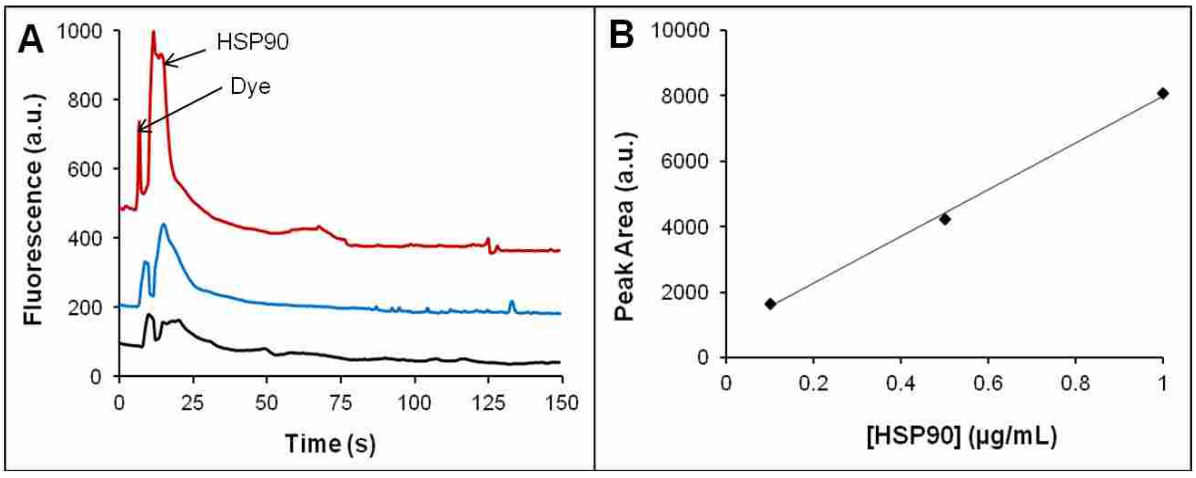


**Figure 4.9.** On-chip labeling and elution of HSP90 using a BMA column. a) Elution traces. Chromatograms are offset vertically for clarity (bottom: 0.1 µg/mL, middle: 0.5 µg/mL and top: 1 µg/mL). b) Plot of peak area as a function of HSP90 concentration. The slope is 7200 ± 140, and the intercept is 830 ± 170.

Unlike typical on-chip labeling where the on-line mixing of high concentrations of fluorescent dyes with sample can interfere with the separation process, in my work protein samples are enriched in addition to being labeled and purified from the unreacted dye. These results demonstrate that unlabeled protein samples can be readily assayed by a simple and sensitive procedure that is favorable for automation. Integration of my reversed-phase columns with an up-stream affinity extraction module would further increase the selectivity of the method, especially for complex biological samples. Multiple analytes could also be extracted, labeled and separated in my integrated system.

## 4.4 REFERENCES


(1) Angelescu, D. E. *Highly Integrated Microfluidics Design*; Artech House, 2011.
(2) Yang, H.; Mudrik, J. M.; Jebrail, M. J.; Wheeler, A. R. *Anal. Chem.* **2011**, *83*, 3824-3830.
(3) Hagan, K. A.; Reedy, C. R.; Bienvenue, J. M.; Dewald, A. H.; Landers, J. P. *Analyst* **2011**, *136*, 1928-1937.
(4) Yang, W.; Yu, M.; Sun, X.; Woolley, A. T. *Lab Chip* **2010**, *10*, 2527-2533.
(5) Hua, Y.; Jemere, A. B.; Harrison, D. J. *J. Chromatogr. A* **2011**, *1218*, 4039-4044.
(6) Tennico, Y. H.; Remcho, V. T. *Electrophoresis* **2010**, *31*, 2548-2557.
(7) Yu, M.; Wang, Q.; Patterson, J. E.; Woolley, A. T. *Anal. Chem.* **2011**, *83*, 3541-3547.
(8) Wu, J.; Ferrance, J. P.; Landers, J. P.; Weber, S. G. *Anal. Chem.* **2010**, *82*, 7267-7273.
(9) Nge, P. N.; Yang, W.; Pagaduan, J. V.; Woolley, A. T. *Electrophoresis* **2011**, *32*, 1133-1140.
(10) Beyor, N.; Yi, L.; Seo, T. S.; Mathies, R. A. *Anal. Chem.* **2009**, *81*, 3523-3528.
(11) Nandi, P.; Desai, D. P.; Lunte, S. M. *Electrophoresis* **2010**, *31*, 1414-1422.
(12) Mecker, L. C.; Martin, R. S. *Anal. Chem.* **2008**, *80*, 9257-9264.
(13) Wu, A.; Wang, L.; Jensen, E.; Mathies, R.; Boser, B. *Lab Chip* **2010**, *10*, 519-521.
(14) Bhatta, D.; Michel, A. A.; Marti Villalba, M.; Emmerson, G. D.; Sparrow, I. J. G.; Perkins, E. A.; McDonnell, M. B.; Ely, R. W.; Cartwright, G. A. *Biosens. Bioelectron.* **2011**, *30*, 78-86.
(15) Verbarg, J.; Kamgar-Parsi, K.; Shields, A. R.; Howell, P. B., Jr.; Ligler, F. S. *Lab Chip* **2012**, *12*, 1793-1799.
(16) Svec, F. *J. Chromatogr. B* **2006**, *841*, 52-64.
(17) Njoroge, S. K.; Witek, M. A.; Battle, K. N.; Immethun, V. E.; Hupert, M. L.; Soper, S. A. *Electrophoresis* **2011**, *32*, 3221-3232.
(18) Nguyen, T.; Pei, R.; Stojanovic, M.; Lin, Q. *Microfluid. Nanofluid.* **2009**, *6*, 479-487.
(19) Wang, C.; Jemere, A. B.; Harrison, D. J. *Electrophoresis* **2010**, *31*, 3703-3710.
(20) Long, Z.; Shen, Z.; Wu, D.; Qin, J.; Lin, B. *Lab Chip* **2007**, *7*, 1819-1824.
(21) Woodward, S. D.; Urbanova, I.; Nurok, D.; Svec, F. *Anal. Chem.* **2010**, *82*, 3445-3448.
(22) Yang, Y.; Li, C.; Lee, K. H.; Craighead, H. G. *Electrophoresis* **2005**, *26*, 3622-3630.
(23) Kang, Q.-S.; Li, Y.; Xu, J.-Q.; Su, L.-J.; Li, Y.-T.; Huang, W.-H. *Electrophoresis* **2010**, *31*, 3028-3034.
(24) Liu, J.; Chen, C.-F.; Tsao, C.-W.; Chang, C.-C.; Chu, C.-C.; DeVoe, D. L. *Anal. Chem.* **2009**, *81*, 2545-2554.
(25) Faure, K.; Albert, M.; Dugas, V.; Crétier, G.; Ferrigno, R.; Morin, P.; Rocca, J.-L. *Electrophoresis* **2008**, *29*, 4948-4955.
(26) Ladner, Y.; Crétier, G.; Faure, K. *J. Chromatogr. A* **2010**, *1217*, 8001-8008.
(27) Ramautar, R.; de Jong, G. J.; Somsen, G. W. *Electrophoresis* **2012**, *33*, 243-250.
(28) Huang, B.; Wu, H.; Kim, S.; Zare, R. N. *Lab Chip* **2005**, *5*, 1005-1007.
(29) Jacobson, S. C.; Hergenroder, R.; Moore, A. W., Jr.; Ramsey, J. M. *Anal. Chem.* **1994**, *66*, 4127-4132.
(30) Jacobson, S. C.; Koutny, L. B.; Hergenroeder, R.; Moore, A. W., Jr.; Ramsey, J. M. *Anal. Chem.* **1994**, *66*, 3472-3476.
(31) Antes, B.; Oberkleiner, P.; Nechansky, A.; Szolar, O. H. J. *J. Pharmaceut. Biomed. Anal.* **2010**, *51*, 743-749.

(32) Ye, M.; Hu, S.; Schoenherr, R. M.; Dovichi, N. J. *Electrophoresis* **2004**, *25*, 1319-1326.
(33) Dickerson, J. A.; Ramsay, L. M.; Dada, O. O.; Cermak, N.; Dovichi, N. J. *Electrophoresis* **2010**, *31*, 2650-2654.
(34) Yu, M.; Wang, H.-Y.; Woolley, A. T. *Electrophoresis* **2009**, *30*, 4230-4236.
(35) Yassine, O.; Morin, P.; Dispagne, O.; Renaud, L.; Denoroy, L.; Kleimann, P.; Faure, K.; Rocca, J.-L.; Ouaini, N.; Ferrigno, R. *Anal. Chim. Acta.* **2008**, *609*, 215-222.
(36) Kelly, R. T.; Woolley, A. T. *Anal. Chem.* **2003**, *75*, 1941-1945.
(37) Michielsen, E. C. H. J.; Diris, J. H. C.; Hackeng, C. M.; Wodzig, W. K. W. H.; Van Dieijen-Visser, M. P. *Clin. Chem.* **2005**, *51*, 222-224.
(38) Illa, X.; Ordeig, O.; Snakenborg, D.; Romano-Rodriguez, A.; Compton, R. G.; Kutter, J. P. *Lab Chip* **2010**, *10*, 1254-1261.
(39) Pagaduan, J. V.; Yang, W.; Woolley, A. T. *Proc. SPIE* **2011**, *8031*, 80311V/80311-80311V/80317.
(40) Urban, J.; Jandera, P. *J. Sep. Sci.* **2008**, *31*, 2521-2540.
(41) Yu, C.; Davey, M. H.; Svec, F.; Fréchet, J. M. J. *Anal. Chem.* **2001**, *73*, 5088-5096.
(42) Armenta, J. M.; Gu, B.; Thulin, C. D.; Lee, M. L. *J. Chromatogr. A* **2007**, *1148*, 115-122.
(43) Augustin, V.; Jardy, A.; Gareil, P.; Hennion, M.-C. *J. Chromatogr. A* **2006**, *1119*, 80-87.
(44) Marchiarullo, D. J. *Development of microfluidic technologies for on-site clinical and forensic analysis: Extraction, amplification, separation, and detection. Dissertation, Doctor of Philosophy, University of Virginia* **2009**.
(45) Wojcik, R.; Swearingen, K. E.; Dickerson, J. A.; Turner, E. H.; Ramsay, L. M.; Dovichi, N. J. *J. Chromatogr. A* **2008**, *1194*, 243-248.
(46) Kyte, J.; Doolittle, R. F. *J. Mol. Biol.* **1982**, *157*, 105-132.
(47) Salgado, J. C.; Rapaport, I.; Asenjo, J. A. *J. Chromatogr. A* **2005**, *1098*, 44-54.
(48) Cummins, P. M.; O'Connor, B. F. *Methods in Molecular Biology*; Walls, D., Loughran, S. T., Eds.; Humana Press, 2011; Vol. 681, Part 2,, 431-437.
(49) Zhang, Y.; Martinez, T.; Woodruff, B.; Goetze, A.; Bailey, R.; Pettit, D.; Balland, A. *Anal. Chem.* **2008**, *80*, 7022-7028.
(50) Mücksch, C.; Urbassek, H. M. *Langmuir* **2011**, *27*, 12938-12943.
(51) The charge density differences between BSA and HSP90 were inferred from their 'grand mean of hydropathicity' (GRAVY) scores of -0.433 and -0.750 respectively *calculated using the PROTPARAM tool:http://us.expasy.org/tools/protparam.html* **accessed May 2, 2012**.
(52) Karenga, S.; El Rassi, Z. *J. Sep. Sci.* **2008**, *31*, 2677-2685.
(53) Wetzl, B. K.; Yarmoluk, S. M.; Craig, D. B.; Wolfbeis, O. S. *Angew. Chem., Int. Ed.* **2004**, *43*, 5400-5402.
(54) Ramsay, L. M.; Dickerson, J. A.; Dovichi, N. J. *Electrophoresis* **2009**, *30*, 297-302.
(55) Jungbauer, L. M.; Yu, C.; Laxton, K. J.; LaDu, M. J. *J. Mol. Recognit.* **2009**, *22*, 403-413.
(56) Nichkova, M.; Dosev, D.; Gee, S. J.; Hammock, B. D.; Kennedy, I. M. *Anal. Biochem.* **2007**, *369*, 34-40.
(57) Liu, K.; Tolley, H. D.; Lee, M. L. *J. Chromatogr. A* **2012**, *1227*, 96-104.
(58) Li, Y.; Tolley, H. D.; Lee, M. L. *J. Chromatogr. A* **2011**, *1218*, 1399-1408.

# 5. CONCLUSIONS AND FUTURE WORK

## 5.1 CONCLUSIONS

### 5.1.1 Integrated affinity and electrophoresis systems for biomarker analysis

In Chapter 2, I reviewed the principles and protocols for the fabrication of PMMA devices and preparation of porous monolithic columns in the devices. Designs on a silicon template, prepared by photolithographic techniques and etching, were transferred to a PMMA piece by hot embossing. The embossed piece was then sealed to a cover plate by thermal bonding. Affinity columns were prepared in these devices by *in situ* photopolymerization of a prepolymer mixture containing glycidyl methacrylate monomer containing epoxy groups that react with protein amine groups. The columns were functionalized with antibodies and used for the extraction of fluorescently labeled cancer biomarkers. Labeling efficiency was determined by performing electrophoresis without affinity extraction. Efficient labeling of the proteins occurred at pH ~9 but TK1 with a higher pI of ~8.75 was better labeled at a higher pH of 10.6. μCE of Alexa Fluor 488-labeled TK1 showed complete separation of the unreacted dye and the labeled protein. Initial affinity extraction experiments with anti-HSP90 functionalized monoliths showed specificity towards HSP90 but not to the unreacted dye. Such systems show great promise for analysis in complex mixtures.

### 5.1.2 Ion-permeable membrane for on-chip preconcentration and separation of cancer marker proteins

I demonstrated that cancer marker proteins can be electrophoretically concentrated and separated in a microdevice using a simple and quick method. On-chip preconcentration was achieved with

an ion-permeable membrane formed by *in situ* photopolymerization just beyond the injection intersection in the microchip. Baseline resolution of two cancer marker proteins with similar electrophoretic mobilities was accomplished at pH 7.0. A 10-fold increase in the signal of these proteins was achieved under my optimized conditions with just a 1 min preconcentration time. Such signal enhancement offers improved limits of detection that are essential in clinical diagnosis where target proteins can be present in low concentrations. The preconcentration and separation process carried out with my device is simple, fast, and generalizable. The simplicity and speed of analysis provide good potential for application in POC analysis. The membrane used in this device could easily be coupled to a suitable pretreatment technique, such as affinity extraction, for the analysis of clinically significant biomolecules in a complex sample matrix. This technique offers the potential for enhanced analysis of multiple cancer biomarkers, which should facilitate diagnosis and monitoring of response to treatment.

### 5.1.3 Microfluidic chips with reversed-phase monoliths for solid phase extraction and on-chip labeling

The difficulties encountered in the integration of sample preparation methods in microfluidic systems present a significant obstacle to miniaturized analysis. Therefore, effective integration of sample labeling moves the field closer to the automation level necessary for application in point-of care diagnostics, for example. I have presented a miniaturized system that combines sample enrichment with on-chip labeling and purification. Samples are enriched through SPE on a BMA monolith in a microfluidic device. Analytes are fluorescently labeled while they are on the column, and much of the unreacted dye is removed in a rinsing step. The labeled protein is more strongly retained compared to the unattached label, enabling further purification during elution. I

have characterized the retention and elution of fluorophores and fluorescently labeled amino acids and proteins. I have also developed conditions for automated on-chip fluorescent labeling and purification of proteins. Importantly, the eluted peak area for on-chip labeled HSP90 scaled linearly with concentration, demonstrating the ability of my method to quantify on-chip labeled samples. The combination of the proven enrichment capacity of SPE with fast labeling and separation yields a simple technique that is well suited for miniaturization. The integration of this approach with affinity extraction should provide an additional dimension of specificity, providing a powerful and automated method for bioanalysis.

## 5.2 FUTURE WORK

### 5.2.1 Affinity extraction coupled with solid phase extraction, on-chip labeling and μCE

In Chapter 2, I provided the protocol for the preparation of porous monolithic columns and their subsequent functionalization with antibodies. Extraction from complex biological samples is easier with a wall-coated column because clogging is not an issue. However, the surface area for antibody immobilization is higher with porous monolith, resulting in the extraction of more analyte. If the pores are large enough, clogging can be avoided. Serial arrangement of an affinity column and a reversed phase column could enable automated determination of analyte concentrations from complex mixtures. Samples could be extracted, concentrated and labeled on-chip, reducing sample loss and overall analysis time compared to off-chip sample preparation methods. Figure 5.1 shows a schematic of a device that could be used for this purpose. Monolith 1 could be made from monomers containing epoxide groups such as glycidyl methacrylate[1] or azlactone groups such as 2-vinyl-4,4-dimethylazlactone,[2,3] which can react with amine groups on

antibodies as described in Section 2.3.3. Monolith 2 would be reversed phase as described in chapter 4.

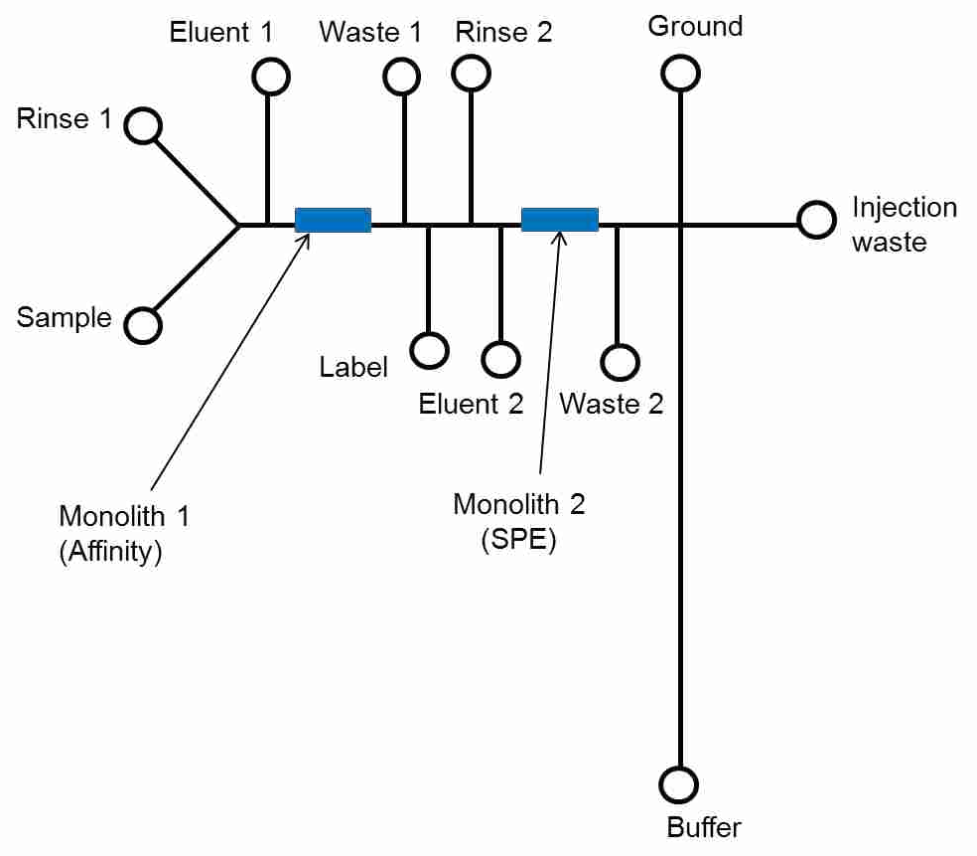


**Figure 5.1.** Schematic of a device for coupling affinity extraction with solid phase extraction, on-chip labeling and μCE.

Application of voltage between the sample and waste 1 reservoirs will cause the sample to flow through monolith 1 (affinity) where the protein of interested will be extracted. Rinsing of excess sample will be done by applying voltage between rinse 1 and waste 1 reservoirs. By applying voltage between eluent 1 and waste 2 reservoirs the sample will be eluted from the affinity column and trapped on the reversed-phase column (monolith 2) where it could be further labeled on-chip by application of voltage between the label and waste 2 reservoirs. Rinsing of excess

label will be performed by the application of voltage between rinse 2 and waste 2 reservoirs. The concentrated sample could then be eluted into the μCE system by application of voltage between the eluent 2 and injection waste reservoirs. The "pinched" injection method could be used to move the sample into the separation channel for μCE. Detection could be carried out near the buffer reservoir with the same LIF system described in Section 2.3.5.

### 5.2.2 On-chip protein digestion coupled with solid phase extraction and μCE

In Chapter 4, I showed that proteins could be concentrated on a monolithic column, fluorescently labeled and then separated. It should be possible for protein identification to be carried out by fragmenting the protein and analyzing the resulting peptide units.[4] This method, known as shotgun or bottom-up proteomics,[4] requires digestion of the protein sample and subsequent analysis of the fragments by MS, after separation, for example by HPLC or capillary electrophoresis. A proteolytic enzyme in solution is commonly used for protein digestion.[1] However, digestion by this method is slow, and autodigestion is common, resulting in unwanted products.[1] Solid-phase microreactors with immobilized proteolytic enzymes have been shown to rapidly digest proteins as well as prevent autodigestion.[2] Moreover, because of the high enzyme-to-substrate ratio in solid-phase microreactors, the digestion efficiency is high.[5] Several solid supports have been employed in microfluidic systems for the digestion of proteins including agarose beads,[6] micropost structures,[5] fiberglass[7] and polymer monoliths.[1,3] The ease of fabrication of monolithic columns in microdevices gives it an advantage over the other solid supports.

Two monoliths fabricated in series could be used for protein digestion and solid phase extraction of the generated peptide fragments. The first monolith could be prepared as before (see Section 2.3.3) to react with amine groups on proteolytic enzymes such as pepsin[8] or trypsin.[2] The second monolith would be the same type of reversed phase monolith described in chapter 4. A schematic of a device design that could be used for these experiments is shown in Figure 5.2. Application of voltage between the sample and waste reservoirs will cause the sample to flow through monolith 1 (enzyme-functionalized) where the protein will be digested as it flows towards monolith 2. The fragmented sample will be trapped on monolith 2. The fragments on monolith 2 will be labeled by applying a voltage between the label and waste reservoirs, and the lightly retained label will be rinsed off by the application of voltage between the rinse and waste reservoirs. Elution of labeled fragments will be done by applying voltage between the eluent and injection waste reservoirs, and the eluted fragments will be injected into the separation column by "pinched" injection where they will be separated by μCE.

Though digestion efficiencies may be high, it is difficult to achieve 100% digestion, so the resulting mixture will consist of multiple peptides along with some undigested protein. Separation efficiencies for such complex mixtures are lower with shorter separation channels,[9] so a serpentine separation channel will be used to improve resolution. Detection will be carried out by the LIF system described in Section 2.3.5.

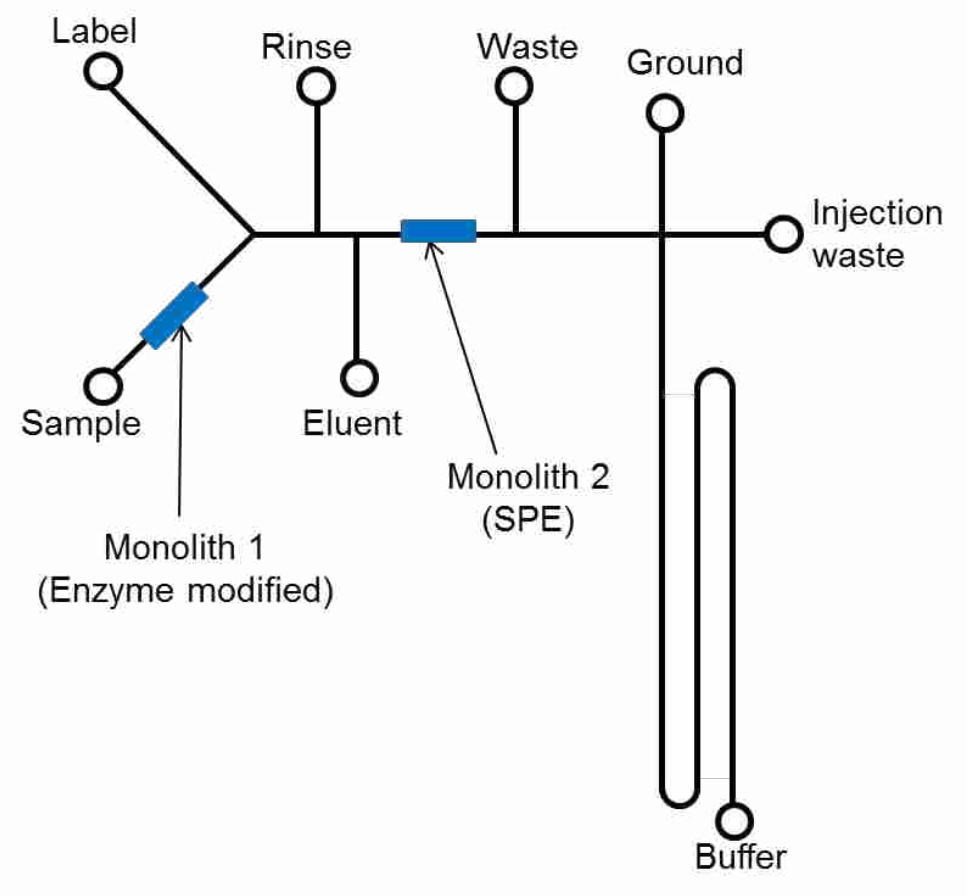


**Figure 5.2.** Schematic of a device for coupling protein digestion with solid phase extraction, on-chip labeling and μCE.

### 5.2.3 On-chip immuno-extraction coupled with protein digestion, preconcentration and MS detection

Mass spectrometry has been successfully applied to protein identification because the method is accurate and can give information about post-translational modification.[6] However, its efficiency is improved if the sample is fractionated and separated before detection.[10] Mellors et al.[11, 12] have shown that μCE can be coupled to ESI-MS by directing the separation channel to the corner of the microdevice to serve as the electrospray tip. An EOF pump at the junction between three channels facilitated the transfer of solution to the ESI emitter.

Analysis of biological samples would be simplified with initial purification to obtain the desired analyte, as demonstrated by the use of immunoaffinity columns.[13] Immuno-extraction of a specific protein followed by on-chip digestion and MS detection would present a rapid and efficient means of determining small structural differences between proteins such as variants, isoforms and post-translational modifications. It is important to be able to identify these subtle changes because as a disease progresses protein modifications also can occur.[14] Additionally, knowing the location of post-translational modification within a protein can provide useful information for some biochemical processes.[6] With the use of three monolithic columns proteins could be extracted, digested and concentrated on-chip before MS detection. A schematic of such a device is shown in Figure 5.3. Monoliths 1 and 2 could both be made as before (Section 2.3.3) to facilitate reaction with amine groups on antibodies (monolith 1) and proteolytic enzymes (monolith 2). Monolith 3 would be the same type of reversed phase monolith described in chapter 4. Monolith 1 would be functionalized with an antibody that targets a specific analyte while monolith 2 would be functionalized with a proteolytic enzyme. A complex biological sample would be loaded on monolith 1 by application of voltage between the sample and waste 1 reservoirs, enabling specific extraction. Lightly retained sample would be removed by application of voltage between the rinse and waste 1 reservoirs. The protein can then be eluted from the column by application of voltage between eluent 1 and waste 2 reservoirs. In this process the eluted protein would flow through monolith 2, where it would be digested, and move on to monolith 3 to be trapped and concentrated. Coupling of μCE with MS could be done by eluting the sample into the injection intersection by the application of voltage between the eluent 2 and injection waste reservoirs. The eluted fragments will be injected into the separation column

by “pinched” injection where they will be separated by μCE. The separation voltage would be applied between the ground and side channel reservoirs. The side channel would be positioned so that it meets the separation channel at a point that is close to the outlet leading to the MS system, so that sample can be sprayed into the MS system as it reaches the junction.

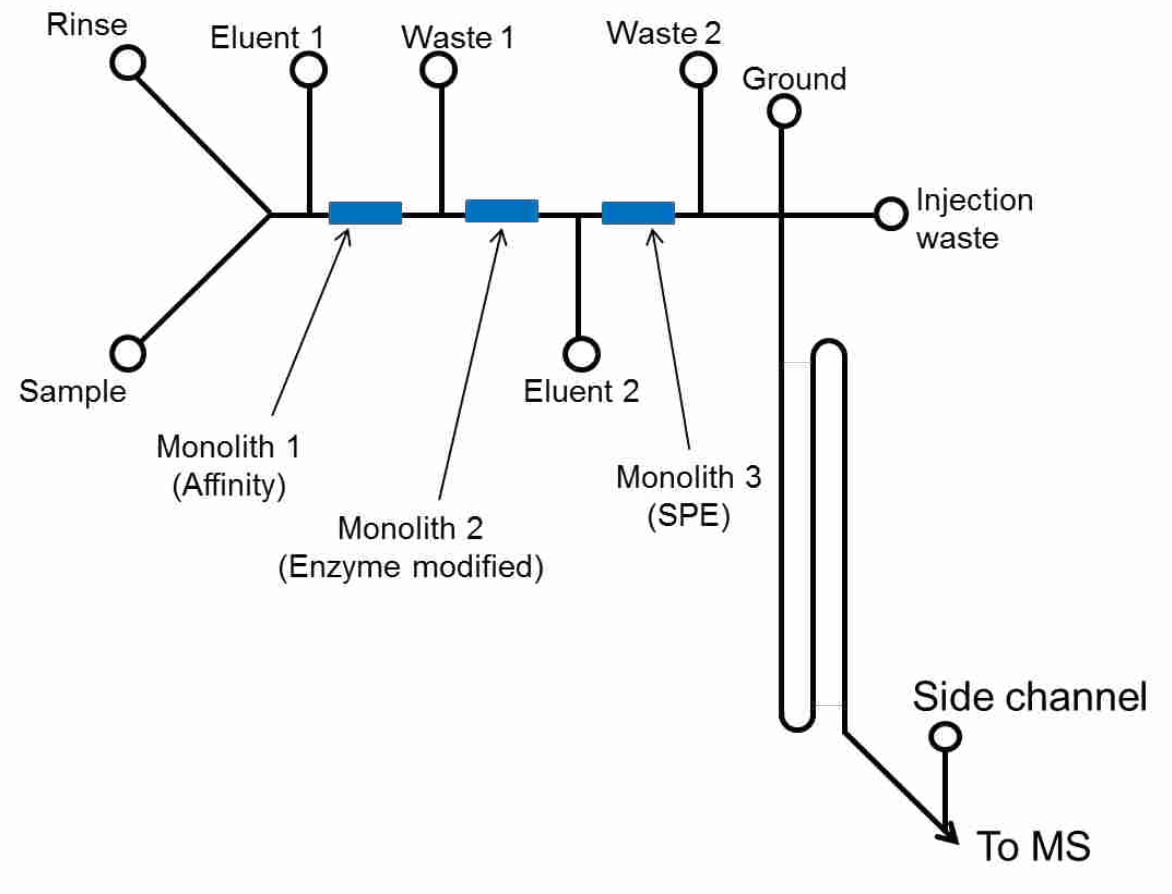


**Figure 5.3.** Schematic of a device for coupling on-chip affinity extraction with MS detection.

In summary, my research has been aimed at developing techniques for the integration of sample preparation methods in microchips. Sample preconcentration has been achieved by *in situ* preparation of hydrogel membranes and polymer monoliths. In addition, fluorescent labeling which is typically performed off-chip has been integrated and coupled with purification and

μCE. Further studies in the combination of affinity extraction with preconcentration and on-chip labeling will advance the applications of micro total analysis systems, and lead to rapid determination of biomarkers. The coupling of microfluidics with mass spectrometry should also advance proteomics by enabling the determination of protein structures and providing further insight into biochemical processes.

## 5.3 REFERENCES


(1) Calleri, E.; Temporini, C.; Gasparrini, F.; Simone, P.; Villani, C.; Ciogli, A.; Massolini, G. *J. Chromatogr. A* **2011**, *1218*, 8937-8945.
(2) Peterson, D. S.; Rohr, T.; Svec, F.; Fréchet, J. M. J. *Anal. Chem.* **2002**, *74*, 4081-4088.
(3) Chen, H.-X.; Huang, T.; Zhang, X.-X. *Talanta* **2009**, *78*, 259-264.
(4) Geiser, L.; Eeltink, S.; Svec, F.; Fréchet, J. M. J. *J. Chromatogr. A* **2008**, *1188*, 88-96.
(5) Lee, J.; Soper, S. A.; Murray, K. K. *Analyst* **2009**, *134*, 2426-2433.
(6) Yue, G. E.; Roper, M. G.; Balchunas, C.; Pulsipher, A.; Coon, J. J.; Shabanowitz, J.; Hunt, D. F.; Landers, J. P.; Ferrance, J. P. *Anal. Chim. Acta.* **2006**, *564*, 116-122.
(7) Fan, H.; Chen, G. *Proteomics* **2007**, *7*, 3445-3449.
(8) Kato, M.; Sakai-Kato, K.; Jin; Kubota, K.; Miyano, H.; Toyo'oka, T.; Dulay, M. T.; Zare, R. N. *Anal. Chem.* **2004**, *76*, 1896-1902.
(9) Zhuang, Z.; Mitra, I.; Hussein, A.; Novotny, M. V.; Mechref, Y.; Jacobson, S. C. *Electrophoresis* **2011**, *32*, 246-253.
(10) Liu, J.; Chen, C.-F.; Yang, S.; Chang, C.-C.; DeVoe, D. L. *Lab Chip* **2010**, *10*, 2122-2129.
(11) Mellors, J. S.; Gorbounov, V.; Ramsey, R. S.; Ramsey, J. M. *Anal. Chem.* **2008**, *80*, 6881-6887.
(12) Mellors, J. S.; Jorabchi, K.; Smith, L. M.; Ramsey, J. M. *Anal. Chem.* **2010**, *82*, 967-973.
(13) Yang, W.; Yu, M.; Sun, X.; Woolley, A. T. *Lab Chip* **2010**, *10*, 2527-2533.
(14) Guzman, N. A.; Phillips, T. M. *Electrophoresis* **2011**, *32*, 1565-1578.